

PFAS Visualization and Modeling Workshop: Site Characterization, Remediation and Forensics

Presented By
Grant Carey, Ph.D.

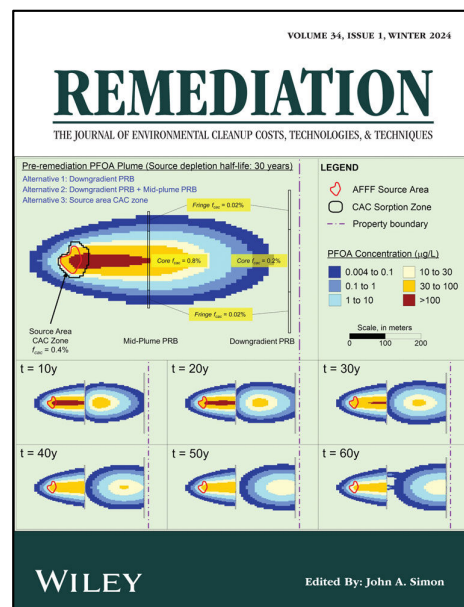
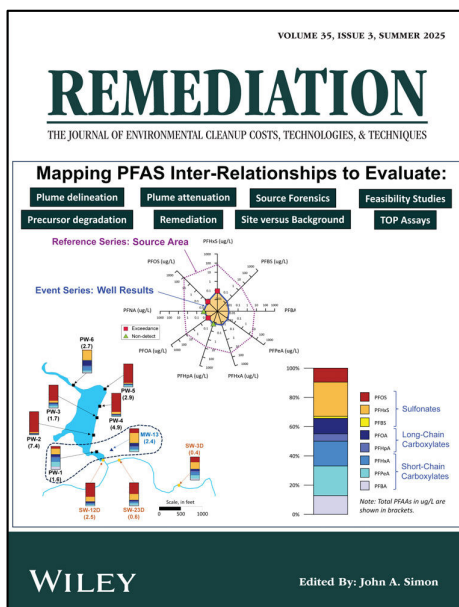
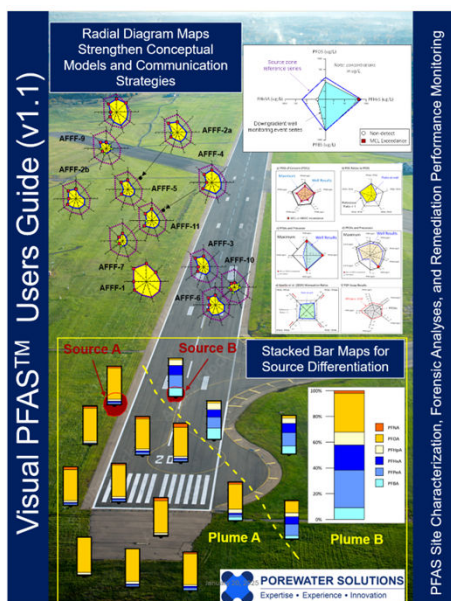
Porewater Solutions
Email: gcarey@porewater.com



POREWATER SOLUTIONS

Expertise • Experience • Innovation

Presented At
2025 REMTEC & Emerging Contaminants Summit



October 13, 2025

Table of Contents

1. Introduction

2. PFAS and AFFF Overview

2.1 PFAS Primer

2.2 Adsorption

2.3 Precursor Transformations

2.4 Regulations

2.5 AFFF Composition and Forensics

3. Visualization Case Studies

3.1 Ellsworth AFB Case Study – AFFF Forensics

- AFFF use differentiation

- Evidence for precursor transformations

- TOP assay visualization

3.2 Michigan AFB – Groundwater discharge forensics

3.3 New Jersey Statewide Soil Survey Forensics

3.4 Other Visualization Examples

4. PFAS Soil Cleanup Criteria and Ellsworth AFB Case Study

4.1 Adsorption to the Air-Water Interface

4.2 Site-specific Soil Screening Levels

4.3 Ellsworth AFB Case Study – Lysimeter Assessment

5. In-Situ Remediation Using Colloidal Activated Carbon

5.1 Adsorption to Activated Carbon

5.2 Case Study No. 1: Navy Pilot Test

5.3 Case Study No. 2: Barrier Placement Alternatives

5.4 Case Study No. 3: Coastal Site Barriers

5.5 Long-Term Remediation Strategies

Appendix A – Carey CV

Appendix B – 2025 PFAS Visualization Journal Paper

Introduction

Section 1

Copyright 2025 Porewater Solutions

1-1

Agenda

- 1** Introduction
- 2** PFAS and AFFF Overview
- 3** Visualization Case Studies
 - Site characterization, remediation, forensics
- 4** PFAS in the Vadose Zone
 - Soil screening levels, modeling, case study
- 5** In-Situ Remediation Case Studies

Copyright 2025 Porewater Solutions

1-2

About Grant Carey, Ph.D.



Grant Carey, Ph.D.
Porewater Solutions

- President of Porewater Solutions
- Over 30 years experience investigating and remediating impacted sites
- PFAS visualization and modeling
- Seven SERDP-ESTCP projects (PFAS remediation)
- Adjunct Research Professor – Carleton U.
- Adjunct Professor – U. of Toronto



Copyright 2025 Porewater Solutions

1-3

Porewater Solutions Involvement In SERDP-ESTCP PFAS Projects



1. SERDP ER21-3959

An Investigation of Factors Affecting **In Situ PFAS Immobilization** by Activated Carbon

2. SERDP ER21-1070

Hydraulic, Chemical, and Microbiological Effects on the Performance of **In Situ Activated Carbon Sorptive Barriers** for PFAS Remediation at Coastal Sites

3. ESTCP ER20-5182

Validation of **Colloidal Activated Carbon** for Preventing the Migration of PFAS in Groundwater

4. ESTCP ER24-8200

Two PFAS Remediation Models for Understanding and Managing PFAS in the Saturated Zone

5. ESTCP ER25-8624

Colloidal Activated Carbon for **In Situ PFAS Remediation at Coastal Sites**: Field Assessment and Modeling of Long-Term Efficacy

6. ESTCP ER25-8483

Demonstrating the **SERDP-ESTCP e-Learning Platform** for Enhancing Technology Transition

7. ESTCP ER25-8875

Evaluation of an **Injected Surface Modified Clay Permeable Adsorptive Barrier** for PFAS Sequestration

Copyright 2025 Porewater Solutions

1-4

ESTCP ER25-8483: PFAS e-Learning Development

Course Resources including:

- Link to course survey
- Printable course notes and reference list
- Links to related SERDP-ESTCP project web pages and other documents

1.2 SERDP and ESTCP PFAS Efforts

SERDP
Strategic Environmental Research and Development Program

ESTCP
Environmental Security Technology Certification Program

Funding broad range of PFAS-related projects

TIP Click on category titles to access project descriptions at the SERDP-ESTCP web site

Legend:

- Treatment
- Ecotoxicity
- Fate, Transport and Characterization
- Analytical and Sampling Methods
- PFAS-Free AFPE

Table of Contents:

- 1.1 PFAS at Joint Bases
- 1.2 PFAS Remediation and Assessment Overview
- 1.3 CAC Sorption
- 1.4 CAC Transport Behavior
- 2. PFAS Adsorption to CAC
- 3. CAC Models & Simulation Results
- 4. CAC Modeling & Performance at Coastal Sites
- 5. CAC Study & Effect of CAC Heterogeneity

Case Studies of PFAS Remediation Using Colloidal Activated Carbon

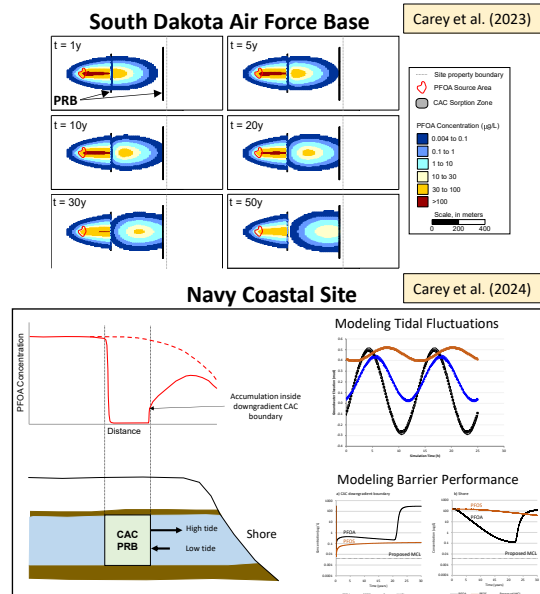
Presented By: David S. Gentry, Ph.D.
February 14, 2024

Copyright 2025 Porewater Solutions

1-5

In-Situ Remediation Model (ISR Model)

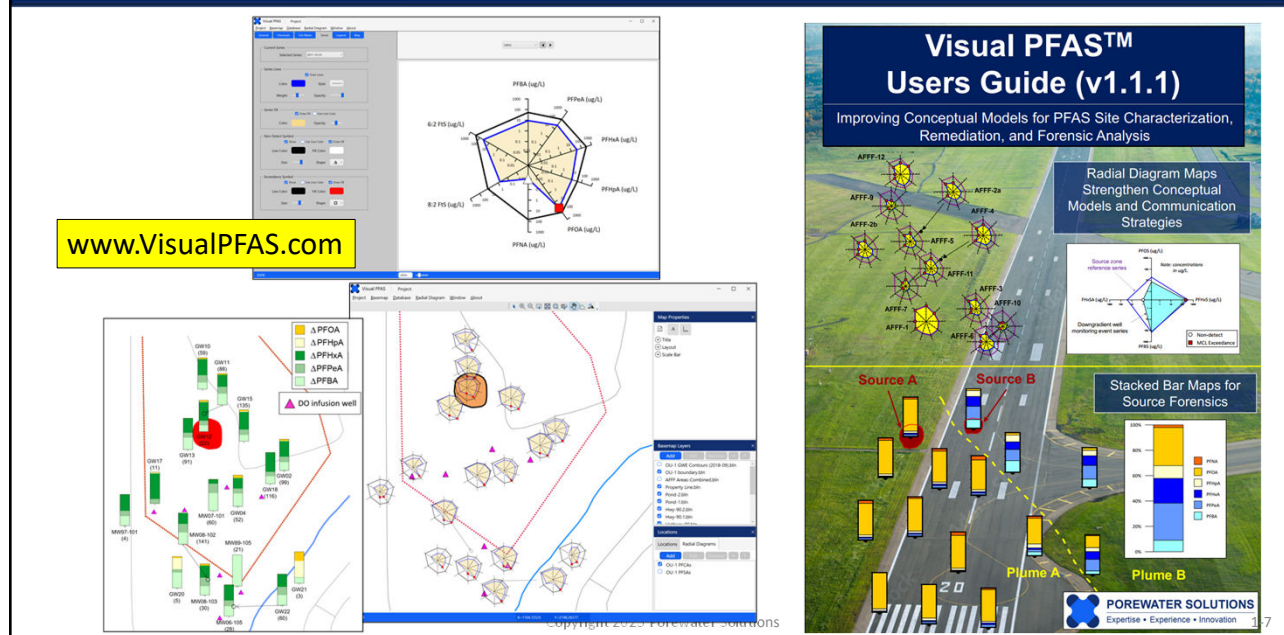
- Originally developed in 1998 as BioRedox-MT3DMS
 - Field and research projects since 2017
 - PFAS-related functionality
 - ✓ PFAS adsorption to CAC
 - ✓ Kinetic sorption
 - ✓ Competitive adsorption
 - ✓ CAC aging
 - ✓ Colloid transport
 - ✓ Branched decay chains
- In progress



Copyright 2025 Porewater Solutions

1-6

Visual PFAS™ for Mapping PFAS Inter-Relationships

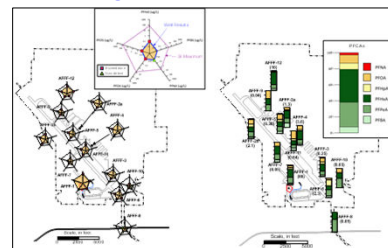


NGWA PFAS Forensic Methods White Paper



National Ground Water Association PFAS Forensic Methods White Paper (Draft)

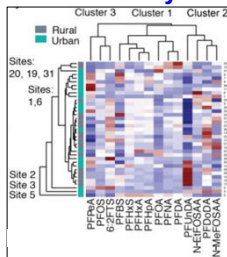
Radial Diagram & Stacked Bar Maps



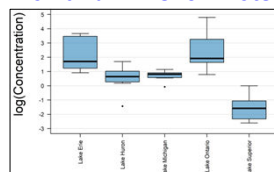
Heat Maps



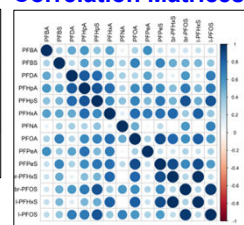
Cluster Analysis



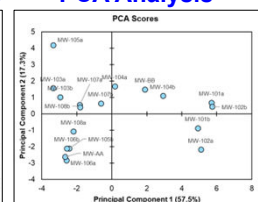
Box and Whisker Plots



Correlation Matrices



PCA Analysis



Copyright 2025 Porewater Solutions

1-8

Administration

- Questions and discussion are always encouraged!
- Course Resources
 - Reference papers and presentations
 - Guidance documents and reports
- Certificates of Attendance
- Coffee
- Bathroom breaks



Copyright 2025 Porewater Solutions

1-9

Porewater Solutions Team at RemTEC Summit



Kiera Rooney



Sabrina Moga



Mia Rebeiro-Tunstall

Copyright 2025 Porewater Solutions

1-10

PFAS and AFFF Overview

Section 2

Section 2 Outline

- 2.1 PFAS Primer
- 2.2 Adsorption
- 2.3 Precursor Transformations
- 2.4 Regulations
- 2.5 AFFF Composition and Forensics




POP QUIZ - Forensics

What Are PFAS?

ITRC Advancing Environmental Solutions
WWW.ITRCWEB.ORG

What Are Per- and Polyfluoroalkyl Substances (PFAS)?

- Large class of surfactants (~~>3,000?~~ ^{>10,000}) with unique chemical & physical properties that make ~~many~~ ^{some} of them extremely persistent and mobile in the environment
- Used since 1940s in wide range of consumer and industrial applications



ITRC (2018)

2-3

PFAS Challenges

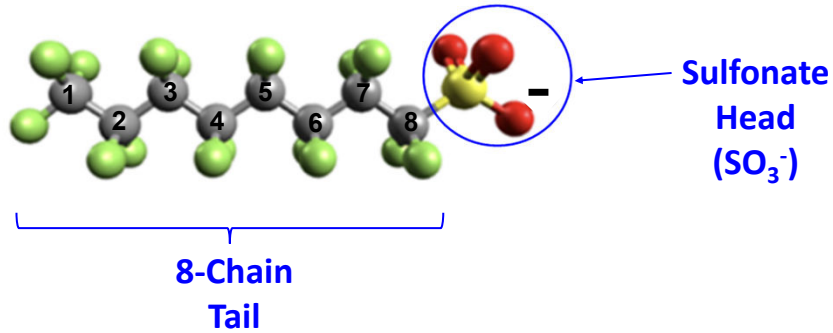
- Used in many products since the 1950s
- Widespread in soil, water, air, and human blood
- PFAS engineered to resist degradation "Forever Chemicals"
- Bioaccumulate in fish, wildlife, and humans
- Some PFAS are toxic at low concentrations



2-4

PFOS Molecule (C8, and 8-Carbon tail)

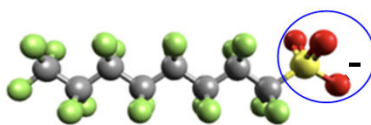
PFOS



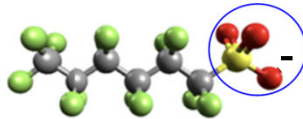
C8: Total number of Carbon atoms in the molecule

2-5

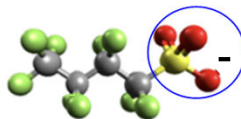
PFAS Overview: Sulfonates (PFSAs)



PFOS (C8)



PFHxS (C6)



PFBS (C4)

Long-chain Sulfonates

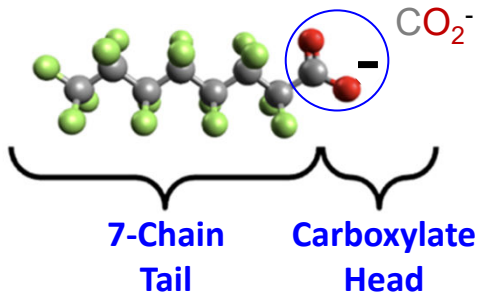
- Stronger adsorption
- Higher bioaccumulation

2-6

PFOA and PFOS Comparison

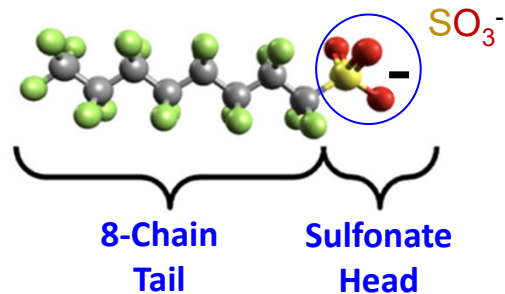
Carboxylate (PFCA)

PFOA (C8)



Sulfonate (PFSA)

PFOS (C8)



2-7

PFAA Naming Convention






PFAAs

Total No. Carbon	Term	PFSAs	PFCAs
		<i>Sulfonates</i>	<i>Carboxylates</i>
9	nona	PFNS	PFNA
8	octa	PFOS	PFOA
7	hepta	PFHpS	PFHpA
6	hexa	PFHxS	PFHxA
5	penta	PFPeS	PFPeA
4	buta	PFBS	PFBA

Long-chain: More toxic

Short-chain: Less toxic

2-8

EPA Method 1633 (40 Analytes)				
PFAAs		Precursors		PFEAs
PFBS (C4) PFPeS (C5) PFHxS (C6) PFHpS (C7) PFOS (C8) PFNS (C9) PFDS (C10) PFDoS (C12)	PFBA (C4) PFPeA (C5) PFHxA (C6) PFHpA (C7) PFOA (C8) PFNA (C9) PFDA (C10) PFUnA (C11) PFDoA (C12) PFTTrDA (C13) PFTA (C14)	NEtFOSA (C10) NMeFOSA (C9) PFOSA (C8) NEtFOSAA (C12) NMeFOSAA (C11) NEtFOSE (C12) NMeFOSE (C11) Biodegrade to: PFOS	3:3 FTCA (C6) 5:3 FTCA (C8) 7:3 FTCA (C10) 4:2 FTS (C6) 6:2 FTS (C8) 8:2 FTS (C10) Biodegrade to: C4 to C8 Carboxylates	11Cl-PF3OUdS (C10) 9Cl-PF3ONS (C8) ADONA (C7) HFPO-DA (C6) NFDHA (C5) PFEEA (C4) PFMB (C5) PFMPA (C4)
				
Sulfonates	Carboxylates	ECF-Based	FT-Based	Replacements

2-9

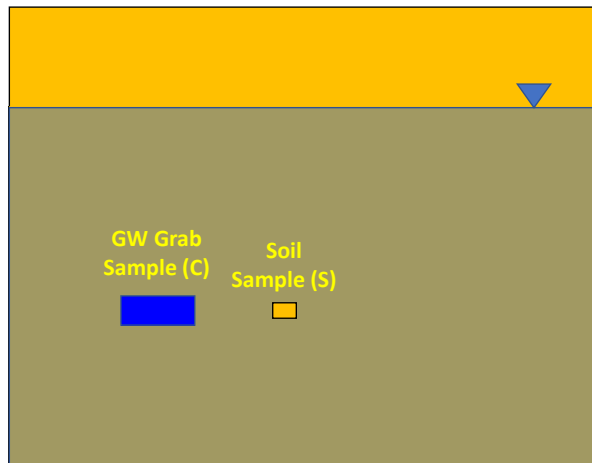
PFAS Adsorption

Section 2.2

2-10

Empirical Approach to Sorption Coefficient Estimation

Collocated soil and groundwater grab samples



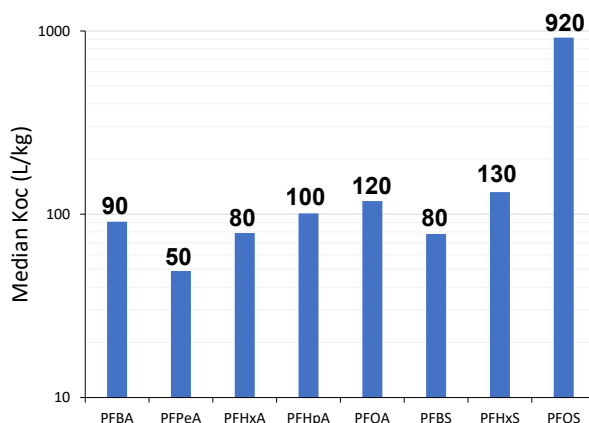
$$K_d = K_{oc} f_{oc} = \frac{S}{C}$$

$$K_{oc} = \frac{S}{C f_{oc}}$$

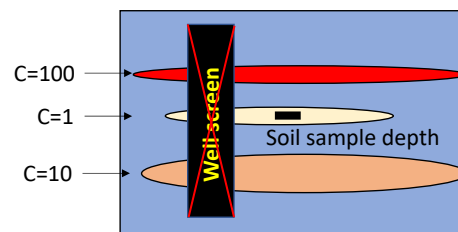
2-13

Site-Specific K_{oc}: South Dakota AFB

Carey et al. (2019-SI) median K_{oc}



Be careful about collecting representative groundwater and soil samples for K_d estimates.
Use short, temporary well screens.



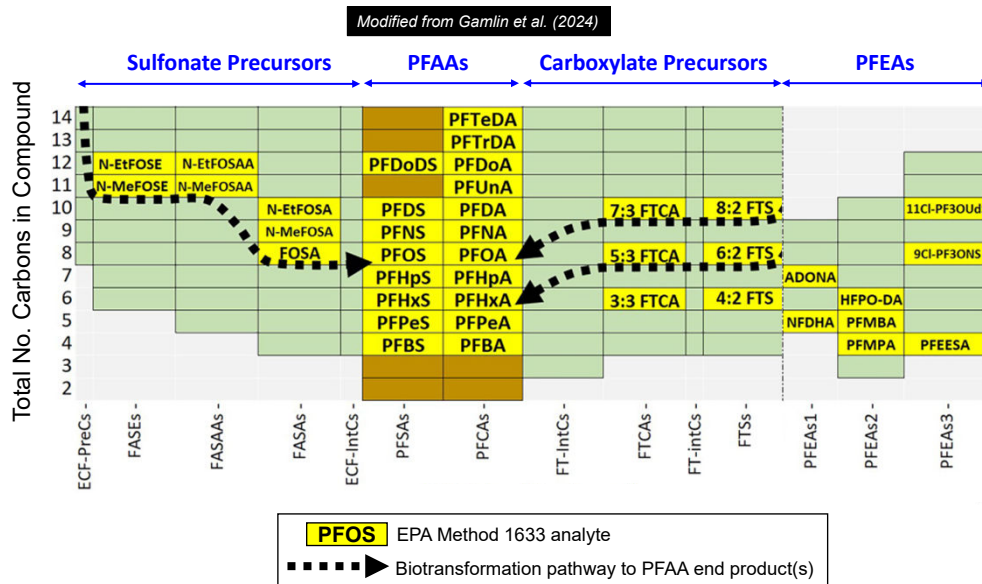
2-14

Precursor Transformations

Section 2.3

2-15

Example of Precursor Transformation Pathways



2-16

Table of PFAA Parent Precursors

Category	Abbreviation	Total No. Carbon Atoms	Aerobic Precursors	Anaerobic Precursors
PFAA - Carboxylates	PFBA	4	4:2 FTS, 6:2 FTS, 5:3 FTCA	8:2 FTOH, 7:2 sFTOH,
	PFPeA	5	6:2 FTS	8:2 FTOH, 7:2 sFTOH
	PFHxA	6	6:2 FTS, 8:2 FTS, 5:3 FTCA	8:2 FTOH, 7:2 sFTOH, 6:2 FTOH
	PFHpA	7	8:2 FTS, 7:3 FTCA	8:2 FTOH, 7:2 sFTOH
	PFOA	8	8:2 FTS	8:2 FTOH, 7:2 sFTOH, 6:2 FTOH
	PFNA	9		
	PFDA	10	10:2 FTCA / FTUCA	
	PFUnA	11		
	PFDoA	12		
	PFTiDA	13		
	PFTA	14		
PFAA - Sulfonates	PFBS	4	FBSA	
	PFPeS	5		
	PFHxS	6	FHxSA, PFHxSAmS, PFHxSAm	
	PFHpS	7		
	PFOS	8	PFOSA, NEtFOSA, NEtFOSE, SAmPAP, PFOSA, NMeFOSA, NMeFOSAA, NMeFOSE	
	PFNS	9		
	PFDS	10		
	PFDoS	12		

2-17

Method 1633 Precursors that May Biodegrade to PFAAs

Precursor Category	Abbreviation	Total No. Carbon Atoms	Aerobic Terminal PFAAs	Anaerobic Terminal PFAAs
FASA	NEtFOSA	10	PFOS	
	NMeFOSA	9	PFOS	
	PFOSA	8	PFOS	
FASAA	NEtFOSAA	12	PFOS	
	NMeFOSAA	11	PFOS	
FASE	NEtFOSE	12	PFOS	
	NMeFOSE	11	PFOS	
FTCA	3:3 FTCA	6		
	5:3 FTCA	8	PFPeA, PFBA	
	7:3 FTCA	10		
FTS	4:2 FTS	6	PFBA	
	6:2 FTS	8	PFHxA, PFPeA, PFBA	
	8:2 FTS	10	PFOA, PFHpA, PFHxA	

2-18

Summary of Precursor Transformations

- Typically, precursor transformation to regulated PFAS only occurs under aerobic conditions
 - More limited pathways under anaerobic conditions (FtOHs to PFCAs)
 - Investigations should include aerobic/anaerobic zone delineation
- Enhanced remediation technologies like bioremediation or in-situ chemical oxidation (ISCO) used for non-PFAS chemicals
 - Can change redox conditions in groundwater
 - May cause increase in regulated PFAS concentrations

2-19

2.5 PFAS Regulations: EPA MCLs and RSLs

MCL

Maximum Chemical Limit

- MCLs are enforceable standards for drinking water quality.

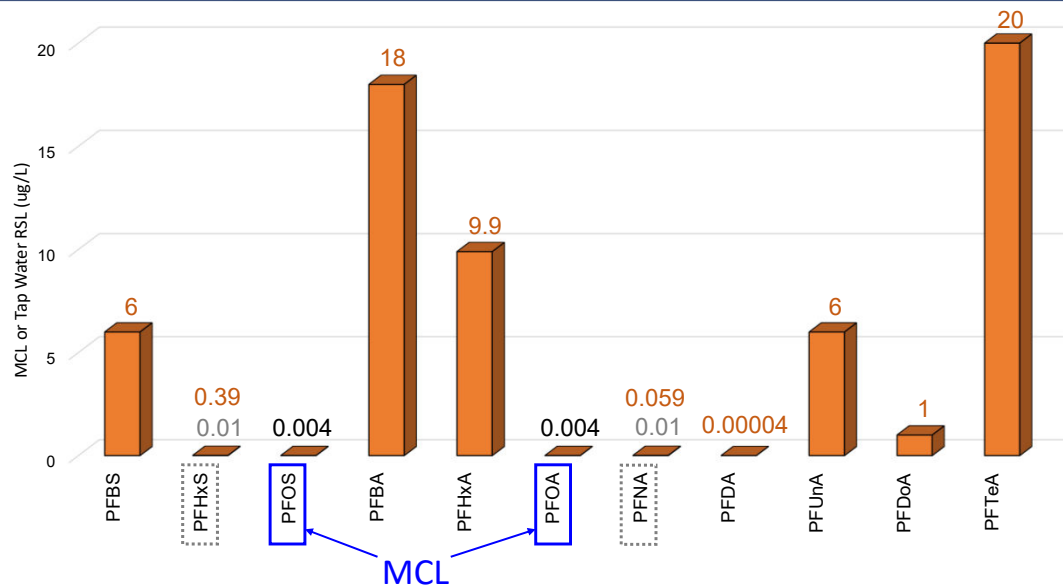
RSL

Regional Screening Level

- RSLs are non-enforceable, risk-based screening levels used to identify chemicals at Superfund Sites which may warrant further investigation.

2-20

PFAS Regulations: EPA MCLs & RSLs



2-21

PFAS Regulations: States

Summary of State Drinking Water/Groundwater Regulated PFAS

Category	Name	No. states with chemical criteria	States (if <10 w. regs)	Median (ug/L)	Minimum (ug/L)	Maximum (ug/L)
Sulfonate	PFBS	16		3.45	0.1	400
	PFHxS	21		0.02	0.01	0.7
	PFHpS	1	HI	0.038	0.038	0.038
	PFOS	28		0.03	0.0007	0.56
Precursor	PFDS	2	HI, TX	0.164	0.038	0.29
	6:2 FTS	1	HI	1.5	1.5	1.5
	8:2 FTS	1	CO	0.07	0.07	0.07
	PFOSA	3	CO, HI, TX	0.07	0.046	0.29
	NMeFOSAA	1	CO	0.07	0.07	0.07
	NEtFOSAA	1	CO	0.07	0.07	0.07
PFEA	HFPO-DA (Gen-X)	11		0.01	0.01	0.37
	8:2 Cl-PFESA	1	CT	0.005	0.005	0.005
Carboxylate	PFBA	7	CT, HI, ME, MN, NC, TX, WA	8	1.8	24
	PFPeA	2	HI, TX	6.75	1.5	12
	PFHxA	8	CT, HI, ME, MI, MN, NC, TX, WA	6	0.2	400
	PFHpA	5	HI, MA, RI, TX, VT	0.02	0.02	0.56
	PFOA	28		0.02	0.000001	0.29
	PFNA	19		0.013	0.006	0.29
	PFDA	4	HI, MA, RI, TX	0.02	0.0077	0.37
	PFUnA	2	HI, TX	0.1545	0.019	0.29
	PFDoA	2	HI, TX	0.158	0.026	0.29
	PFTeA	2	HI, TX	0.158	0.026	0.29

Notes: 1. Reference: ITRC PFAS regulations summary (last updated April 2025)
 2. Yellow-highlighted PFAS are regulated in 10 or more states.

Q: Which two chemicals have the highest number of states where they are regulated?

- ☐ a) PFOS and PFHxS
- ☐ b) PFOA and PFNA
- ☐ c) PFOS and PFNA
- ☐ d) PFOS and PFOA

2-22

AFFF Product Composition

1. Electrochemical Fluorination (ECF)
2. Fluorotelomerization (FT)



2-23

Historical AFFF Manufacturing Processes

1. Electrochemical Fluorination (ECF)

- Feedstock: PFOS, and sulfonate precursors of that mainly degrade to PFOS, PFHxS, PFBS
 - PFOA is 1% of PFOS (since 1989)
- Only 3M used the ECF process
- All 3M AFFF products are ECF-based



2. Fluorotelomerization (FT)

- Feedstock: Fluorotelomers
- All other manufacturers: FT-based AFFF



2-24

History of AFFF Products on Qualified Products List

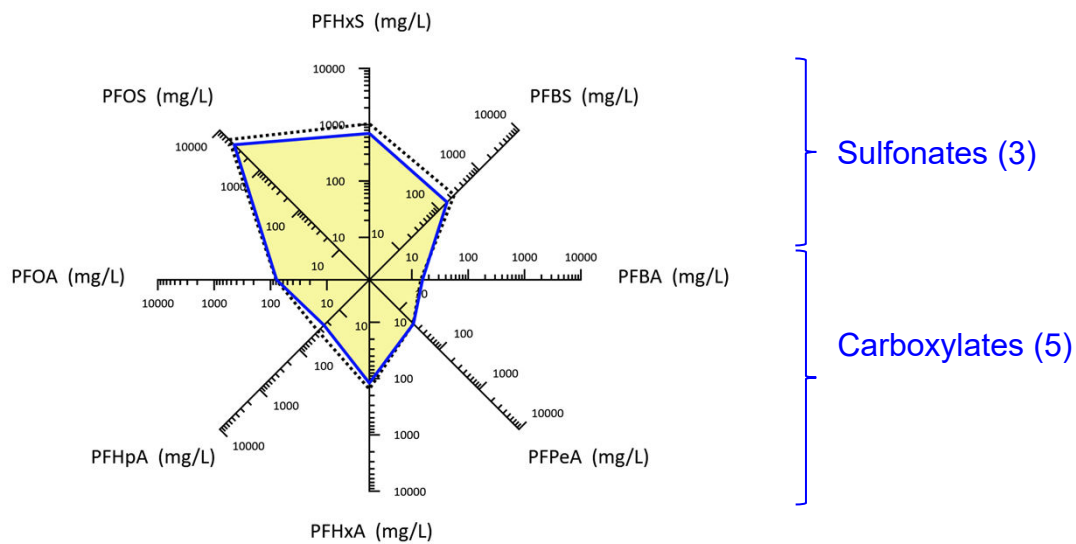
AFFF (3/6%) Manufacturer	1970	1980	1990	2000	2010
3M					
National Foam*					
Ansul or Tyco/Ansul					
Angus					
Chemguard or Tyco/Chemguard					
Kidde					
Buckeye					
Kidde/National/Angus					
Fire Service Plus					
ICL Performance Products					
Amerex/Solberg					
*National Foam or CHUBB National Foam or Kidde/National Foam or Kidde/National/Angus					



ESTCP ER-201574 FAQs Re AFFF Use

2-25

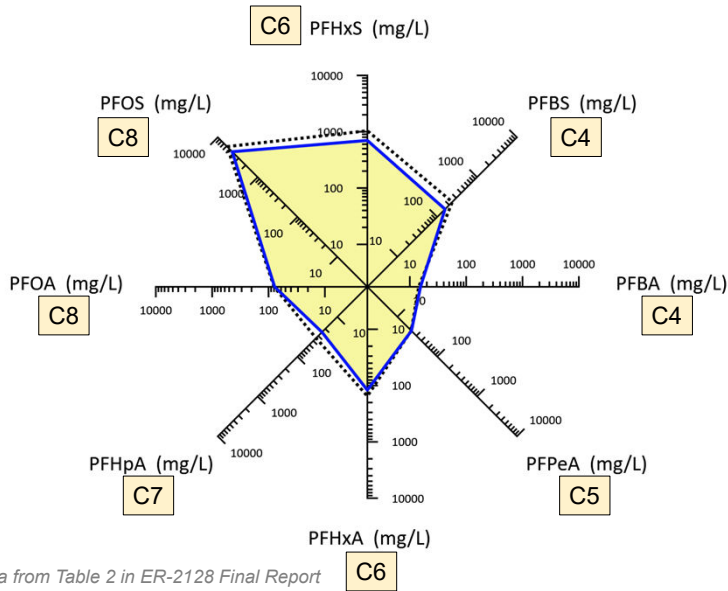
AFFF Composition: ECF-Based PFAAs (3M)



Note: Data from Table 2 in ER-2128 Final Report

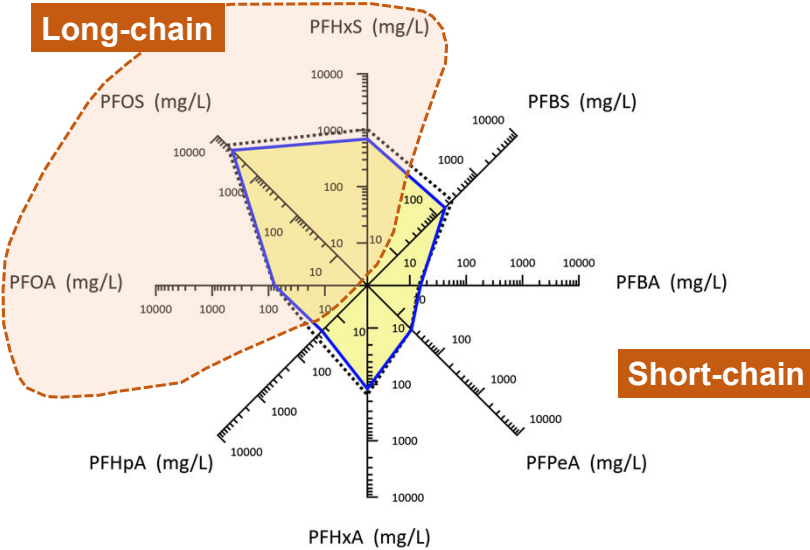
2-26

AFFF Composition: ECF-Based PFAAs (3M)



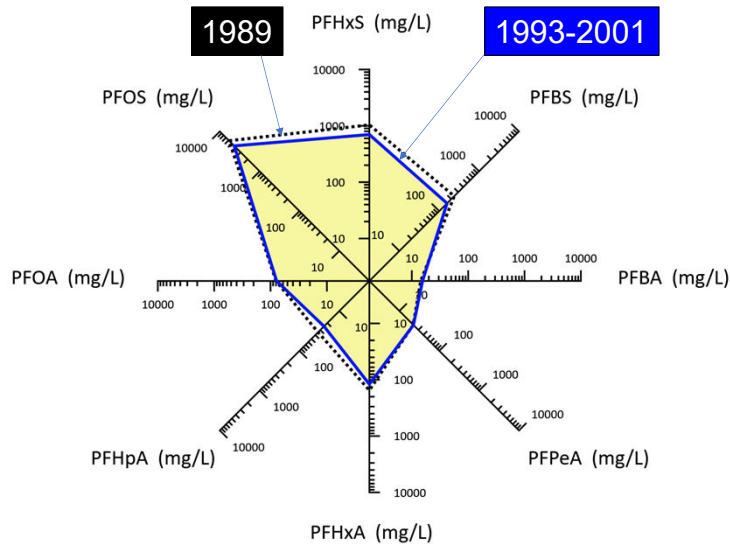
2-27

AFFF Composition: ECF-Based PFAAs (3M)



2-28

AFFF Composition: ECF-Based PFAAs (3M)



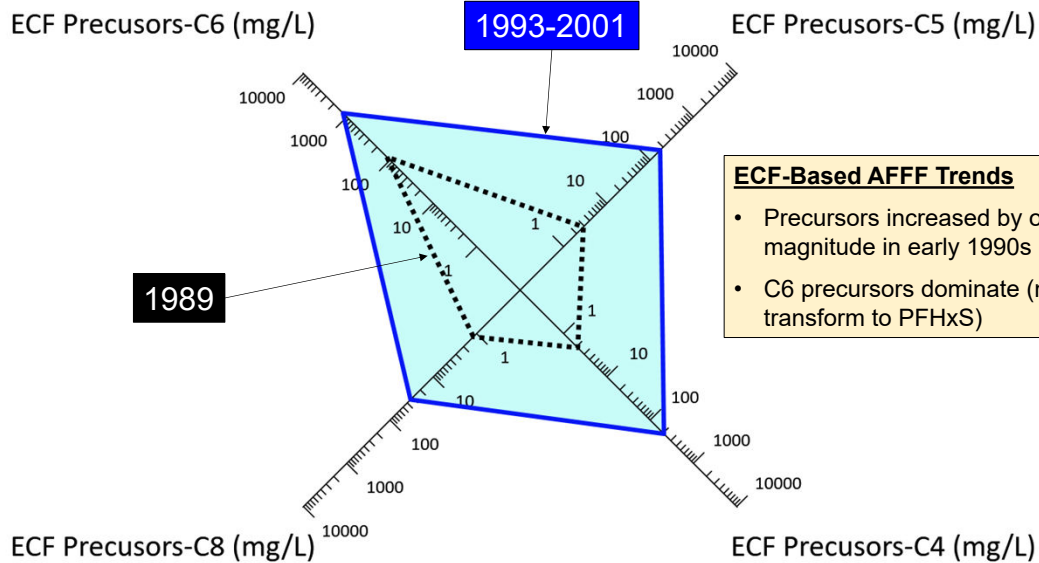
ECF-Based AFFF Trends

- Predominantly PFOS
- PFOS is 5-10x higher than PFHxS
- PFOA is about 1% of PFOS
- Carboxylates negligible since at least 1989

Note: Data from Table 2 in ER-2128 Final Report

2-29

AFFF Composition: ECF-Based Precursors



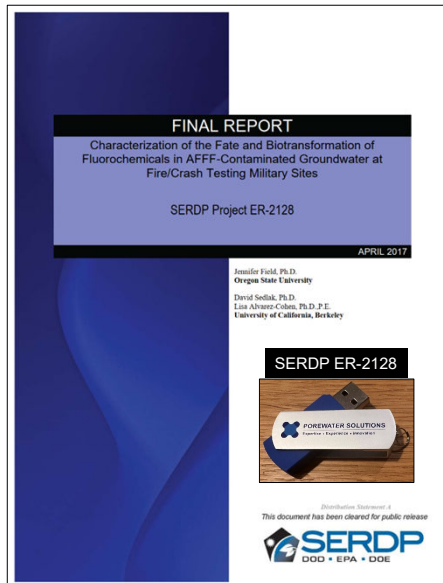
ECF-Based AFFF Trends

- Precursors increased by order of magnitude in early 1990s
- C6 precursors dominate (may transform to PFHxS)

Note: Data from Table 2 in ER-2128 Final Report

2-30

AFFF Composition: FT-Based



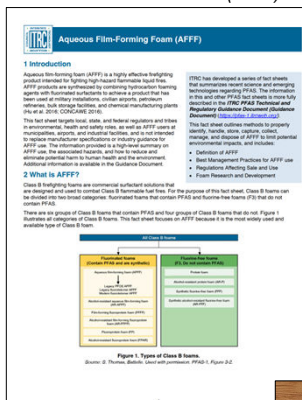
FT-Based Composition Findings

- Detected FT-based precursors only
 - Carboxylates, Sulfonates not detected
- Precursors for long- and short-chain carboxylates
- Fluorotelomer sulfonates (e.g., 6:2 FtS and 8:2 FtS) were low
 - n:2 FtS are intermediate byproducts

2-31

Impacts from AFFF Products

ITRC AFFF Fact Sheet (2024)



ECF: Electrochemical Fluorination
FT: Fluorotelomerization

Legacy ECF
(Late 1960s-2002)

Legacy FT
(Late 1970s-2016)

Modern FT

Long-chain

Short-chain

Soil/GW Impacts:
High PFOS, PFHxS
Lower PFCAs (e.g., PFOA)

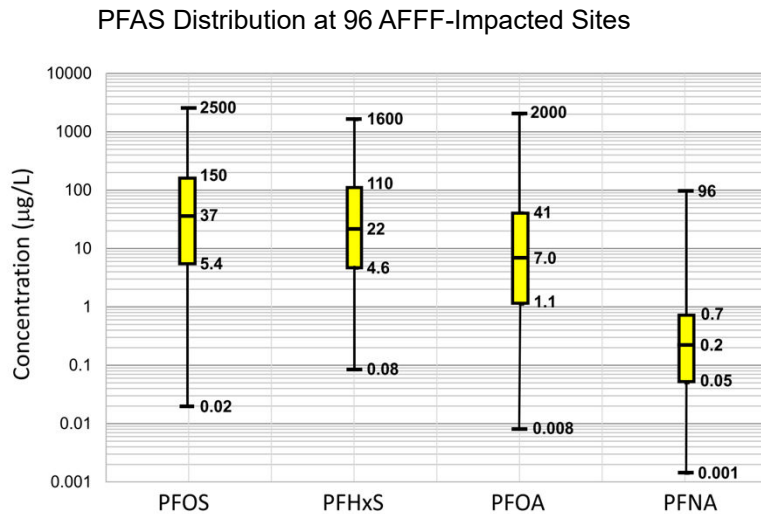
Soil/GW Impacts:
High FtS
High PFCAs (PFBA → PFOA)
Lower PFSA

Product differentiation clues:

- PFSA vs PFCAs
- Long-chain vs short-chain PFCAs

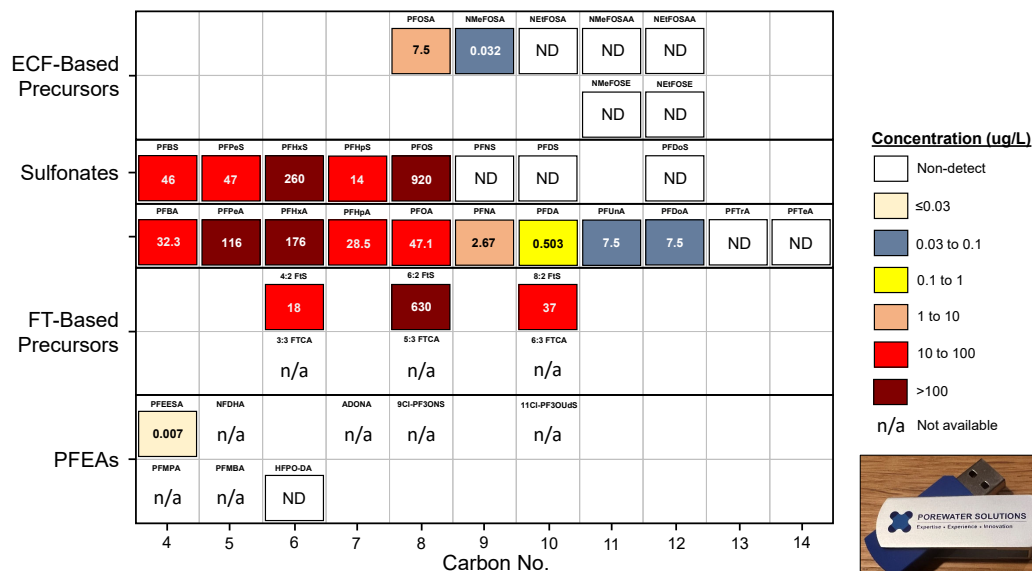
2-32

PFAS Concentrations At AFFF vs Aerospace Sites



2-33

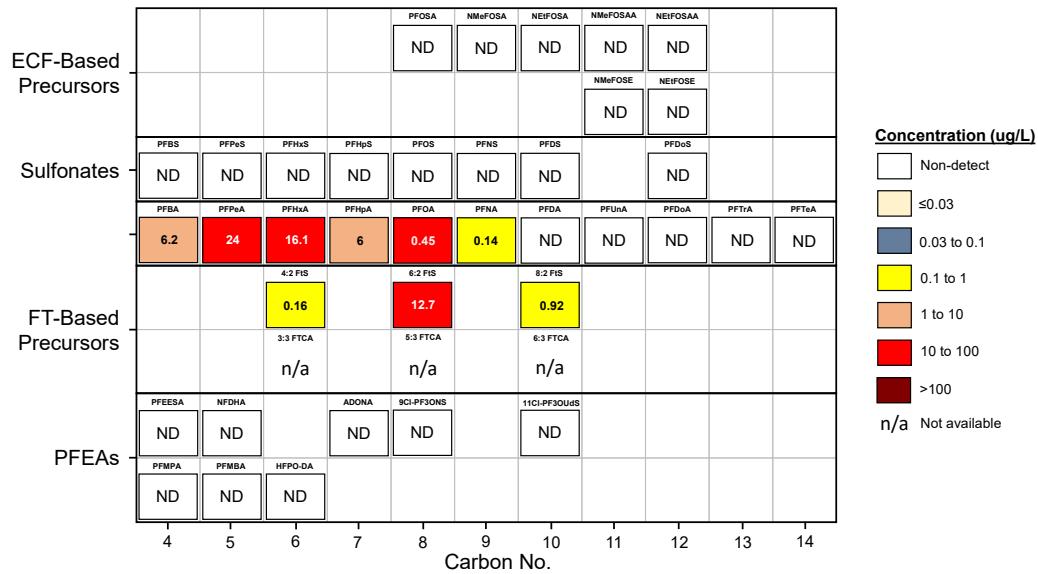
Q1: Which AFFF Products Used At This Site



Utilities\Method 1633 Heat Matrix Template.pptx

2-34

Q2: What was the Dominant Product Used At This Site



2-35

Questions?

Grant R. Carey, Ph.D.

Porewater Solutions

gcarey@porewater.com



POREWATER SOLUTIONS

Expertise • Experience • Innovation

36

Visualization Case Studies

Section 3



Copyright 2025 Porewater Solutions

3-1

Challenges in Characterizing PFAS Sites

Need to assess:

- Plume extent
- Attenuation trends along flow path
- Source differentiation
- Background fingerprinting
- Redox zones



Copyright 2025 Porewater Solutions



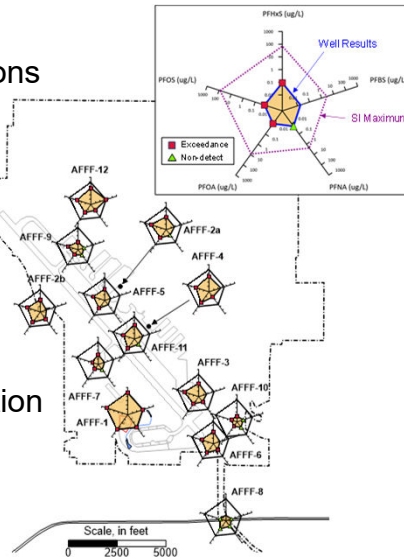
3-2

PFAS Inter-Relationships Are Important to Source Forensics

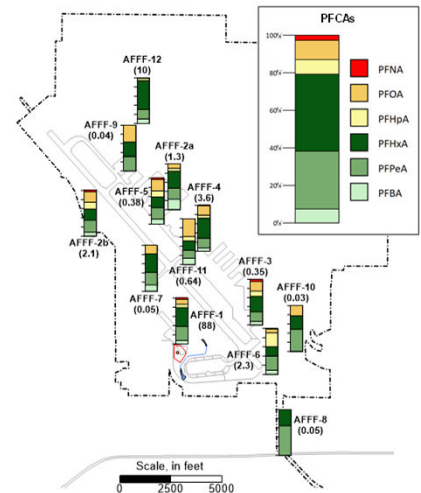
To Evaluate:

1. Exceedance & ND locations
2. Short vs long-chain
3. Precursor degradation
4. Flow path attenuation
5. Site vs background
6. TOP assay results
7. Time + spatial differentiation

Radial Diagram Maps



Stacked Bar Maps



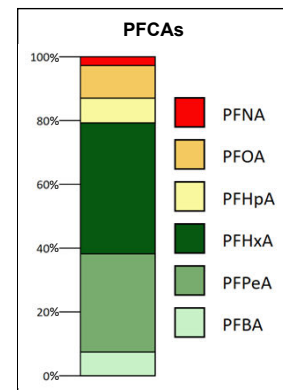
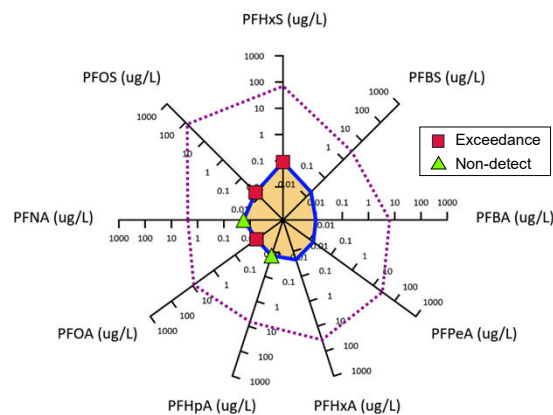
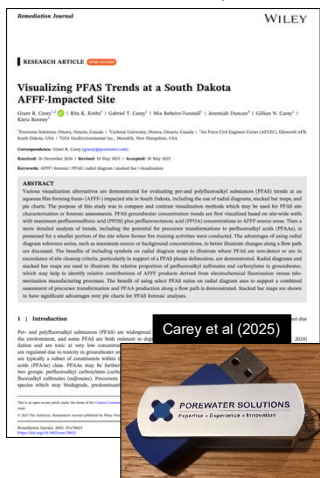
Copyright 2025 Porewater Solutions

3-5

PFAS Site Characterization South Dakota AFB

Remediation Journal (Open Source)

Section 3.1



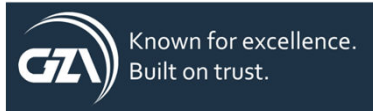
Copyright 2025 Porewater Solutions

3-6

Acknowledgements



Rita Krebs



Jeremiah Duncan, Ph.D.

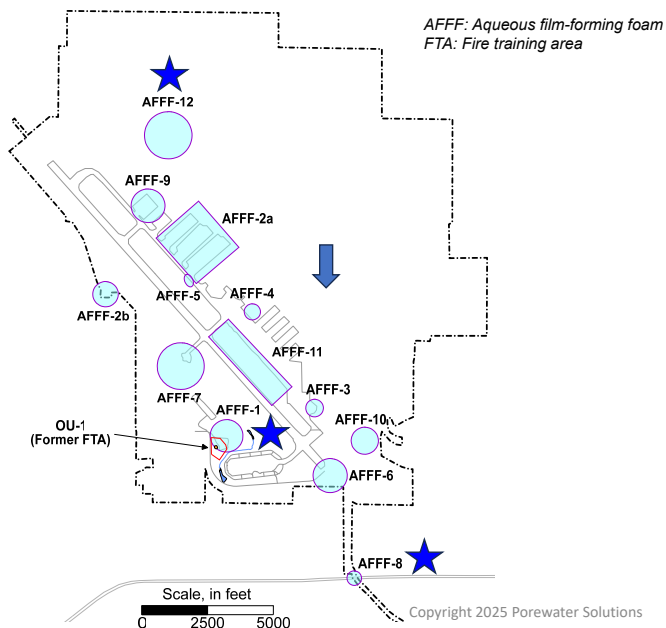


Gabriel Carey
Mia Rebeiro-Tunstall
Gillian Carey
Kiera Rooney

Copyright 2025 Porewater Solutions

3-7

Site Inspection: AFFF Source Areas

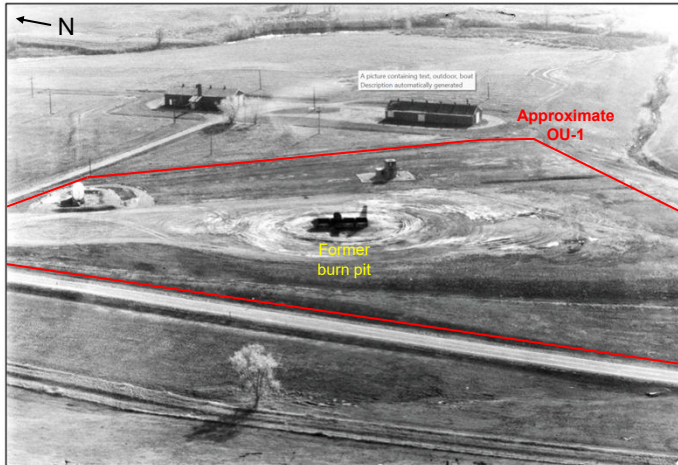


AFFF Area	Location
★ AFFF-1	Current FTA
AFFF-2a AFFF-2b AFFF-3	70, 80, 90 Rows; and Outfall #3 Building 618
AFFF-4	Former Fire Station (Building 7506)
AFFF-5	B-52 Crash (1972)
AFFF-6	B-1 Crash (1988)
AFFF-7	Delta Taxiway West Crash (2000)
★ AFFF-8	Marten Crash (2006)
AFFF-9	Crash 4 (2001)
AFFF-10	Wastewater Treatment Plant
AFFF-11	Spray Nozzle Test Area
★ AFFF-12	Building 88240
★ OU-1	Former Fire Training Area

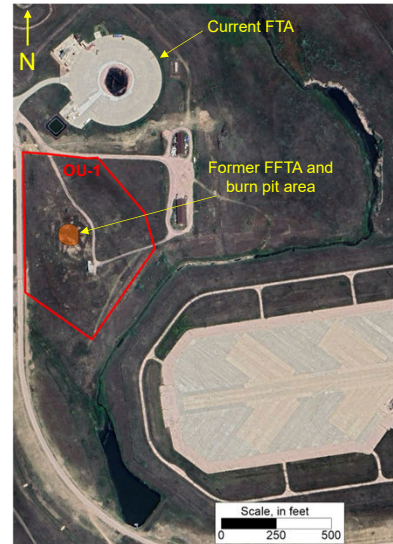
3-8

Current and Former Fire Training Areas

a) Former fire training area in 1985 (Rita Krebs, 2025)



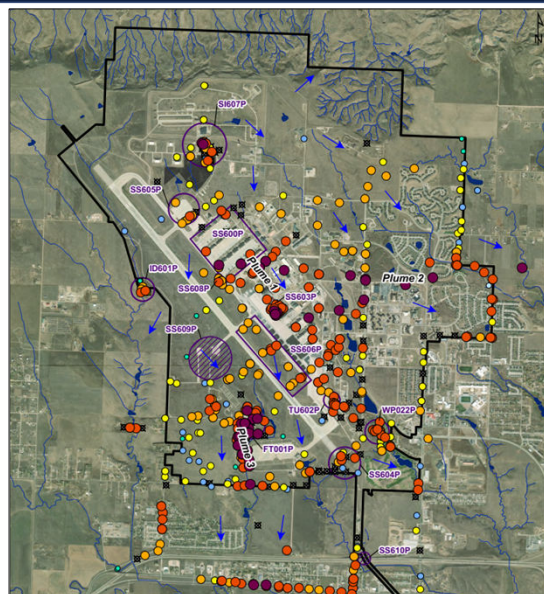
b) Current and former fire training areas



Copyright 2025 Porewater Solutions

3-9

Exceedance Factors (EFs) – Single Species or Max. EF



$$EF = \text{Concentration} / \text{Criterion}$$

Legend

Groundwater Sample PFOS Concentration

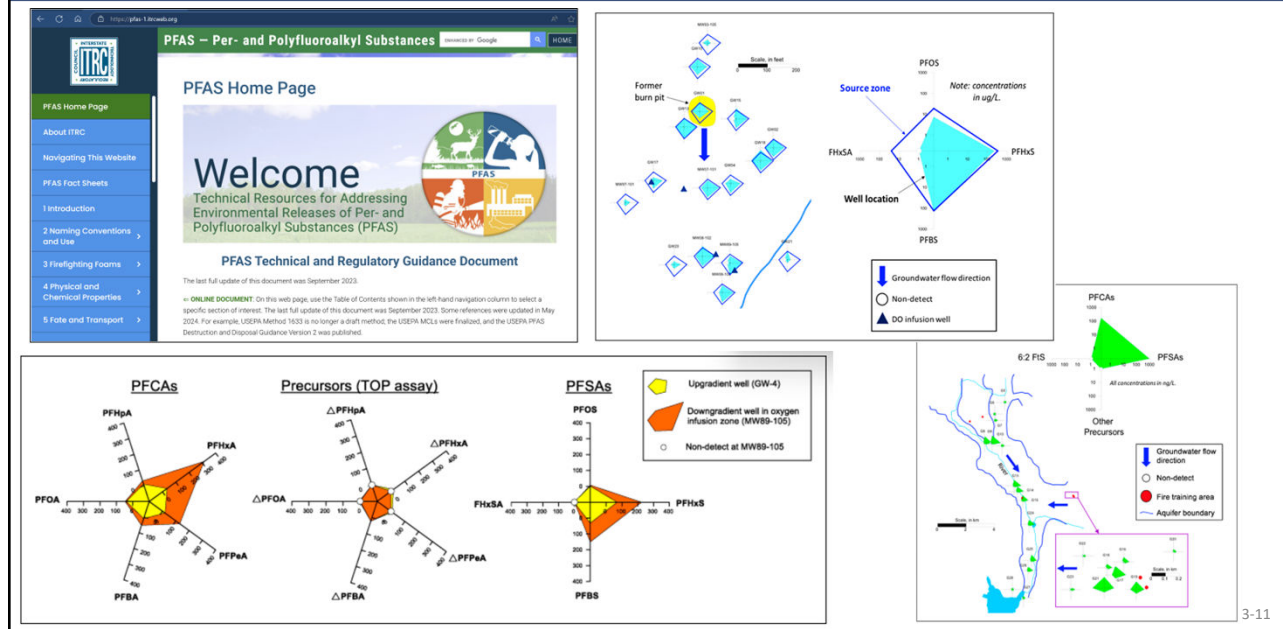
- Greater than 1,000x SL
- Between 100x SL and 1,000x SL
- Between 10x SL and 100x SL
- Between SL and 10x SL
- Detection < SL
- Non-detect (RL > SL)
- Non-detect (RL ≤ SL)
- Dry Groundwater Sample Location During RI

- Air Force Base Boundary
- PFAS Source Area - Sampled
- PFAS Source Area - Unvalidated, Not Sampled
- Waterbody
- Stream/Creek
- Inferred Groundwater Flow Direction

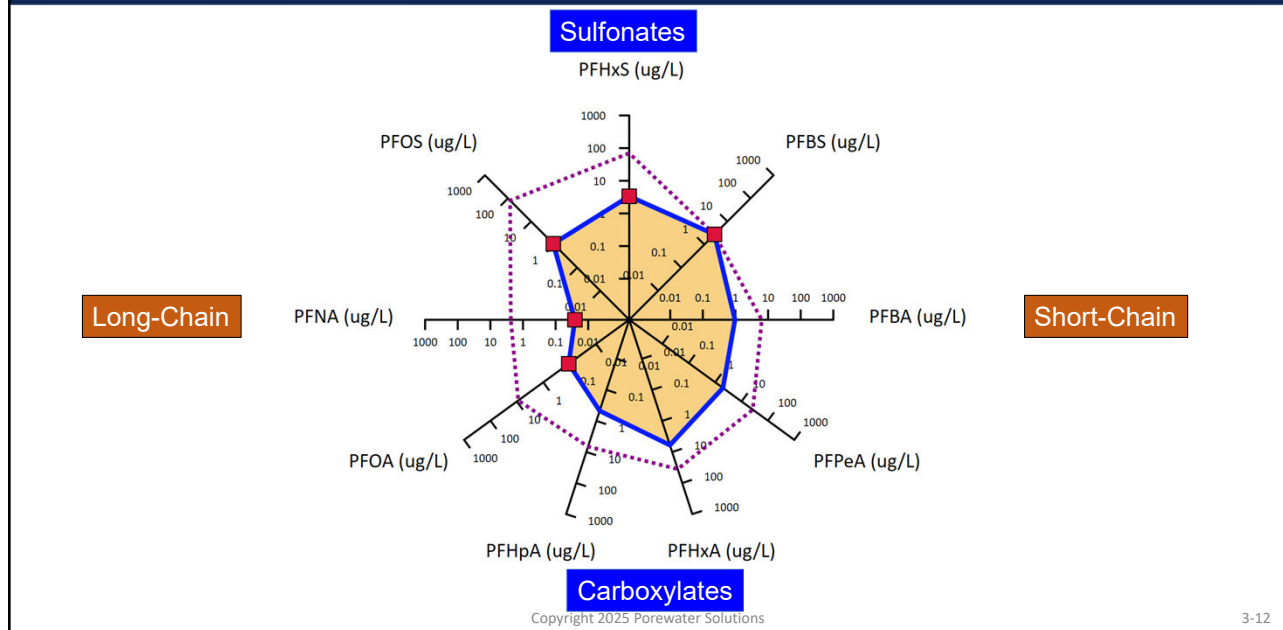
Copyright 2025 Porewater Solutions

3-10

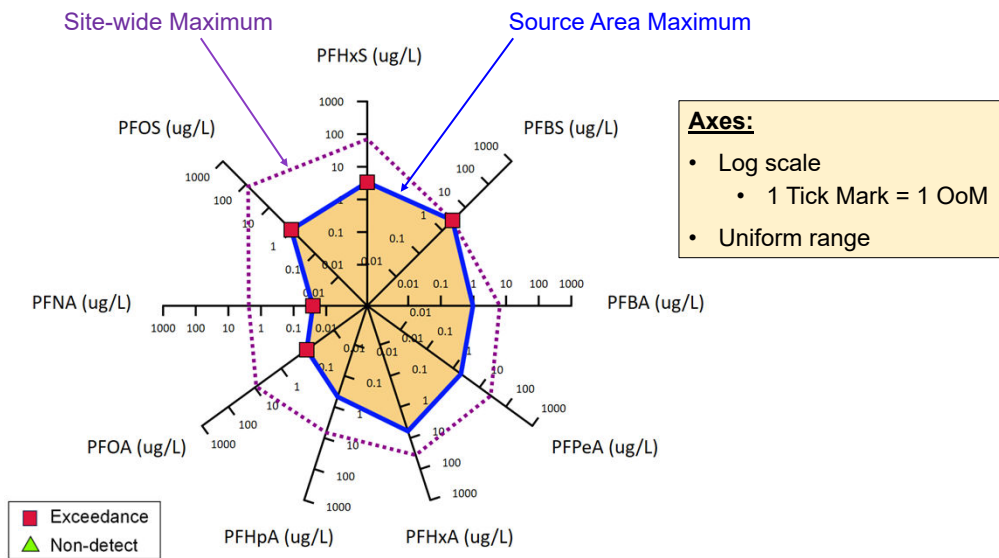
ITRC PFAS Guidance: Radial Diagram Examples



AFFF Source Area Radial Diagrams: AFFF-12



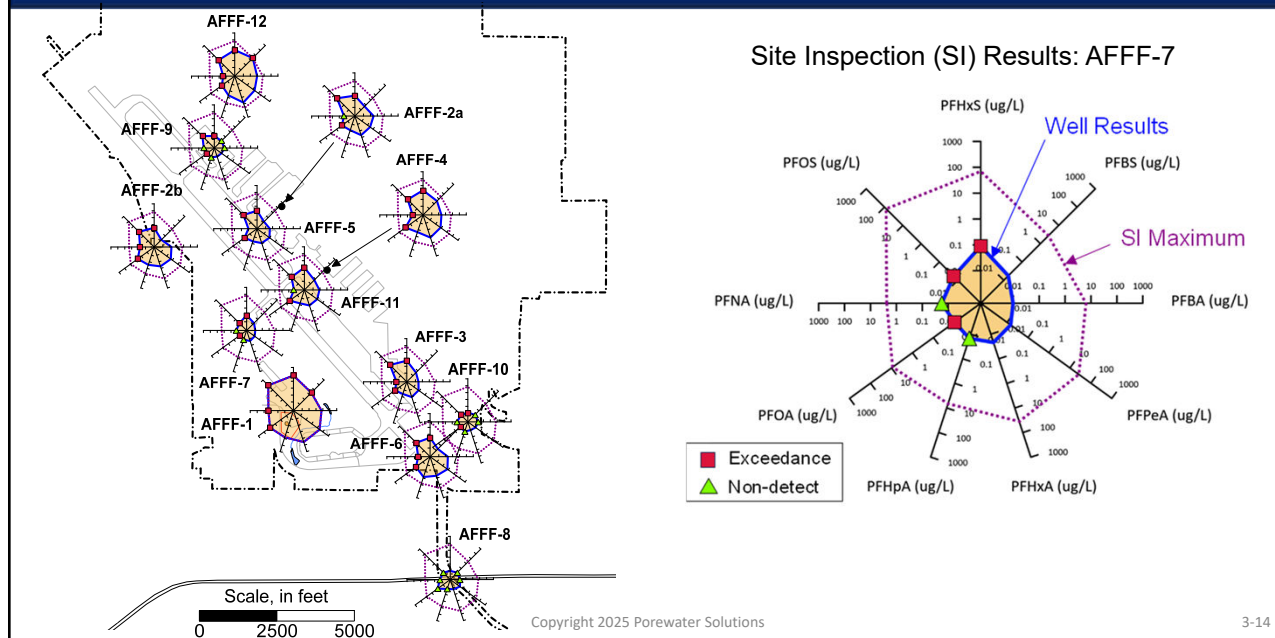
AFFF Source Area Radial Diagrams: AFFF-12



Copyright 2025 Porewater Solutions

3-13

AFFF Source Area Radial Diagrams



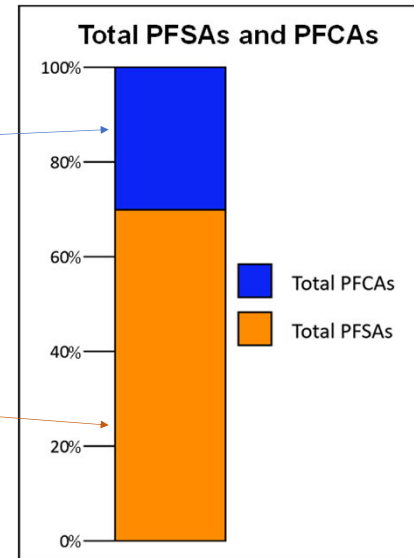
Copyright 2025 Porewater Solutions

3-14

Stacked Bar Chart Example: AFFF-7

AFFF Product:
Fluorotelomerization
(FT) Process

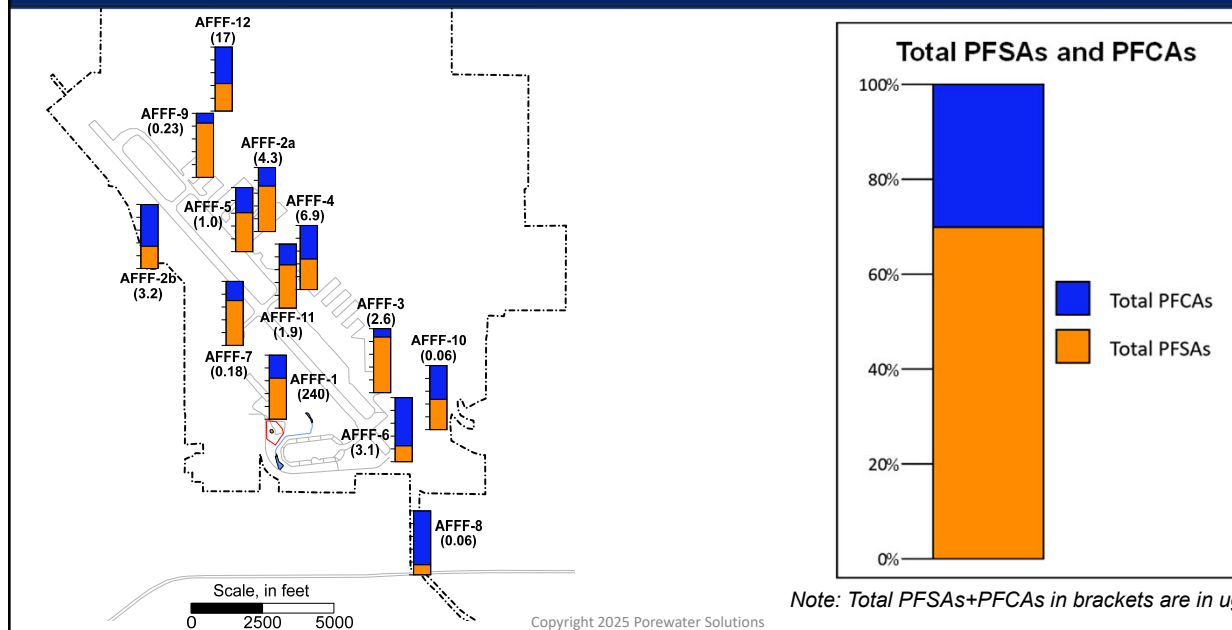
AFFF Product:
Electrochemical Fluorination
(ECF) Process



Copyright 2025 Porewater Solutions

3-15

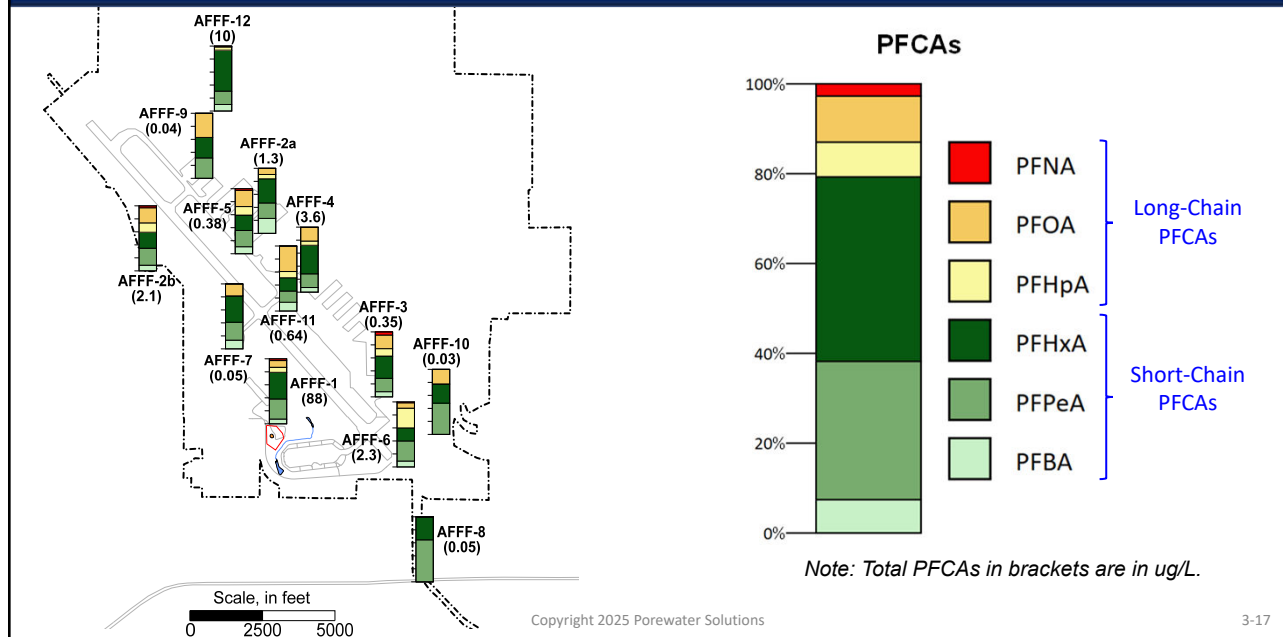
Stacked Bar Chart Example



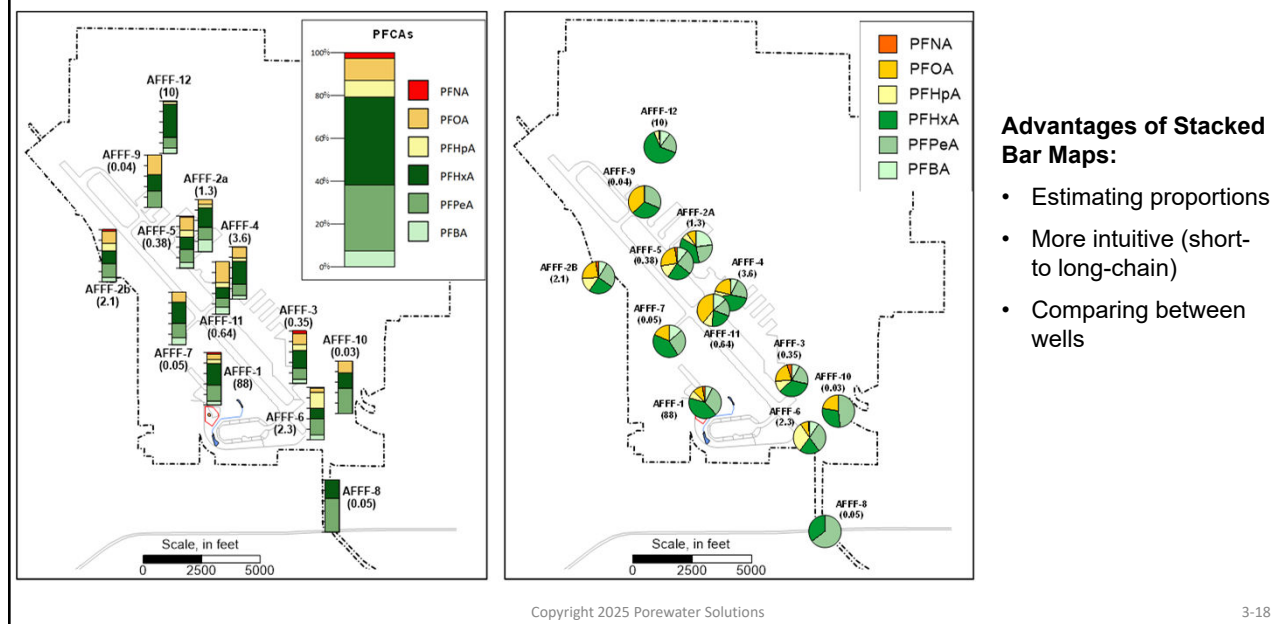
Copyright 2025 Porewater Solutions

3-16

Source Area Short vs Long-Chain PFCAs



Stacked Bar vs Pie Chart Maps



Ratios as Evidence of Precursor Transformations

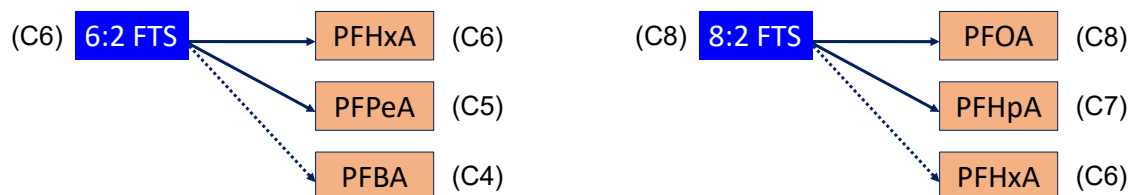
Section 3.1.1

Copyright 2025 Porewater Solutions

3-19

6:2 FTS and 8:2 FTS Transformation Pathways

Precursor Transformation Pathways

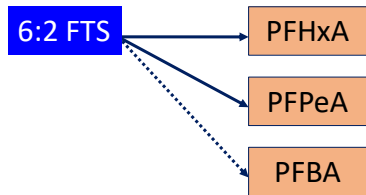


Note: Fluorotelomer sulfonates biodegrade to carboxylates, not sulfonates.

Copyright 2025 Porewater Solutions

3-20

South Dakota Installation: 6:2 FTS Ratios at MW89-105



Biodegradation Process

Precursor concentration: ↓

Daughter product (PFAA) concentration: ↑

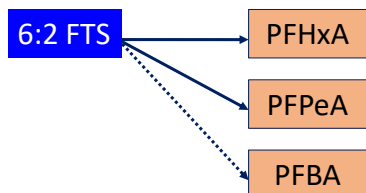
Ratio: ↓

$$\text{Ratio} = \frac{\text{Parent}}{\text{Daughter Product}}$$

Copyright 2025 Porewater Solutions

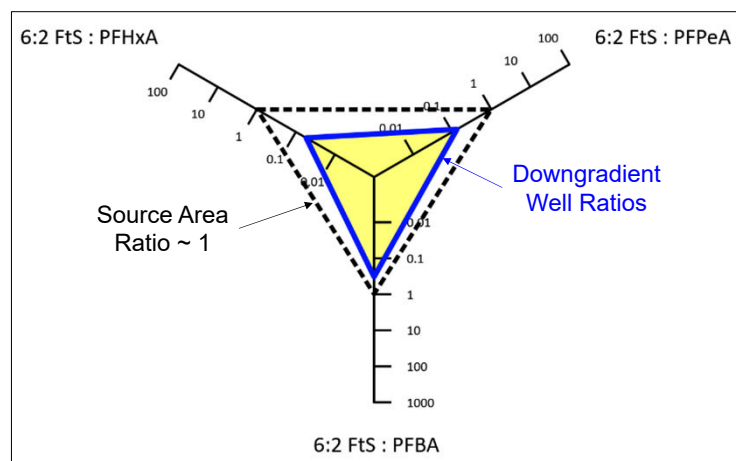
3-21

South Dakota Installation: 6:2 FTS Ratios at MW89-105



$$\text{Ratio} = \frac{\text{Parent}}{\text{Daughter Product}}$$

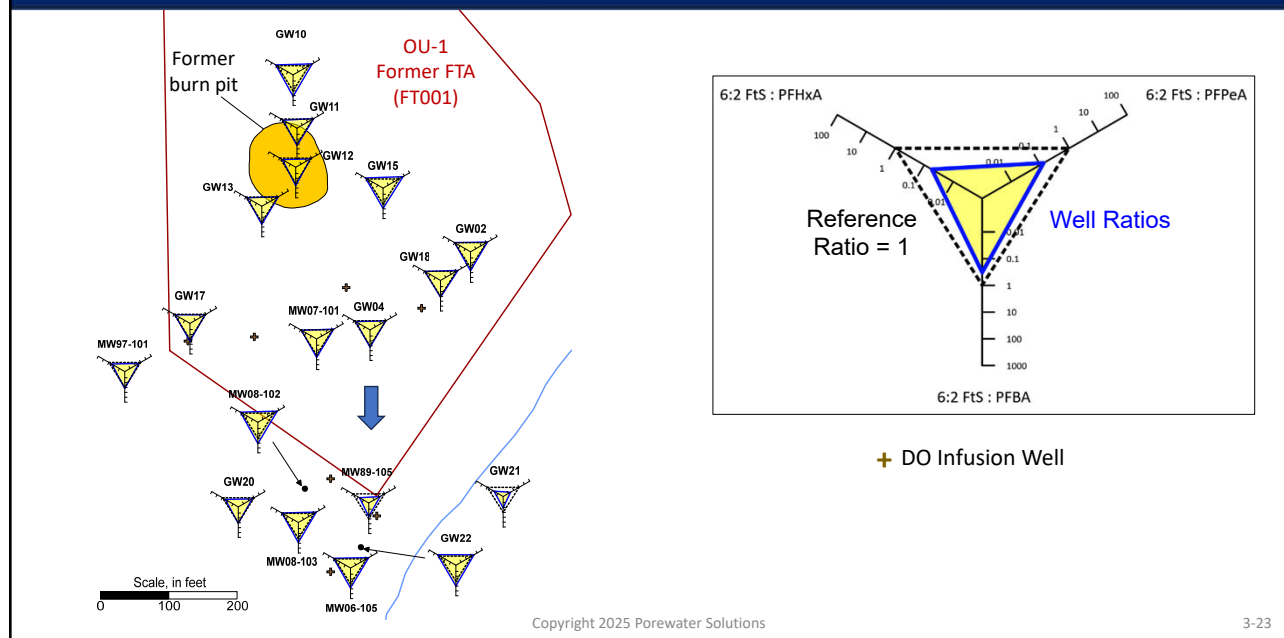
Carey et al. (2025)



Copyright 2025 Porewater Solutions

3-22

OU-1 (Former FTA): 6:2 FtS Ratios



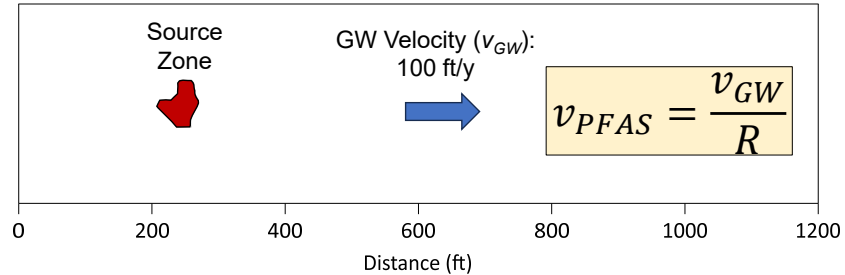
Will Differential Adsorption Affect PFAS Ratios?

$$\text{Ratio} = \frac{\text{Parent (precursor)}}{\text{Daughter Product (PFAA)}}$$

- Two processes which may cause this ratio to decrease along a groundwater flow path:
 - Parent (precursor) biodegradation; and/or
 - Differential adsorption in an expanding plume (precursor slower than PFAA)

Model of Differential Adsorption Effects

Simultaneous releases
starting 50 years ago:
6:2 FtS and PFHxA,
10 ug/L each



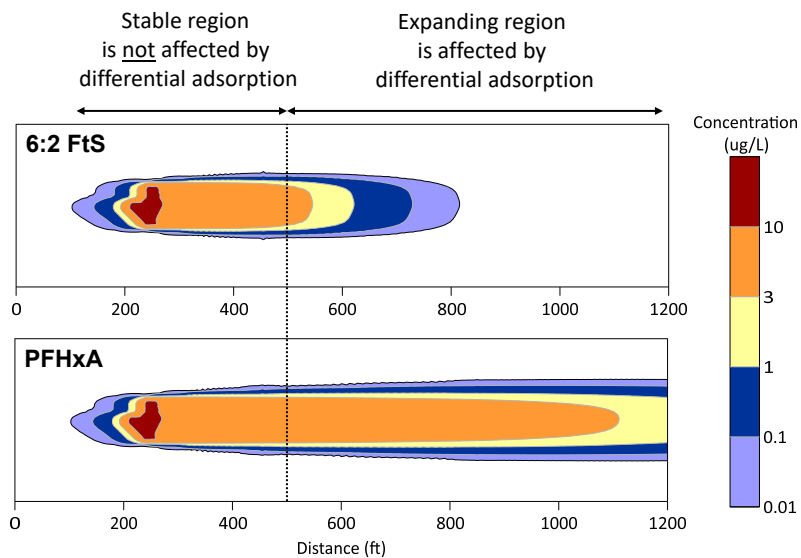
Solute	Koc (L/kg)	Kd (L/kg)	Retardation Coefficient, R (dimensionless)
6:2 FtS	500	0.5	3.0
PFHxA	50	0.05	1.2

Note: $f_{oc} = 0.1\%$

Copyright 2025 Porewater Solutions

3-25

Modeled PFAS Plumes 50 Years After Start of Release



Copyright 2025 Porewater Solutions

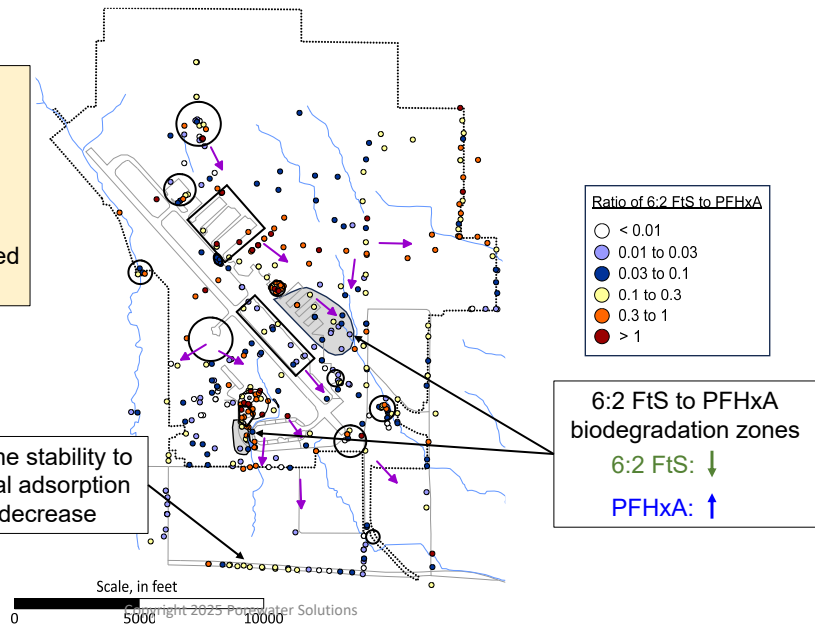
3-26

Ratio of 6:2 FtS versus PFHxA in Groundwater

Note:

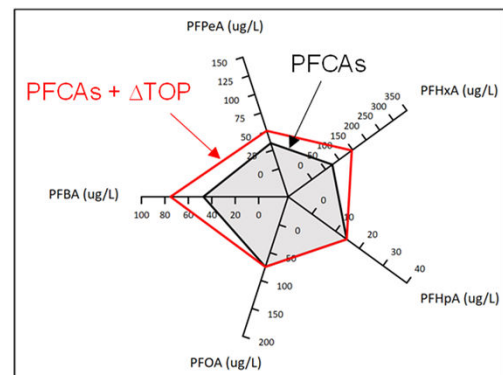
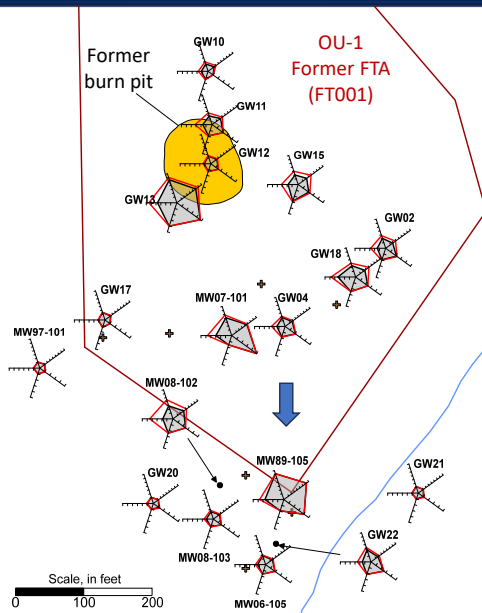
1. Multiple lines-of-evidence approach will strengthen a forensic analysis
2. Potential for differential adsorption needs to be assessed with ratio analyses

Check 6:2 FtS plume stability to confirm if differential adsorption is causing ratio decrease



3-27

OU-1 (Former FTA): TOP Assay Results



Copyright 2025 Porewater Solutions

3-28

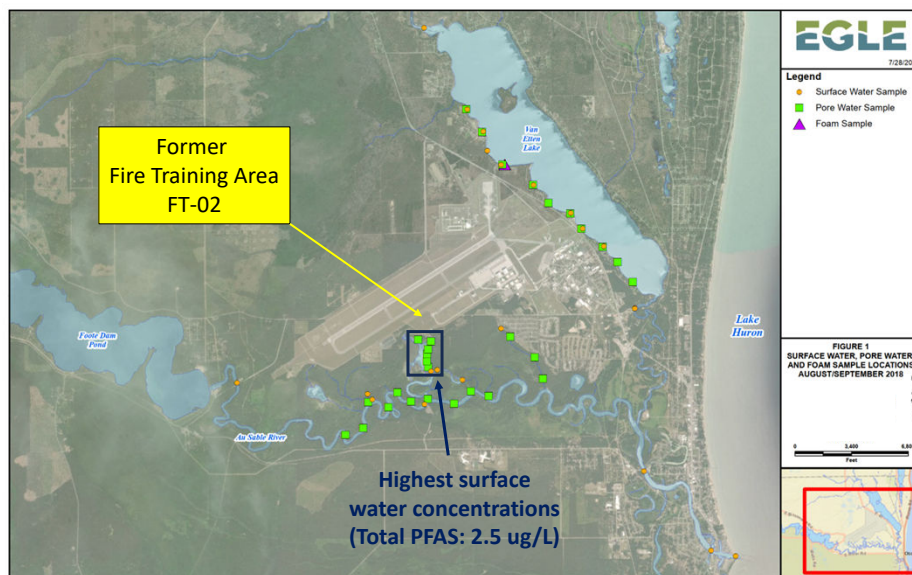
Differentiating Groundwater Impacts to a Pond

Section 3.2

Copyright 2025 Porewater Solutions

3-29

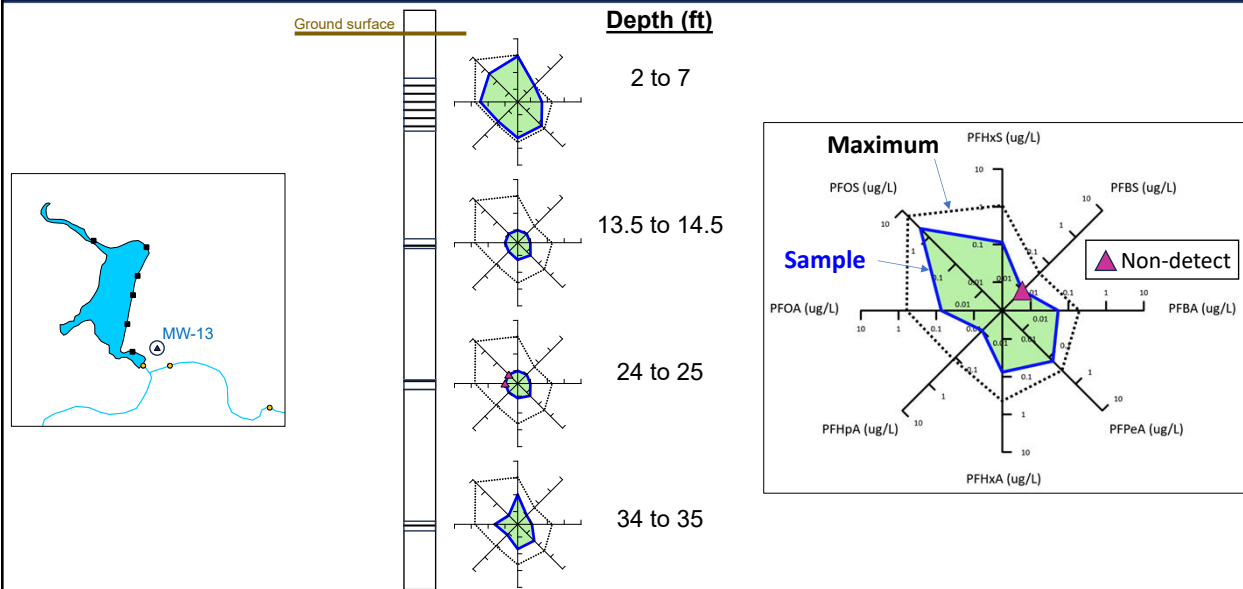
Michigan AFB: 2018 Porewater/Surface Water Samples



Copyright 2025 Porewater Solutions

3-30

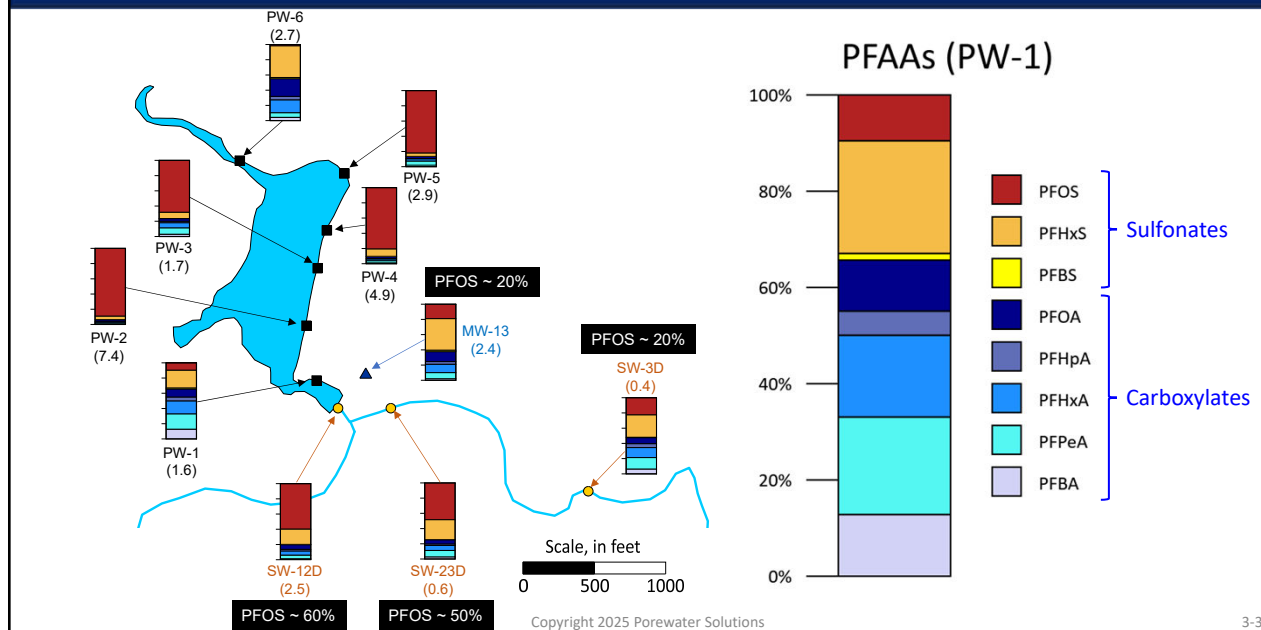
Nested Groundwater Samples (MW-13)



Copyright 2025 Porewater Solutions

3-33

Wurtsmith AFB: GW, PW, SW



Copyright 2025 Porewater Solutions

3-34

New Jersey State-wide Background Soil Survey

Section 3.3

Copyright 2025 Porewater Solutions

3-35

New Jersey Statewide PFAS Soil Survey

Per- and Polyfluoroalkyl Substances in New Jersey Soils: A Statewide Investigation

Authors:

Jennifer Willemssen¹, Greg Toffoli¹, Alex Imnone¹, Lori Lester², Zahid Aziz², Sandra Goodrow¹,
Alissa Metter¹, Nick Procopio¹, Erica Snyder¹, Joe Stefanoni¹

¹New Jersey Department of Environmental Protection, Contaminated Site Remediation and Redevelopment
²New Jersey Department of Environmental Protection, Division of Science and Research

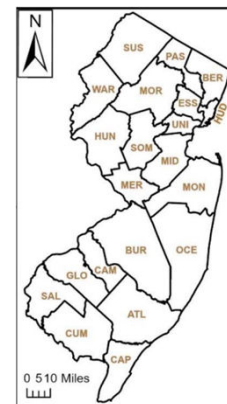
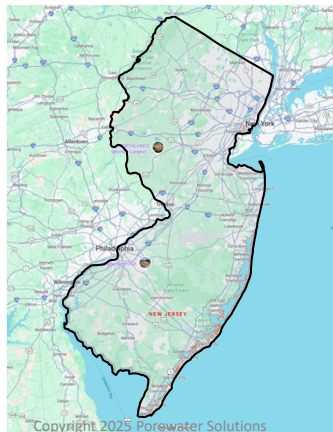
New Jersey Department of Environmental Protection

September 2025



NJDEP (2025)

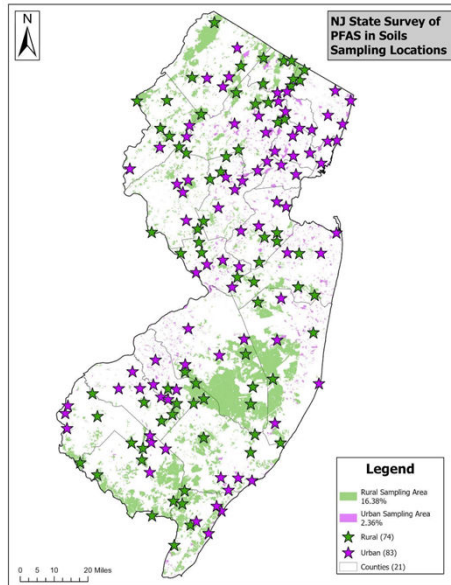
- **Goal:** To assess atmospheric deposition influence on PFAS in shallow soil
- 157 State-wide surficial soil samples



Copyright 2025 Porewater Solutions

3-36

Sampling Locations



- “PFAS atmospheric impacts from a point source can extend far beyond a 0.5-mile radius”
- Samples located at least 0.25 to 0.5 miles from known contamination

Copyright 2025 Porewater Solutions

3-37

State-wide Maximum Surficial Soil Concentrations (ug/kg)

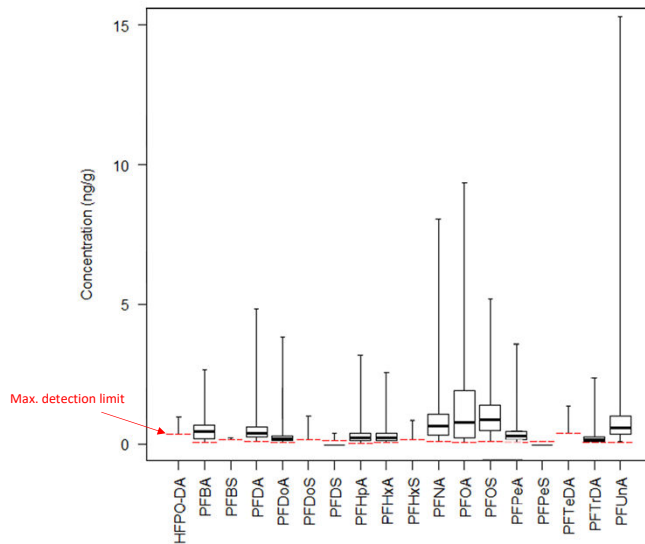
ECF-Based Precursors					PFOSA	NMeFOSA	NEiFOSA	NMeFOSAA	NEiFOSAA					
					ND	ND	ND	ND	ND					
Sulfonates								NMeFOSE	NEiFOSE					
								ND	ND					
Carboxylates	PFBS	PFPeS	PFHxS	PFHpS	PFOS	PFNS	PFDS		PFDoS					
	0.22	0.087	0.83	0.049	5.2	ND	0.379		1.0					
FT-Based Precursors	PFBA	PFPeA	PFHxA	PFHpA	PFOA	PFNA	PFDA	PFUnA	PFDoA	PFTtA	PFTeA			
	2.7	3.6	2.6	3.2	9.4	8.1	4.8	15	3.8	2.4	1.4			
PFEAs			4:2 FTB		6:2 FTB		8:2 FTB							
			ND		0.37		ND							
			3:3 FTCA		5:3 FTCA		6:3 FTCA							
			ND		ND		ND							
	PFESBA	NFDHA		ADONA	9CI-PF3ONS		11CI-PF3OUdS							
	ND	ND		ND	ND		ND							
	PFMPA	PFMBA	HFPO-DA											
	ND	ND	0.95											
	4	5	6	7	8	9	10	11	12	13	14			

Carbon No.



Utilities\Method 1633 Heat Matrix Template.apptx

Box and Whisker Plot

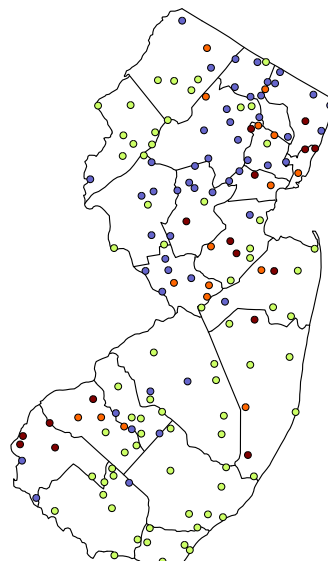


Note: This plot could be improved by grouping carboxylates and sulfonates, and ranking species based on chain length.

Copyright 2025 Porewater Solutions

3-39

Heat Map Example #1: Total PFAS Distribution



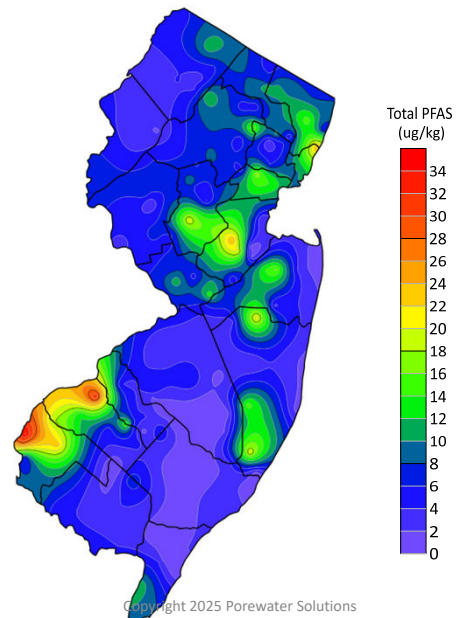
Total PFAS (ug/kg)

- 0 to 5
- 5 to 10
- 10 to 15
- >15

Copyright 2025 Porewater Solutions

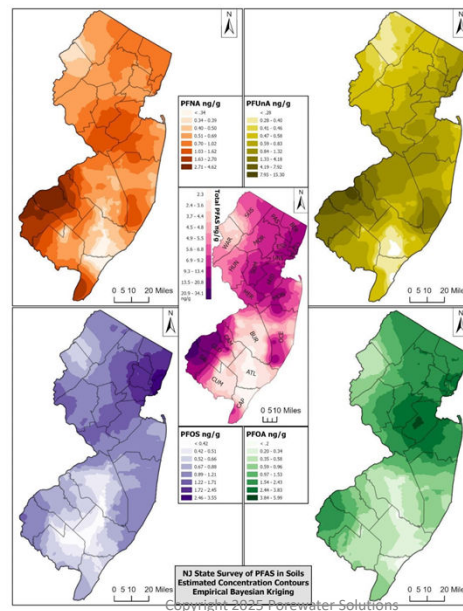
3-40

Heat Map Example #2: Total PFAS Contours

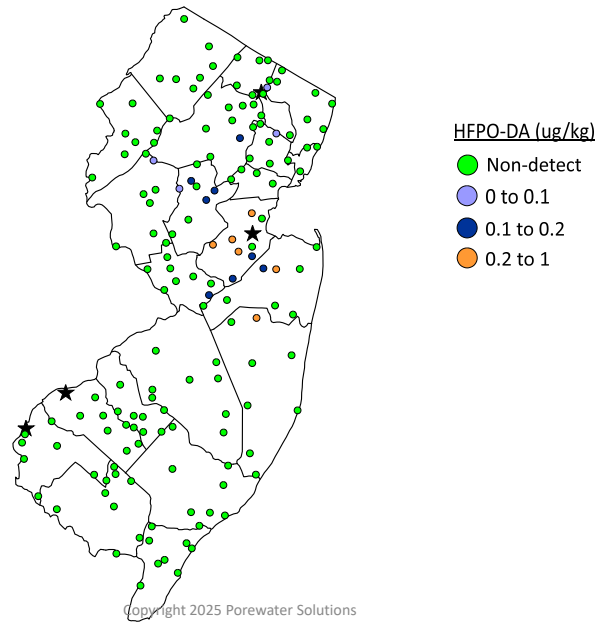


3-41

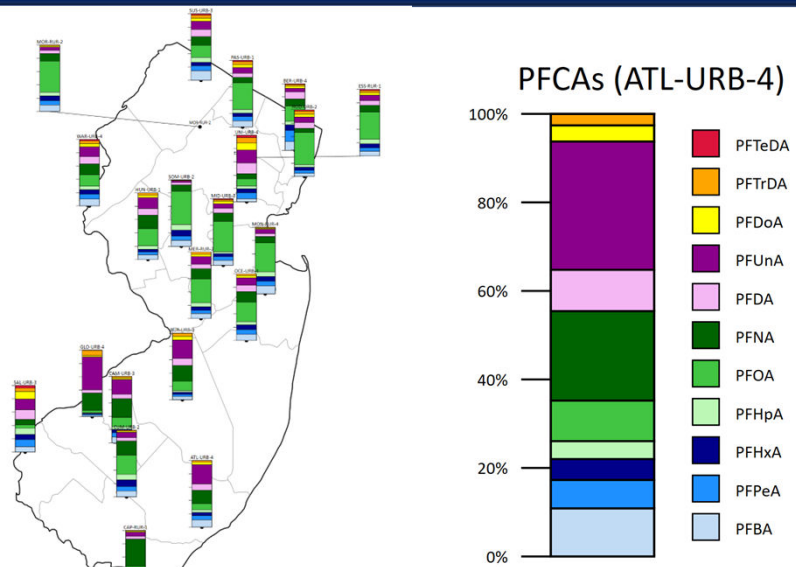
NJDEP Report Heat Maps



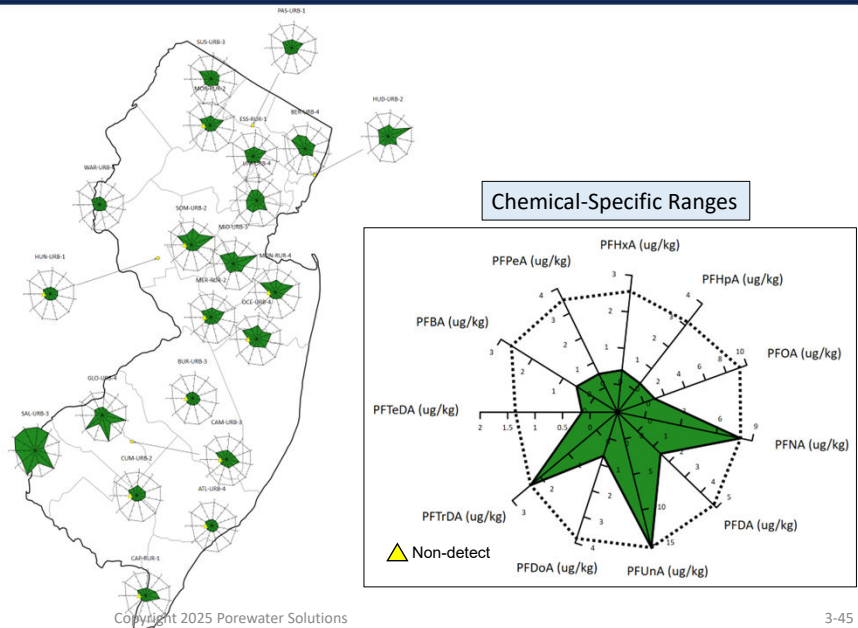
HFPO-DA



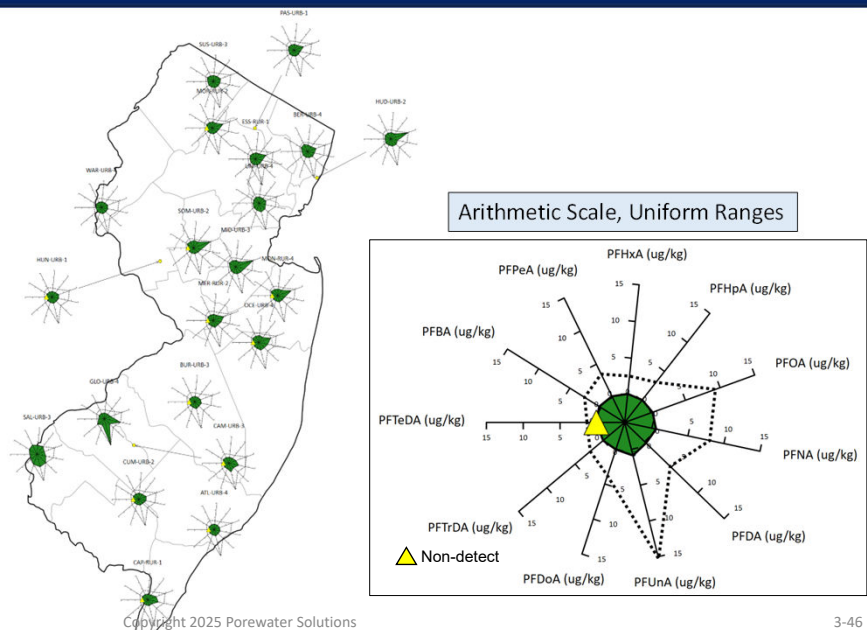
Stacked Bar Map: PFCAs



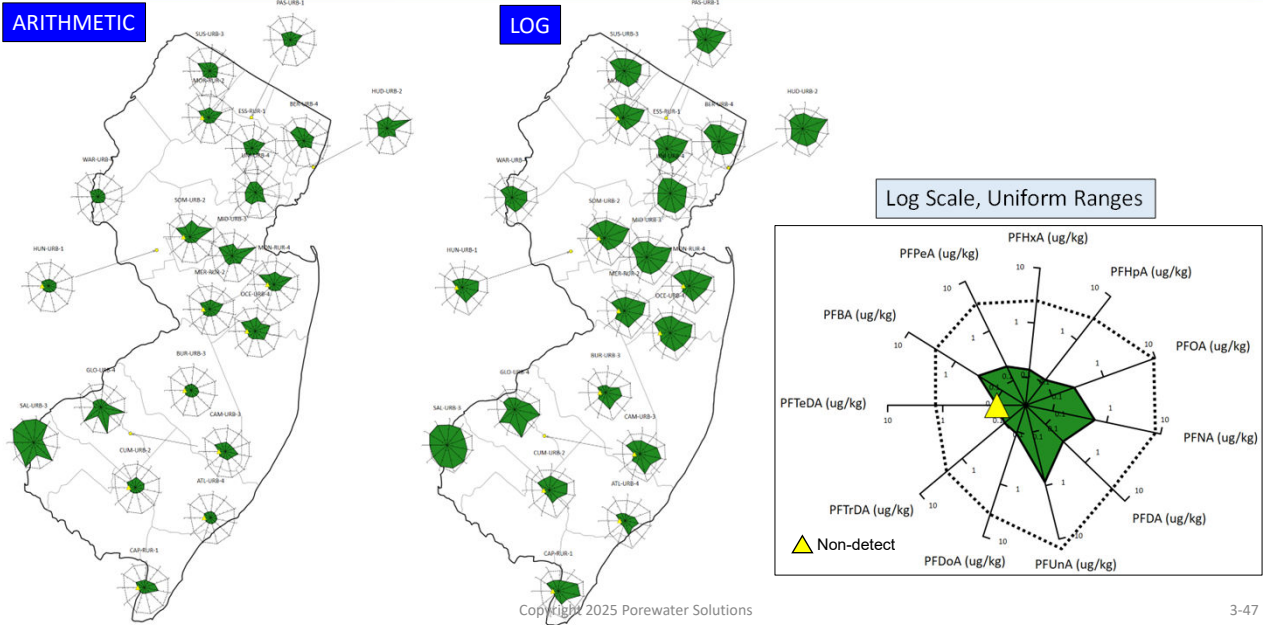
Radial Diagram Map: PFCAs (Arithmetic Scale)



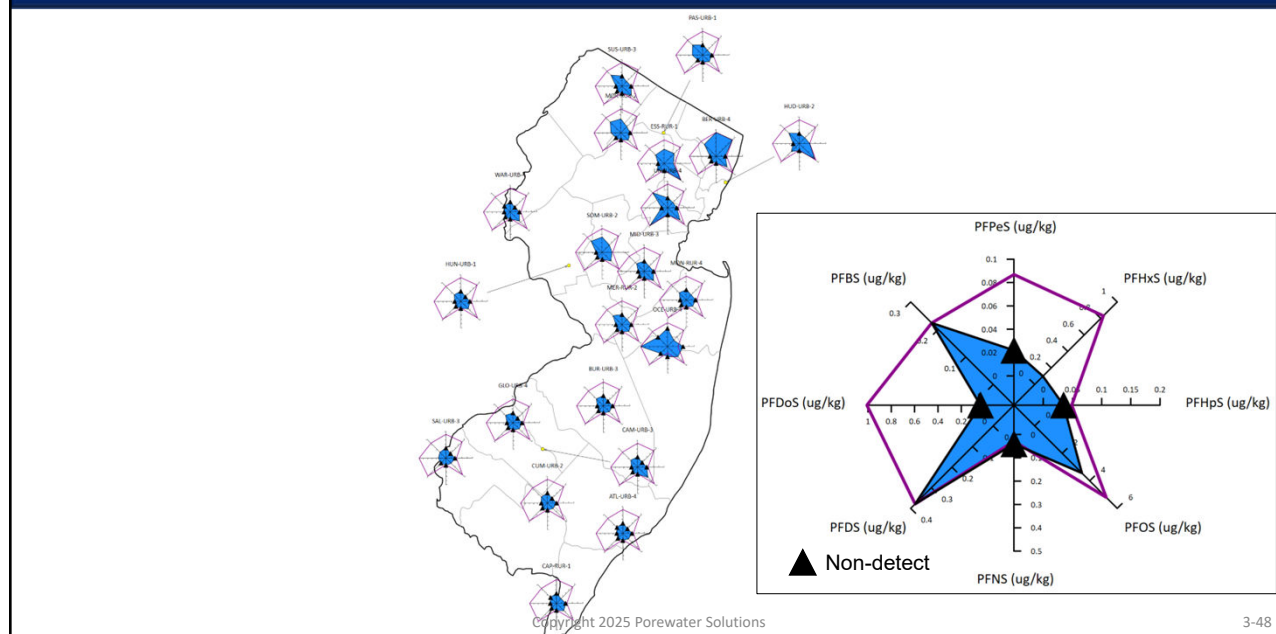
Radial Diagram Map: PFCAs (Uniform Ranges)



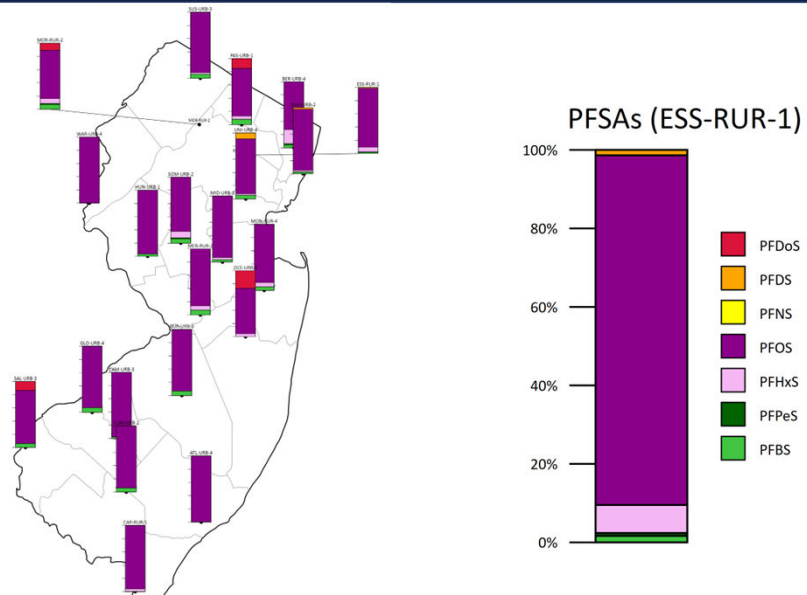
Radial Diagram Map: PFCAs (Log Scale)



Radial Diagram Map: PFSAs (Arithmetic Scale)



Stacked Bar Map: PFSA's



Copyright 2025 Porewater Solutions

3-49

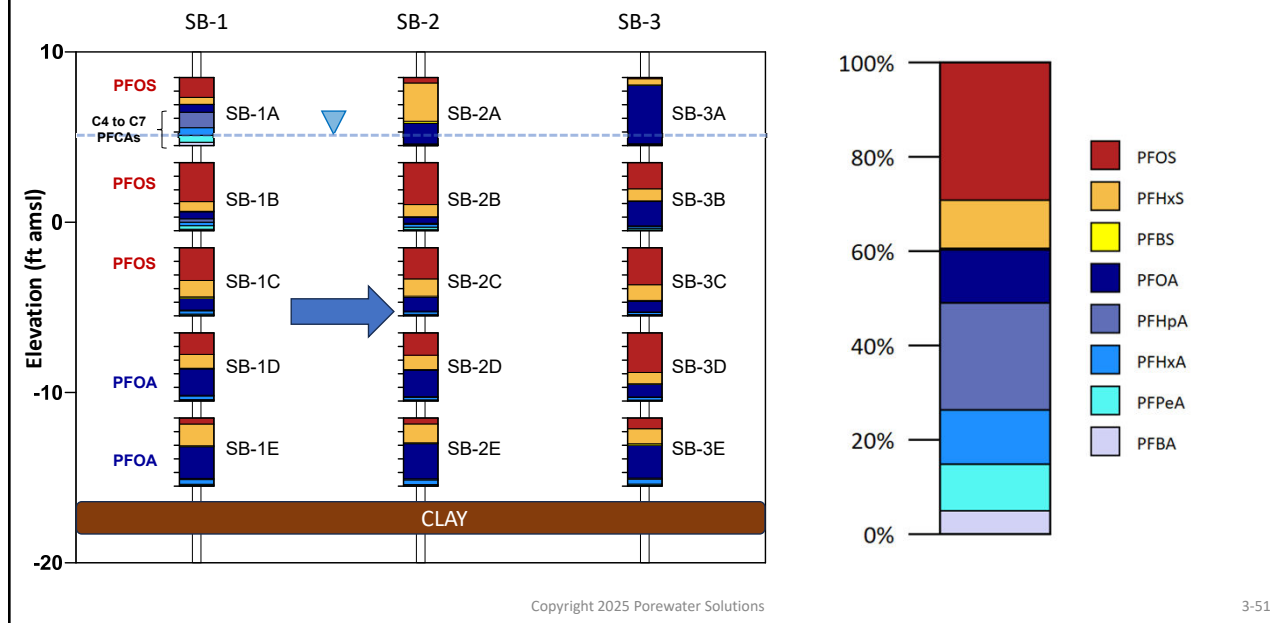
Other Chemical Fingerprinting Examples

Section 3.4

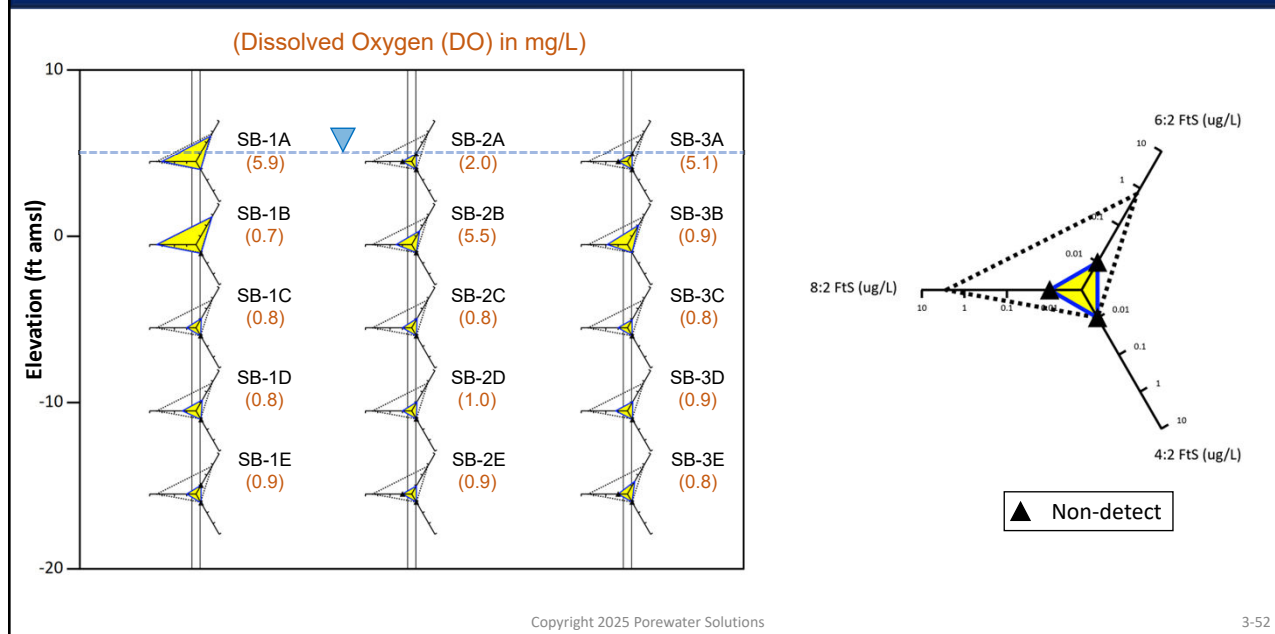
Copyright 2025 Porewater Solutions

3-50

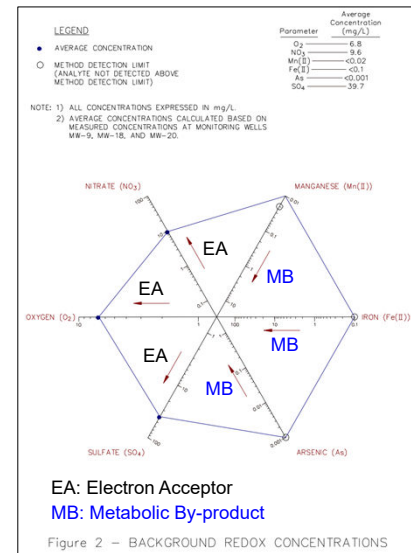
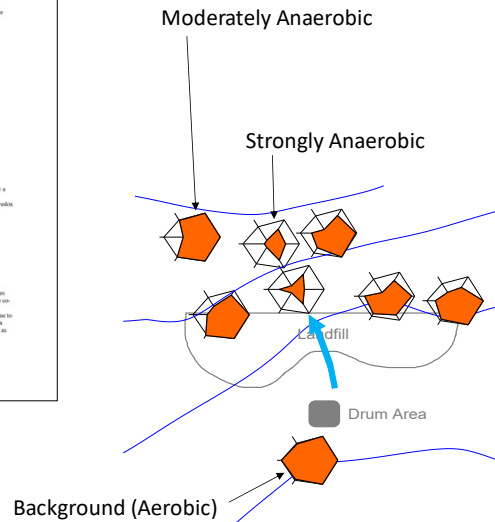
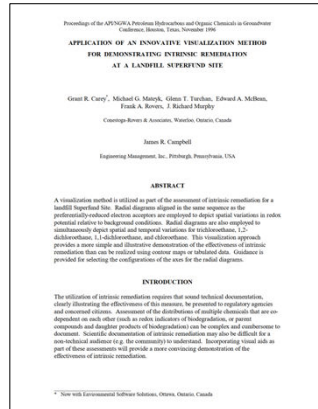
Navy Pre-Pilot Test: PFAAs Stacked Bar Map



Navy Pre-Pilot Test: Precursor Radial Diagrams



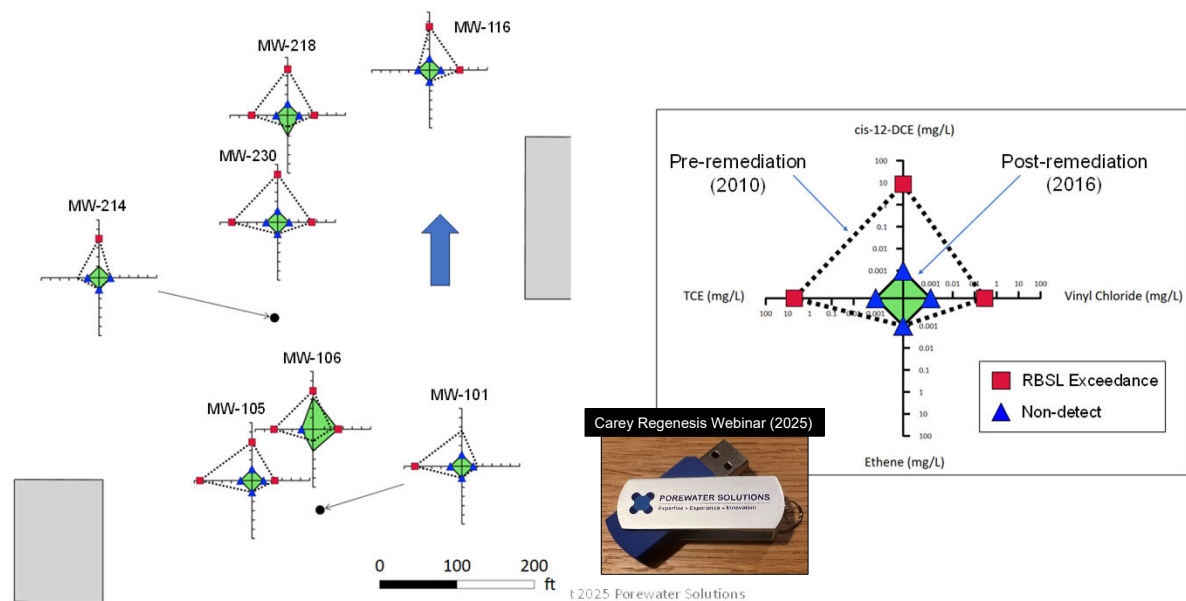
Landfill Superfund Site: Redox Radial Diagrams



Copyright 2025 Porewater Solutions

3-53

Chlorinated Solvent Remediation at Michigan Site



3-54

Conclusions and Recommendations

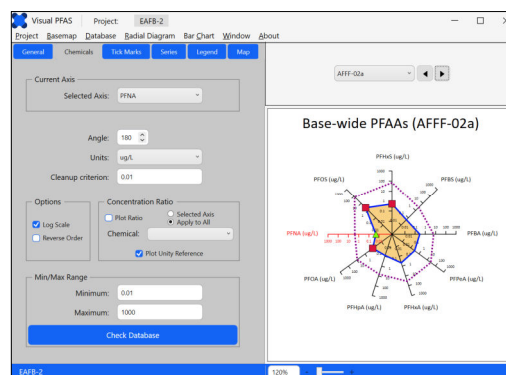
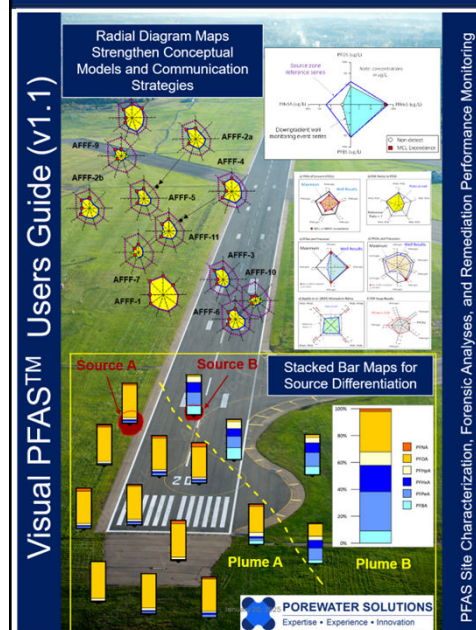
- Pictures are worth a thousand words!
 - Visual aids are the most convincing way to make a case
- Radial diagram and stacked bar maps are powerful tools for visualizing PFAS trends
- Multiple and converging lines of evidence will strengthen forensic assessments
- Differential adsorption only affects a plume in the expanding region
 - Not where the plume is stable



Copyright 2025 Porewater Solutions

3-55

Visual PFAS™ Lite



www.porewater.com/PFAS.html

Email: gcarey@porewater.com

Copyright 2025 Porewater Solutions

3-56

Questions?

Grant R. Carey, Ph.D.

Porewater Solutions
gcarey@porewater.com



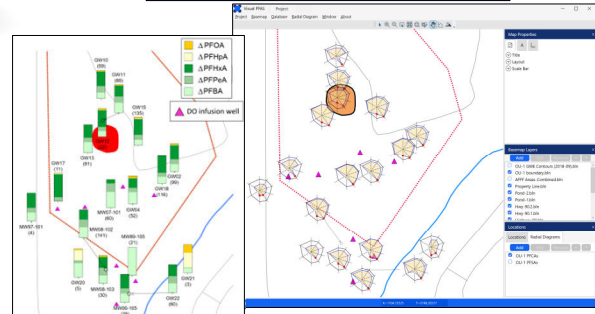
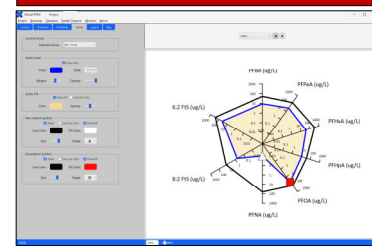
Link to publications:
www.porewater.com/PFAS.html



POREWATER SOLUTIONS

Expertise • Experience • Innovation

www.VisualPFAS.com



Copyright (2025) Porewater Solutions

57

PFAS Transport in the Vadose Zone

October 5, 2025

Copyright (2025) Porewater Solutions

4-1

Section 4 Outline

4.1 Adsorption to Air-Water Interface

4.2 Soil Screening Levels (SSLs)

4.3 Case Study: Ellsworth AFB

- Porewater reproducibility assessment
- Mass discharge based on: a) porewater samples; and b) PFAS-LEACH model

Copyright (2025) Porewater Solutions

4-2

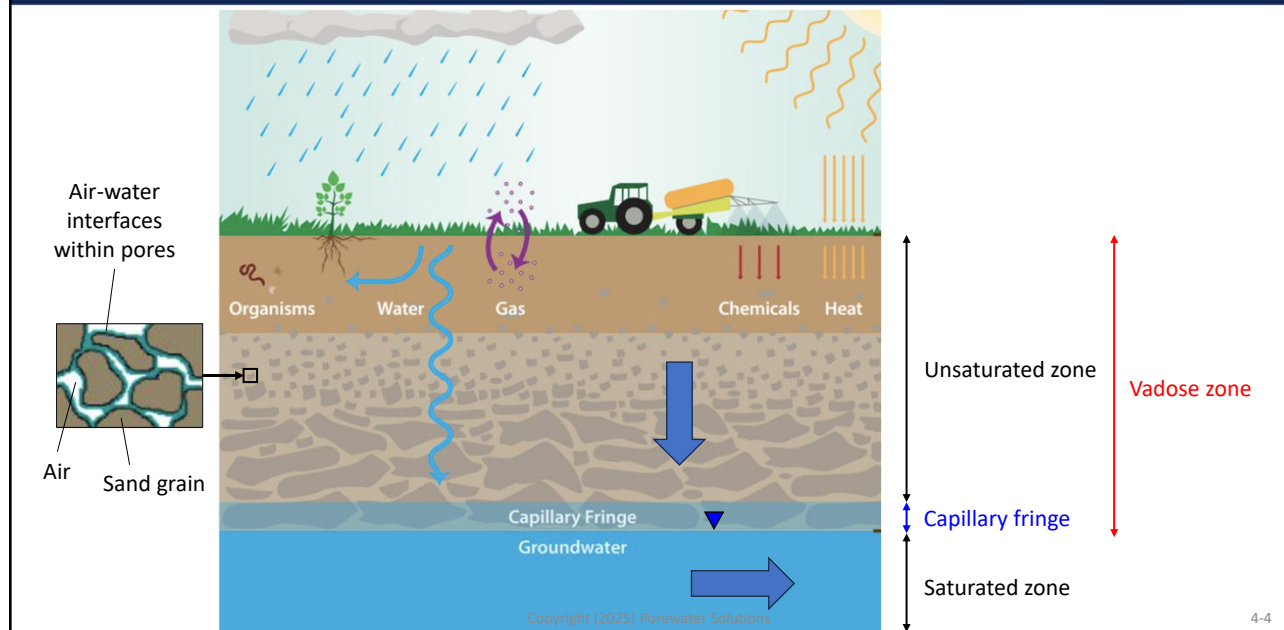
PFAS Adsorption to the Air-Water Interface

Section 4.1

Copyright (2025) Porewater Solutions

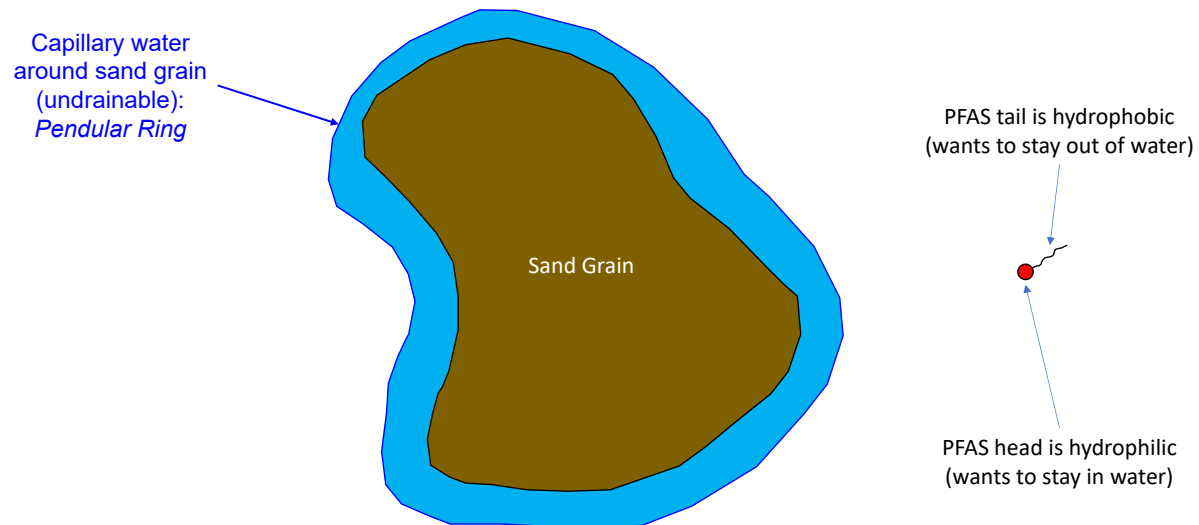
4-3

Vadose Zone Cross-Section



4-4

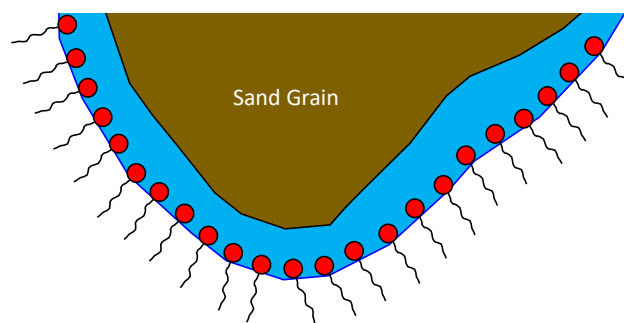
PFAS At Air-Water Interface



Copyright (2025) Porewater Solutions

4-5

PFAS At Air-Water Interface



PFAS surfactant properties cause the molecules to accumulate (adsorb) at air-water interfaces in the vadose zone.

Copyright (2025) Porewater Solutions

4-6

Long-Chain PFAS Adsorb to Air-Water Interfaces

Contents lists available at ScienceDirect

Science of the Total Environment

journal homepage: www.elsevier.com/locate/scitotenv

ELSEVIER

Assessing the potential contributions of additional retention processes to PFAS retardation in the subsurface

Mark L. Brusseau

429 Shantz Bldg, Soil, Water and Environmental Science Department, Hydrology and Atmospheric Sciences Department, School of Earth and Environmental Sciences, University of Arizona, United States

CrossMark

HIGHLIGHTS

- A comprehensive model for PFAS retention in porous media is proposed.
- Adsorption at the air-water interface contributes greatly to PFOA/PFOS retention.
- Adsorption at the NAPL-water interface and NAPL partitioning are also significant.

GRAPHICAL ABSTRACT

Brusseau, 2018

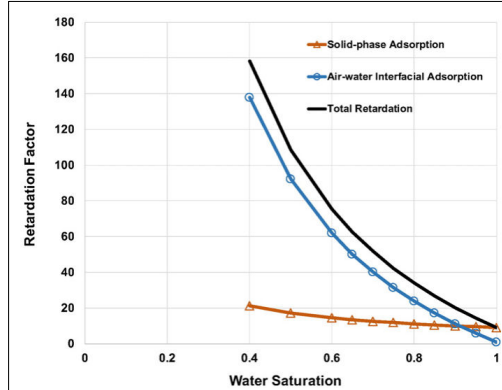


Fig. 2. Impact of water saturation on PFOS retardation factors for solid-phase adsorption, air-water interface adsorption, and the sum of the two (total).

Copyright (2025) Porewater Solutions

4-7

Brusseau and Guo Journal Papers (USB)

Brusseau and Guo (2022)

Chemosphere

PFAS concentrations in soil versus soil porewater: Mass distributions and the impact of adsorption at air-water interfaces

M.L. Brusseau^{a,*}, B. Guo^b

^a Environmental Science Department, The University of Arizona, Tucson, AZ 85721, United States
^b Hydrology and Atmospheric Sciences Department, The University of Arizona, Tucson, AZ 85721, United States

HIGHLIGHTS

- A comprehensive distribution model is developed for PFAS porewater concentration (C_p).
- The ratio between soil concentration (C_s) and C_p is a function of soil and PFAS properties.
- The C_p/C_s may change during long-term leaching due to nonlinear adsorption processes.
- The C_p/C_s changes during infiltration events due to changes in air-water interfacial area.
- Air-water interfacial adsorption has a significant impact on C_p/C_s behavior.

GRAPHICAL ABSTRACT

ARTICLE INFO

Handling Editor: Tom Fisk

Keywords:

PFAS
 Porewater
 Distribution
 Adsorption
 Leaching

ABSTRACT

Determining the risk posed by PFAS leaching from soil to groundwater requires quantification of the magnitude and temporal/spatial variability of PFAS mass discharge from the vadose zone, which is governed in part by the concentrations of PFAS in soil porewater. Porewater concentrations are impacted and excluded by the properties of the PFAS and soil, and multiple transport and fate processes, and site conditions. The objective of this research was to determine the relationship between soil porewater concentrations and soil concentrations, based on a comprehensive model of PFAS mass distribution within a soil sample volume. Measured parameters representing solid-phase sorption and air-water interfacial adsorption are used to illustrate the impact of soil and PFAS properties on the distribution of representative PFAS between soil and soil porewater. Literature data reported for soil and soil porewater concentrations of several PFAS obtained from outdoor leachate experiments are used to test the distribution model. Soil-to-porewater concentration ratios predicted with the model compared very well to the measured concentration ratios. The nondimensional distribution coefficient that describes the distribution of PFAS mass amongst all domains within a soil sample was observed to be a function of PFAS molecular size. Numerical simulations conducted for a model leaching source area were used to illustrate the range in magnitude of soil versus porewater concentrations for representative field conditions. The results of the measured and simulated data are demonstrated the importance of air-water interfacial adsorption for the distribution of the longer-chain PFAS within soil samples. PFAS soil porewater concentrations are anticipated to range from ng/L to ng/L depending upon soil concentrations, which is very dependent upon the nature of the site.

* Corresponding author at: Environmental Science Department, The University of Arizona, Tucson, AZ 85721, United States.
 E-mail address: brusseau@arizona.edu (M.L. Brusseau).

<https://doi.org/10.1016/j.chemosphere.2022.134918>

Received 1 March 2022; Received in revised form 29 April 2022; Accepted 9 May 2022
 Available online 11 May 2022
 0924-6460/© 2022 Elsevier Ltd. All rights reserved.

Brusseau and Guo (2023)

Journal of Hazardous Materials Letters

Revising the EPA dilution-attenuation soil screening model for PFAS

Mark L. Brusseau^{a,*}, Bo Guo^b

^a Environmental Science Department, The University of Arizona, Tucson, AZ 85721, USA
^b Hydrology and Atmospheric Sciences Department, The University of Arizona, Tucson, AZ 85721, USA

ARTICLE INFO

Keywords:

PFAS
 Leaching
 Transport and fate
 Soil contamination

ABSTRACT

For polychlorinated aromatic hydrocarbons (PAHs) have been shown to be ubiquitous in the environment, and one issue of critical concern is the leaching of PAHs from soil to groundwater. The risk posed by contaminants present in soil is often assessed in terms of the anticipated impact to groundwater through the determination of soil screening levels (SSLs). The U.S. Environmental Protection Agency (EPA) established a soil screening model for determining SSLs. However, the model does not consider the unique retention properties of PFAS and, consequently, the SSLs calculated with the model may not represent the actual levels that are protective of groundwater quality. The objective of this work is to revise the standard EPA SSL model to reflect the unique properties and associated retention behavior of PFAS. Specifically, the distribution parameter and to correct soil and groundwater concentrations to soil concentrations is critical to account for adsorption at the air-water interface. Example calculations conducted for PFOA and PFOS illustrate the conserving SSLs obtained with the revised and standard models. A comparison of distribution parameters calculated for a series of PFAS of different chain length shows that the significance of air-water interfacial adsorption can vary greatly as a function of the specific PFAS. Therefore, the difference between SSLs calculated with the revised versus standard models will vary as a function of the specific PFAS, with greater differences typically observed for longer-chain PFAS. It is anticipated that this revised model will be useful for developing improved SSLs that can be used to reduce site investigations and management for PFAS-contaminated sites.

Impact: The widely used EPA SSL model is revised for PFAS applications to account for adsorption at the air-water interface.

Introduction

Recent meta-analysis of field investigations have determined that the vadose zone is a primary reservoir of per and polyfluorinated substances (PFAS) at many PFAS-impacted sites (Lichtenberg et al., 2021; Brusseau et al., 2022). A primary concern for these sites is the leaching of PFAS through the vadose zone to groundwater, and the subsequent impairment of groundwater quality and associated potential risks to human health. The risk posed by contaminants present in the vadose zone is often assessed in terms of the anticipated impact to groundwater. An initial assessment of this risk is typically conducted by computing measured soil concentrations to soil screening levels (SSLs) that are established to be protective of groundwater quality. It is important to note that SSLs are not cleanup standards (EPA, 1996a, 1996b, 1996c). The U.S. Environmental Protection Agency (EPA) established a soil screening guidance in 1996 as a means to develop SSLs (EPA, 1996a, 1996b, 1996c). The SSL is defined as the concentration of contaminants in soil that is determined to be protective of human exposure via a specified exposure pathway. For example, the methodology for calculating SSLs for the migration-to-groundwater pathway was developed to identify concentrations in soil that have the potential to contaminate groundwater. SSLs are risk-based concentrations derived from equations combining exposure information with EPA toxicity data. The exposure information refers to the exposure pathway selected for assessment (such as migration to groundwater) and to the soil concentrations present at the site. The toxicity data refers to the standard used to set the target concentration for the relevant medium, such as a maximum contaminant level used to establish the target groundwater concentration for the migration-to-groundwater pathway.

The primary purpose of the EPA SSL approach is to conserve resources by identifying and targeting the sites that pose the greatest concern and therefore warrant further investigation. It is designed for use during the early stages of site investigation, when there is typically limited information about subsurface properties and conditions. The SSL

Copyright (2025) Porewater Solutions

4-8

Retardation Coefficient (R)

R = Retardation coefficient (dimensionless)
 K_{oc} = organic carbon partitioning coefficient (L/kg)
 f_{oc} = fraction of organic carbon content (g/g)
 ρ_b = dry bulk density (kg/L)
 θ_w = water-filled porosity (m³/m³)
 K_{aw} = air-water interfacial adsorption coefficient (cm³/cm²)
 A_{aw} = air-water interfacial area (cm²/cm³)

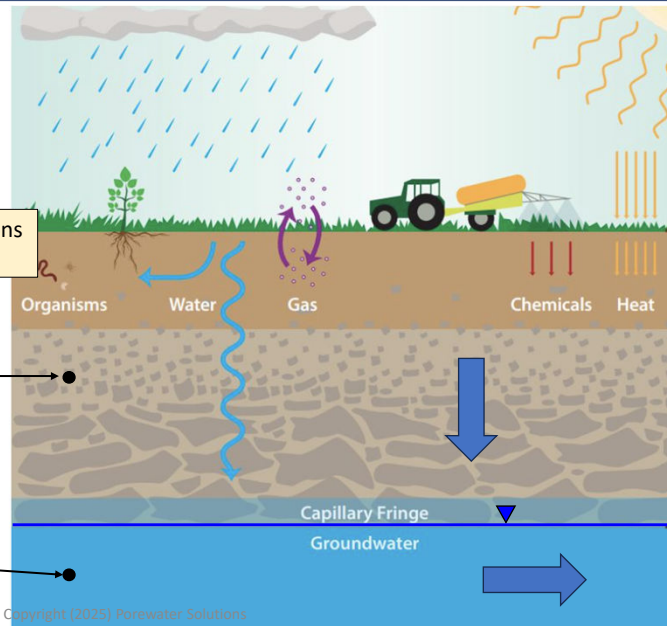
Minimum f_{oc} to account for electrostatic interactions
 e.g., $f_{oc} = 0.1\% = 0.001$ g/g

Unsaturated Zone

$$R = 1 + \frac{\rho_b}{\theta_w} K_{oc} f_{oc} + \frac{K_{aw} A_{aw}}{\theta_w}$$

Saturated Zone

$$R = 1 + \frac{\rho_b}{\theta_w} K_{oc} f_{oc}$$



Copyright (2025) Porewater Solutions

4-9

PFAS Kaw Values

	PFAS	K_{aw} (cm)
C4	PFBA	0.00003
C6	PFHxA	0.0002
C8	PFOA	0.003
C9	PFNA	0.014
C10	PFDA	0.07
C11	PFUnDA	0.128
C13	PFTTrDA	0.26
C4	PFBS	0.00017
C8	PFOS	0.05
	Data Source	Brusseau et al. (2021)



Copyright (2025) Porewater Solutions

4-10

PFAS-LEACH Model (2025)

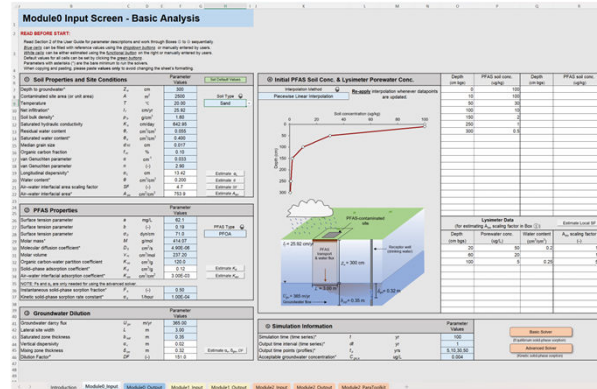


User Guide: Excel tool for Tiers 3 and 4 models of PFAS-LEACH (PFAS-LEACH-Analytical and PFAS-LEACH-DAF)

Version 1.0

M. Ma, J. Smith, M. L. Brusseau, and B. Guo
University of Arizona

October 1, 2025



POINT OF CONTACT

Bo Guo, Ph.D.

Principal Investigator
University of Arizona
Phone: (520) 626-9971

Copyright (2025) Porewater Solutions

4-11

Estimating A_{aw} Using PFAS-LEACH Model

Module0 Input Screen - Basic Analysis

READ BEFORE START:

Read Section 2 of the User Guide for parameter descriptions and work through Boxes ① to ⑤ sequentially. **Blue cells** can be filled with reference values using the **dropdown buttons** or manually entered by users. **White cells** can be either estimated using the **functional button** on the right or manually entered by users. Default values for all cells can be set by clicking the **green buttons**. Parameters with asterisks (*) are the bare minimum to run the solvers. When copying and pasting, please paste **values only** to avoid changing the sheet's formatting.

① Soil Properties and Site Conditions			Parameter Values	Set Default Values
Depth to groundwater*	Z_w	cm	300	
Contaminated site area (or unit area)	A	m^2	2500	
Temperature	T	$^{\circ}C$	20.00	
Net infiltration*	I_f	cm/yr	25.92	
Soil bulk density*	ρ_b	g/cm^3	1.60	
Saturated hydraulic conductivity	K_s	cm/day	642.95	
Residual water content	θ_r	cm^3/cm^3	0.055	
Saturated water content*	θ_s	cm^3/cm^3	0.400	
Median grain size	d_{50}	cm	0.017	
Organic carbon fraction	f_{oc}	%	0.10	
van Genuchten parameter	α	cm^{-1}	0.033	
van Genuchten parameter	n	(-)	2.90	
Longitudinal dispersivity*	α_L	cm	13.42	
Water content*	θ	cm^3/cm^3	0.200	
Air-water interfacial area scaling factor	SF	(-)	5.0	
Air-water interfacial area*	A_{aw}	cm^2/cm^3	366.8	

1. Select soil type

Enter foc as 0.1%, not 0.001 g/g

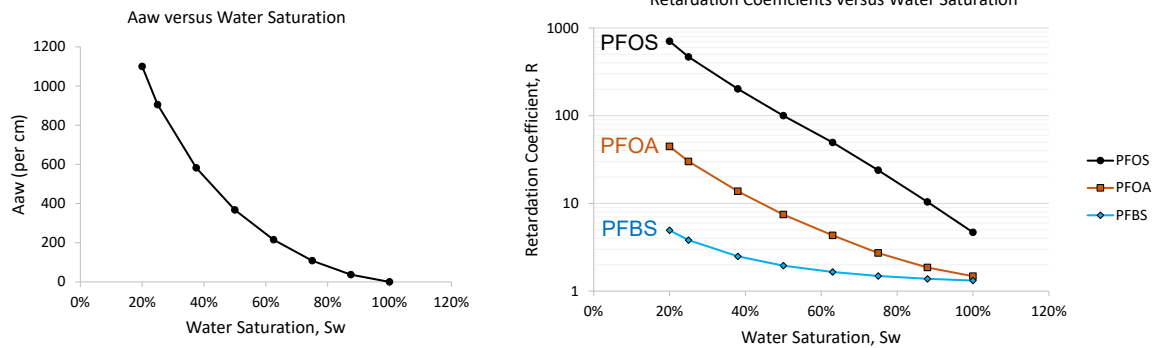
2. Enter site-specific properties

3. Enter water porosity ($S_w = 50\%$)4. Click *Estimate SF* (scaling factor)5. Click *Estimate A_{aw}*

Copyright (2025) Porewater Solutions

4-12

Influence of Water Saturation



$$S_w = \frac{\text{Water Porosity}}{\text{Total Porosity}}$$

Copyright (2025) Porewater Solutions

4-13

Rain Events

- In a humid climate, precipitation events can cause a drainage front to infiltration down through the vadose zone
- S_w increases up to 100% in this drainage front
 - During precipitation events this may cause:
 - Air-water interface to collapse
 - PFOS, PFOA retardation coefficients to drop substantially
 - Increased porewater concentrations
 - Short-term increase in mass discharge to water table
- Paved/covered surfaces will avoid this cycle

Copyright (2025) Porewater Solutions

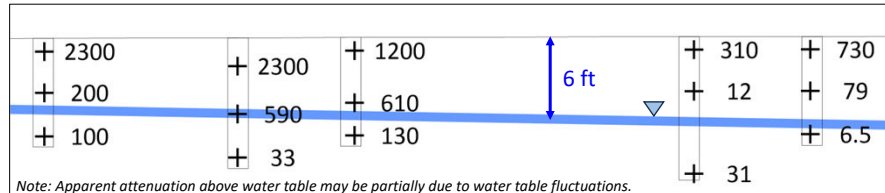
4-14

Case Studies of PFAS Attenuation in Vadose Zone

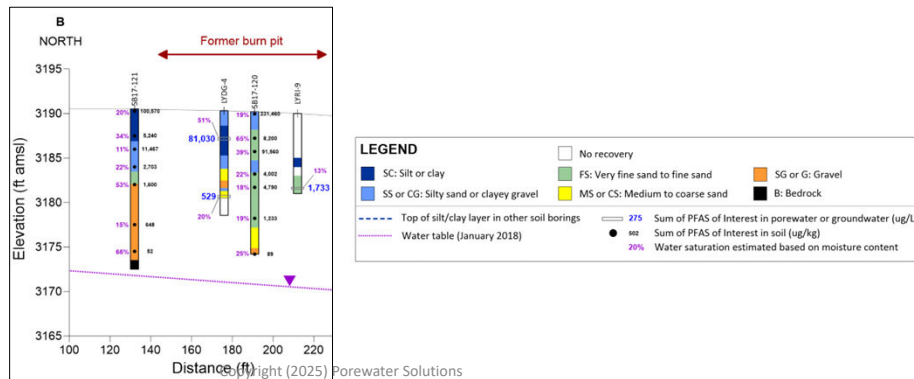
AF_{vz} = Attenuation Factor in vadose zone

+ PFOS soil concentrations in shallow borings (ug/kg)

Humid Climate
(P = 52 inch/year)
 AF_{vz} up to 10x



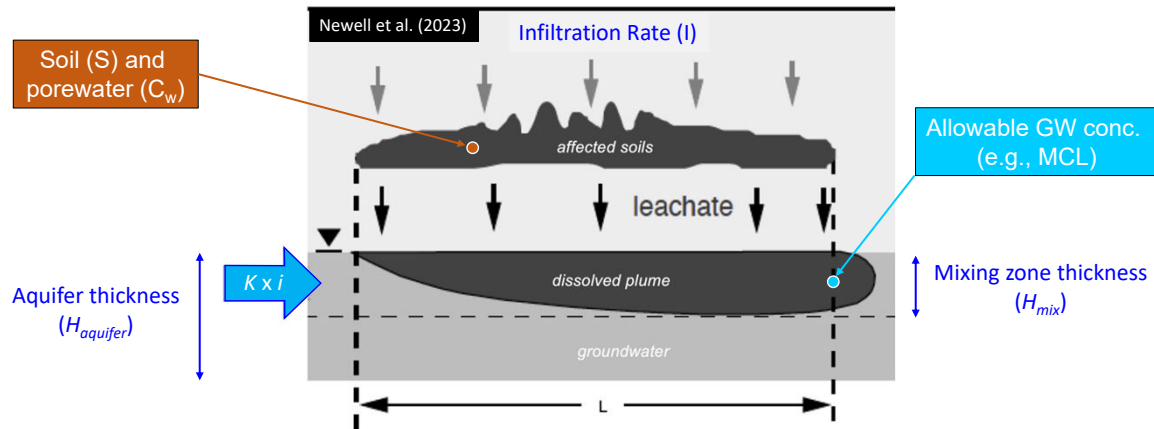
Semi-Arid Climate
(P = 16 inch/year)
 AF_{vz} 2000x



Estimating Soil Screening Levels (SSLs) and Mass Discharge

Section 4.2

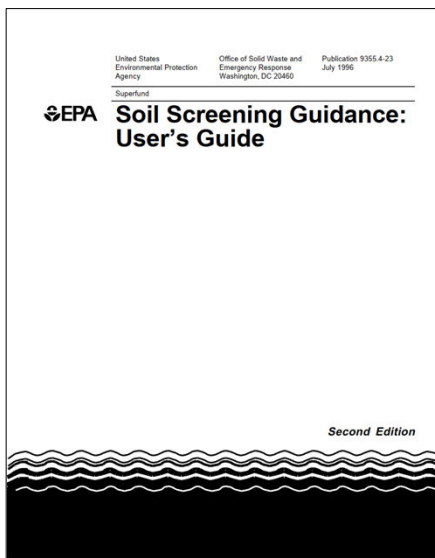
PFAS Migration to Groundwater Exposure Pathway



Copyright (2025) Porewater Solutions

4-17

Equations for Dilution-Attenuation Factor (DAF)



Dilution-Attenuation Factor (DAF)

$$DAF = 1 + \frac{K i H_{mix}}{I L} \quad \text{Default DAF} = 20$$

Mixing Zone Thickness (H_{mix})

$$H_{mix} = \sqrt{0.0112 L^2 + H_{aquifer}} \left[1 - \exp\left(\frac{-L I}{K i H_{aquifer}}\right) \right]$$

K = Hydraulic conductivity (ft/day)

i = Horizontal hydraulic gradient (ft/ft)

I = Infiltration rate (ft/day)

L = Source zone length parallel to groundwater flow (ft)

H_{mix} = Thickness of mixing/dilution zone (ft)

$H_{aquifer}$ = Thickness of aquifer

Copyright (2025) Porewater Solutions

4-18

Estimating Soil Screening Levels

STEP 1: Estimate allowable porewater concentration

1996 EPA Method: Porewater $C_w = GW_{MCL} \times \text{Dilution-Attenuation Factor (DAF)}$

STEP 2: Estimate allowable soil screening level (SSL) concentration

1996 EPA Method: $SSL_{1996} = GW_{MCL} DAF \left[K_{oc} f_{oc} + \frac{\theta_w}{\rho_b} \right]$ * Note: Ignoring PFAS volatilization

Brusseau and Guo (2023)

Tier 4

$$SSL_{2023} = GW_{MCL} DAF \left[K_{oc} f_{oc} + \frac{\theta_w + K_{aw} A_{aw}}{\rho_b} \right]$$

Ignores attenuation with depth in vadose zone

Tier 3

$$SSL_{2023} = AF_{vz} GW_{MCL} DAF \left[K_{oc} f_{oc} + \frac{\theta_w + K_{aw} A_{aw}}{\rho_b} \right]$$

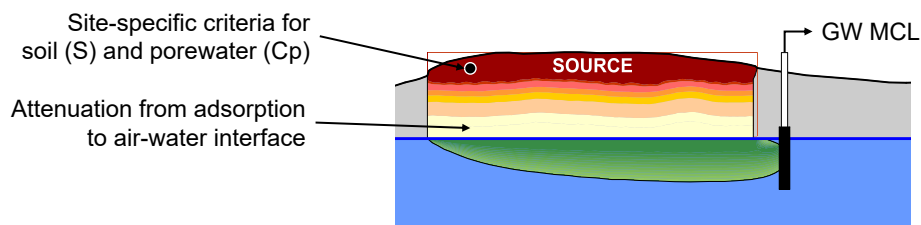
AF_{vz} = attenuation factor in vadose zone

Copyright (2025) Porewater Solutions

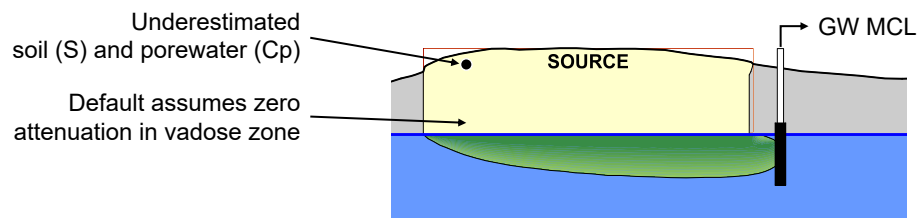
4-19

Site-Specific Soil Cleanup Criteria

Representative Attenuation in Vadose Zone



Default Case: Zero Attenuation in Vadose Zone



Copyright (2025) Porewater Solutions

4-20

Vadose Zone Case Study: Ellsworth AFB

Section 4.3

Copyright (2025) Porewater Solutions

4-21

South Dakota AFB Case Study Acknowledgements



Rita Krebs

Dave Adamson, Ph.D.

Kevin Mumford, Ph.D.
Stephen Brown, Ph.D.

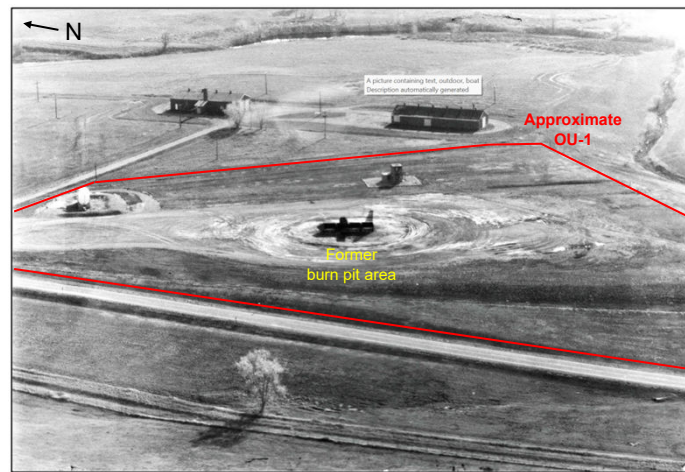
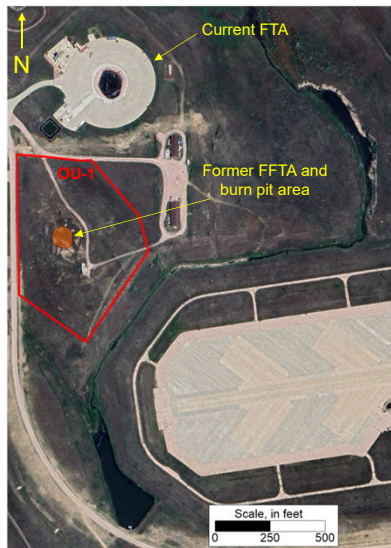
Bo Guo, Ph.D.

Mia Rebeiro-Tunstall
Gabriel Carey
Kiera Rooney
Sabrina Moga

Copyright (2025) Porewater Solutions

4-22

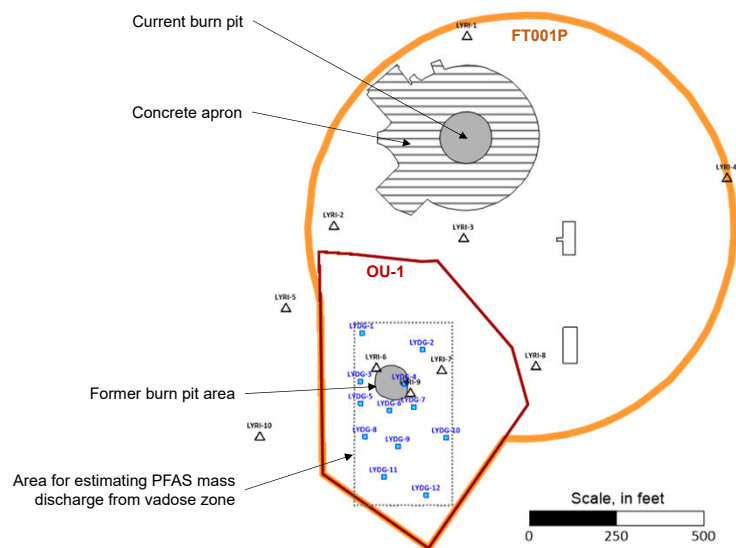
FT001P Area: Former and Current FTAs)



Copyright (2025) Porewater Solutions

4-23

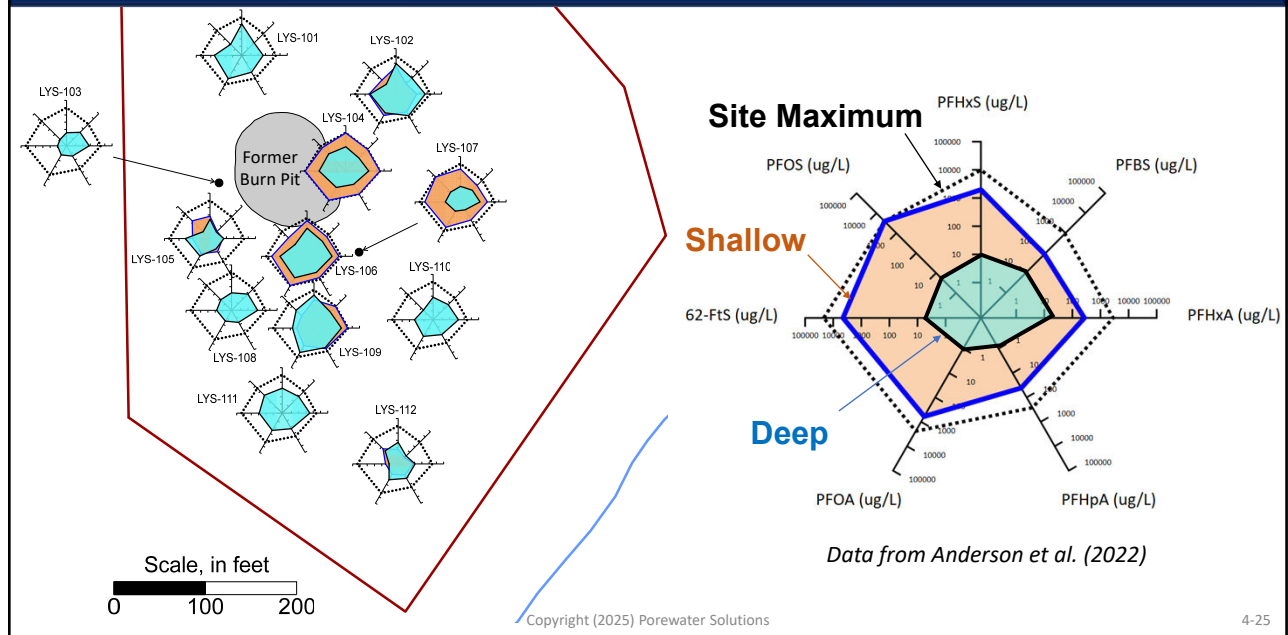
Lysimeter Locations: DGI and RI



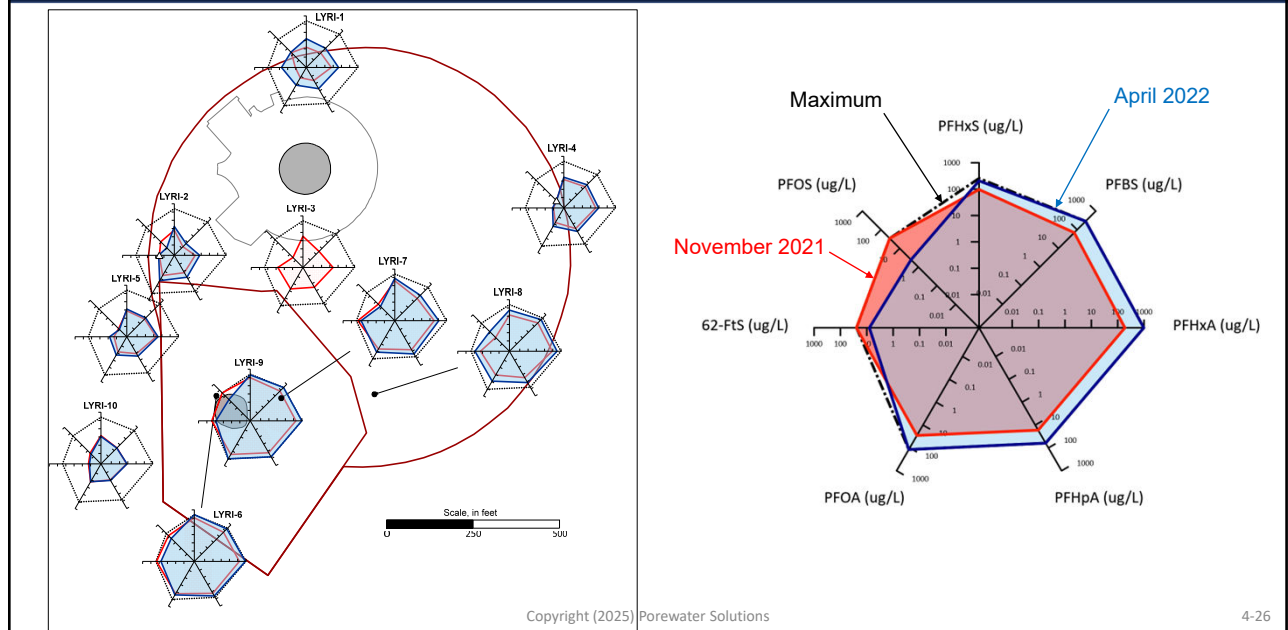
Copyright (2025) Porewater Solutions

4-24

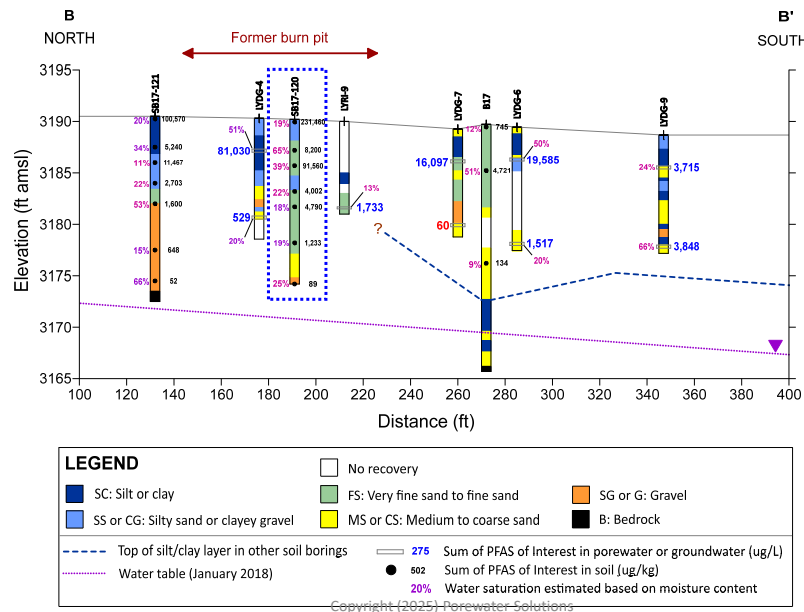
Shallow versus Deep Porewater Concentrations



RI Lysimeters

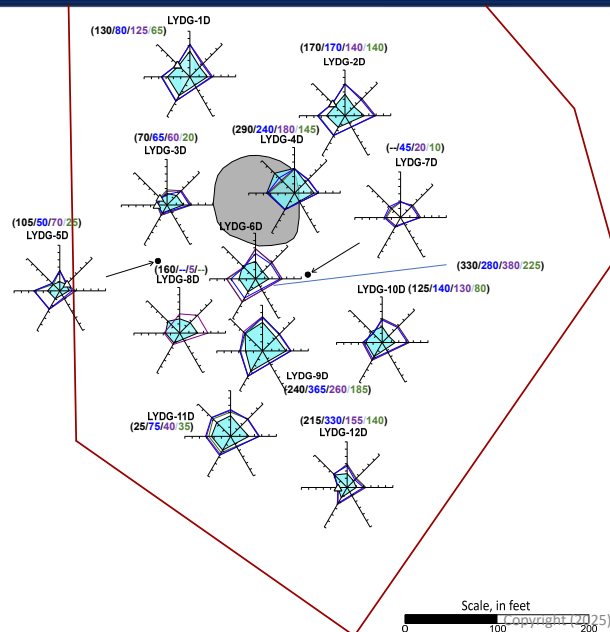


Vadose Zone Cross-Section



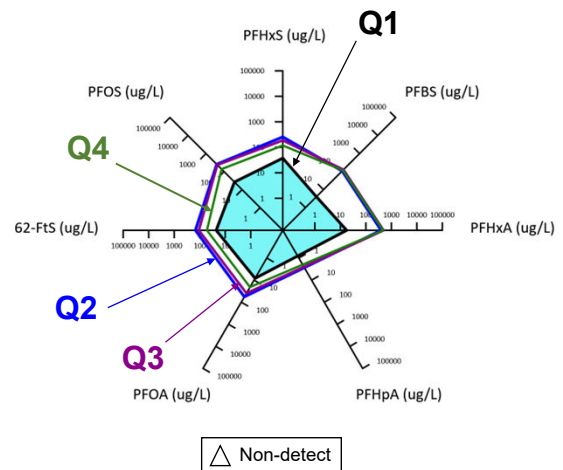
4-27

Checking Porewater Sample Reproducibility



Sample yields (mL) by event:
(25/75/40/35)

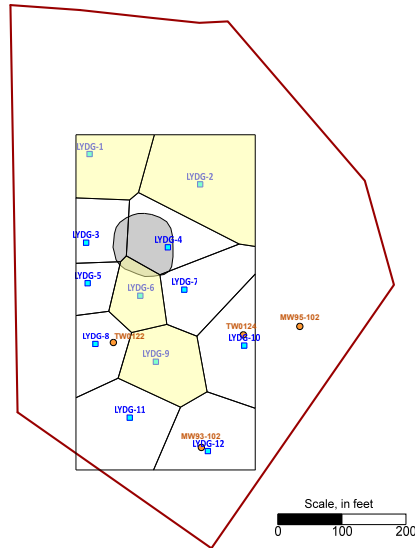
-- Insufficient sample volumetric yield



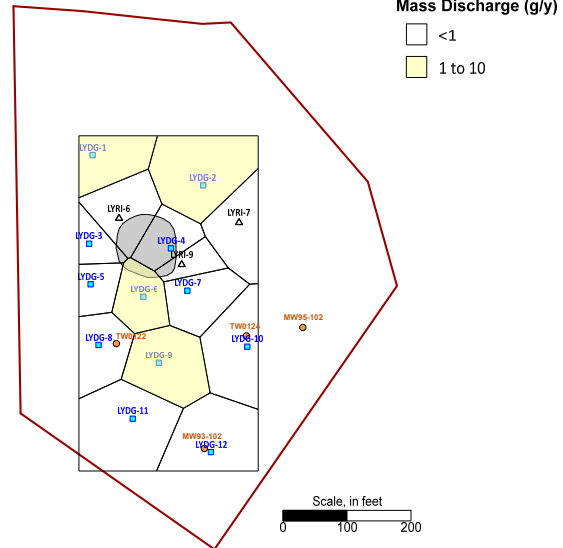
4-28

Theissen Polygons

a) Theissen polygons for DGI lysimeters only



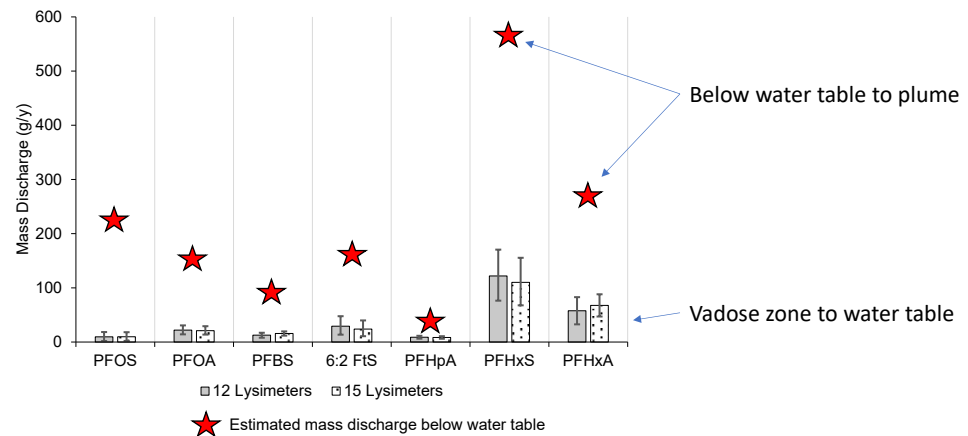
b) Theissen polygons for DGI and RI lysimeters in the FFTA



Copyright (2025) Porewater Solutions

4-29

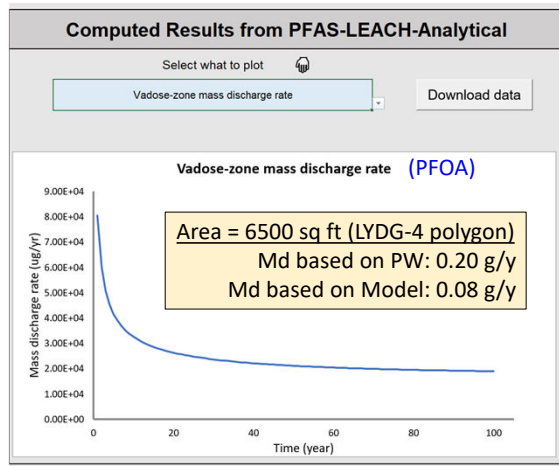
Mass Discharge Estimates



Copyright (2025) Porewater Solutions

4-30

PFAS Leach: Mass Discharge at Former Burn Pit



POINT OF CONTACT

Bo Guo, Ph.D.

Principal Investigator
University of Arizona
Phone: (520) 626-9971



<https://github.com/GuoSFPLab/PFAS-LEACH-Tier-3-4>

Copyright (2025) Porewater Solutions

4-31

Questions?

Grant R. Carey, Ph.D.

Porewater Solutions

gcarey@porewater.com



POREWATER SOLUTIONS

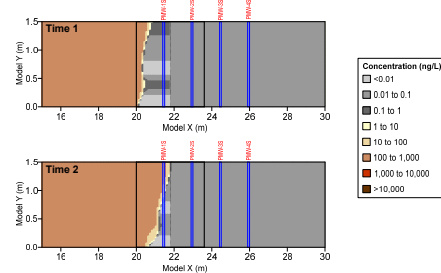
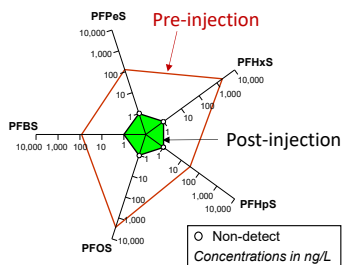
Expertise • Experience • Innovation

Copyright (2025) Porewater Solutions

4-32

Case Studies and Long-Term Strategies for PFAS Remediation Using CAC

Section 5



POREWATER SOLUTIONS
Expertise • Experience • Innovation

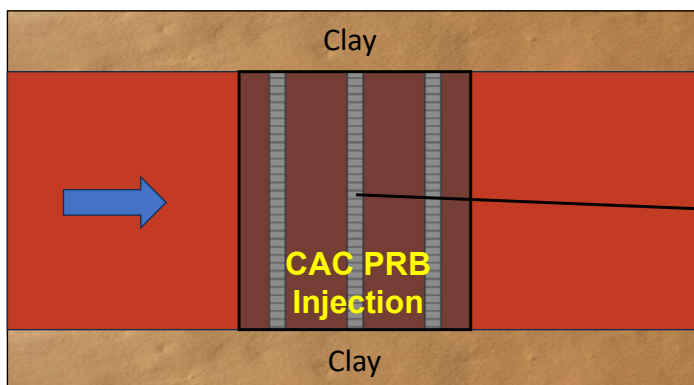
Copyright (2025) Porewater Solutions

5-1

Remediating PFAS With Colloidal Activated Carbon (CAC)

Typical CAC soil concentration in PRBs: 2,000 mg/kg

Fraction of CAC (f_{cac}): 0.2%

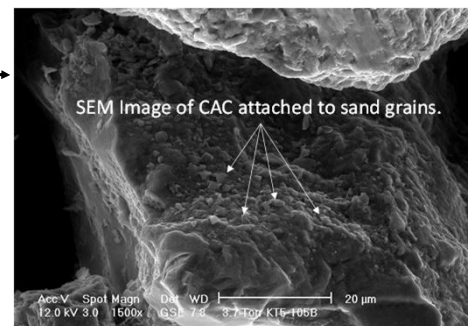


PRB: Permeable Reactive Barrier

Injecting PlumeStop®



Courtesy of Rick McGregor, IRSI

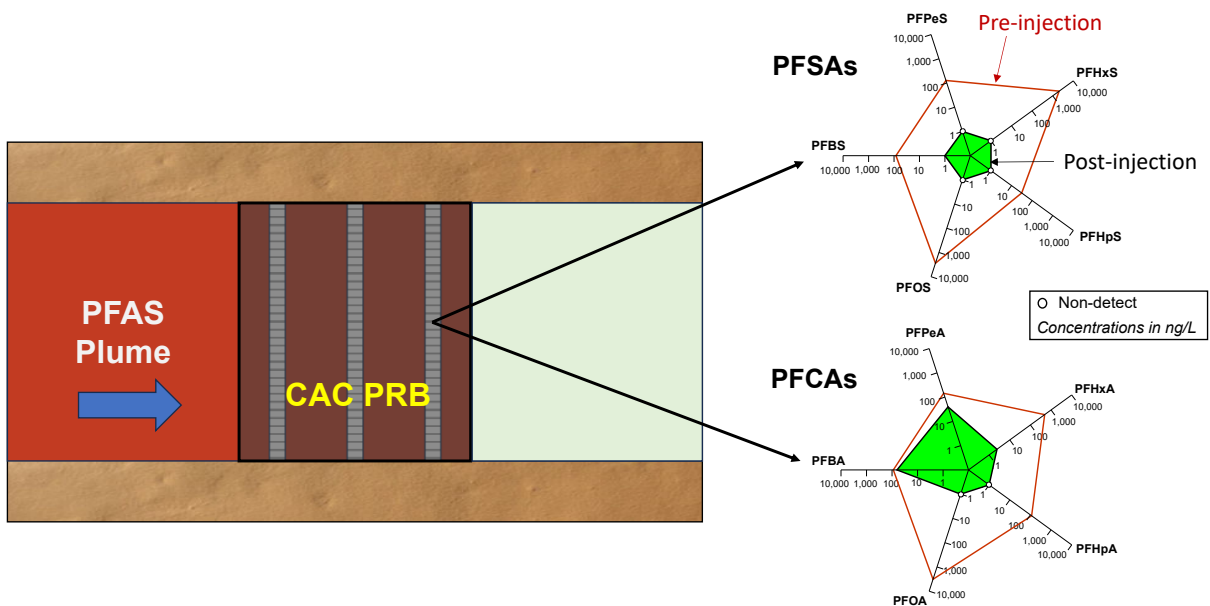


Copyright (2025) Porewater Solutions

Courtesy of REGENESIS

5-2

Remediating PFAS With Colloidal Activated Carbon (CAC)



5-3

Outline

1. Adsorption to Activated Carbon
2. Case Study #1: Navy Pilot Test
3. Case Study #2: Barrier Placement Alternatives
4. Case Study #3: Coastal Site Barrier
5. Long-Term Remediation Strategies

Copyright (2025) Porewater Solutions

5-4

PFAS Adsorption to Activated Carbon

Section 5.1

Copyright (2025) Porewater Solutions

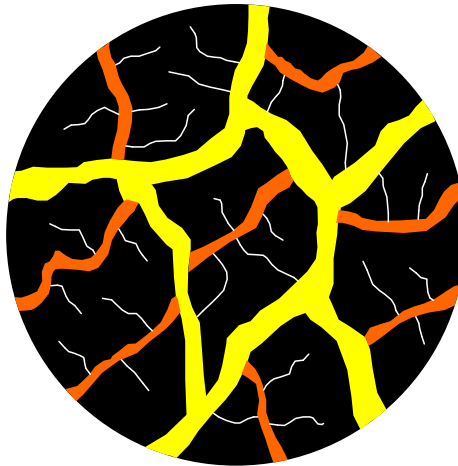
5-5

Activated Carbon

GAC 0.5-1 mm



Granular Activated Carbon (GAC)
0.5 to 1 mm



750 microns

Powdered Activated Carbon (PAC)
0.01 to 0.1 mm



25 microns

Colloidal Activated Carbon (PAC)
0.001 to 0.002 mm

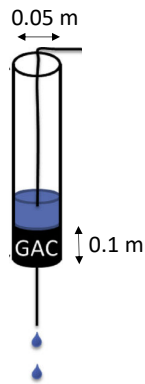


1.5 microns

Copyright (2025) Porewater Solutions

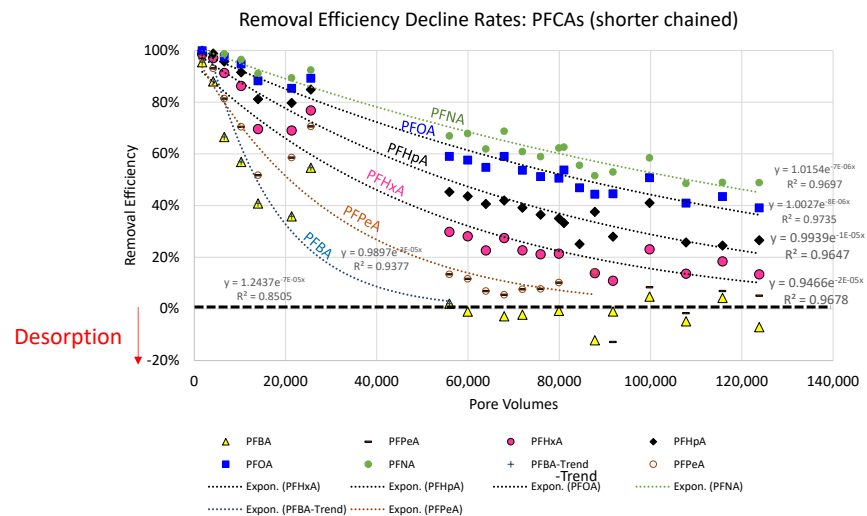
5-6

GAC Bench-Scale Test (Based on McCleaf et al., 2017)



Source: McCleaf et al. (2017)

Velocity = 61 m/day
Retention time = 2 minutes
Length = 0.1 m
Mass flux = 0.002 g/m²/day



Copyright (2025) Porewater Solutions

5-7

NSERC PFAS-PlumeStop® Research Team



Anh Pham, Ph.D.



Seyfollah Gilak



Alannah Taylor



Brent Sleep, Ph.D.



Ezinneifechukwunye Ndubueze



Paul Van Geel, Ph.D.



Mantake Singh



Grant Carey, Ph.D.



Rick McGregor, M.A.Sc., MBA



Paul Erickson, Ph.D.

Copyright (2025) Porewater Solutions

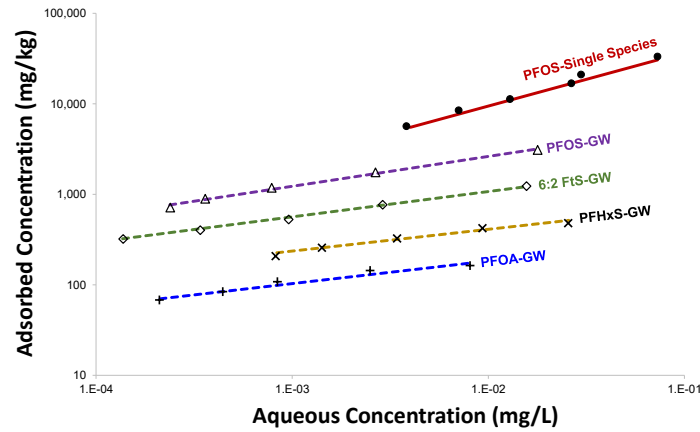
5-8

Evaluating CAC Effectiveness for PFAS Remediation

Carey et al. (2022)



Single Species and Groundwater Sample Isotherms (Freundlich)



Dr. Anh Pham



Seyfollah Gilak Hakimabadi

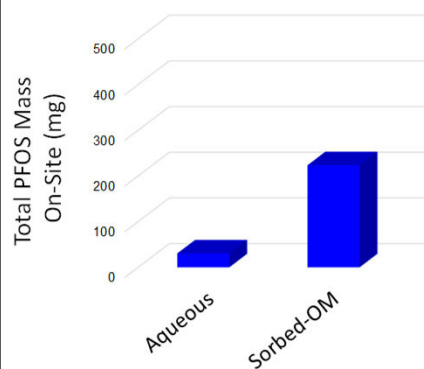
$$\text{Freundlich Isotherm: } S = K_f C_w^a$$

Copyright (2025) Porewater Solutions

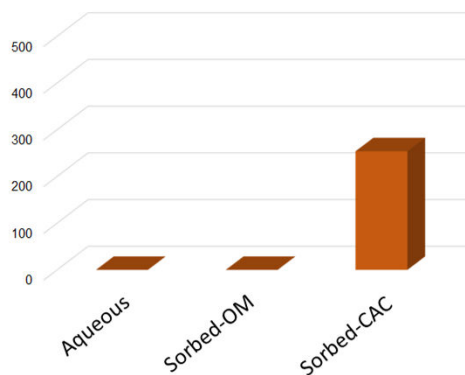
5-9

Modeling CAC Injection: Mass Re-Equilibration

a) Prior to CAC Injection



b) Immediately after CAC Injection



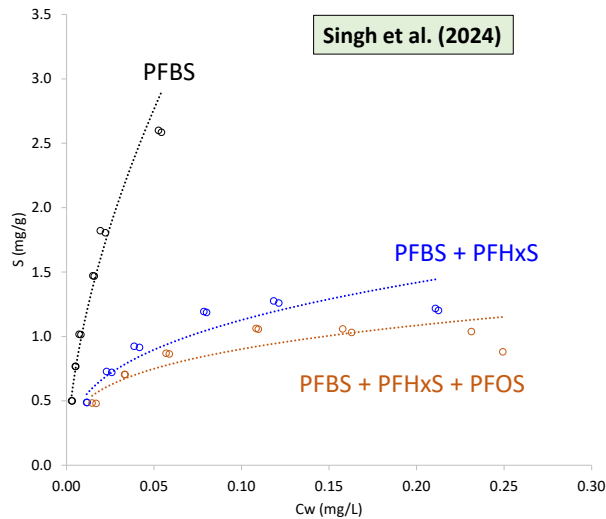
$$C_{adj} = \left[\frac{C_o (\theta + K_{oc} f_{oc} \rho_b)}{K_f f_{cac} \rho_b} \right]^{1/a}$$

C_{adj} = aqueous concentration after PFAS mass has re-equilibrated in the barrier.

Copyright (2025) Porewater Solutions

5-10

Influence of Competition on PFBS Adsorption

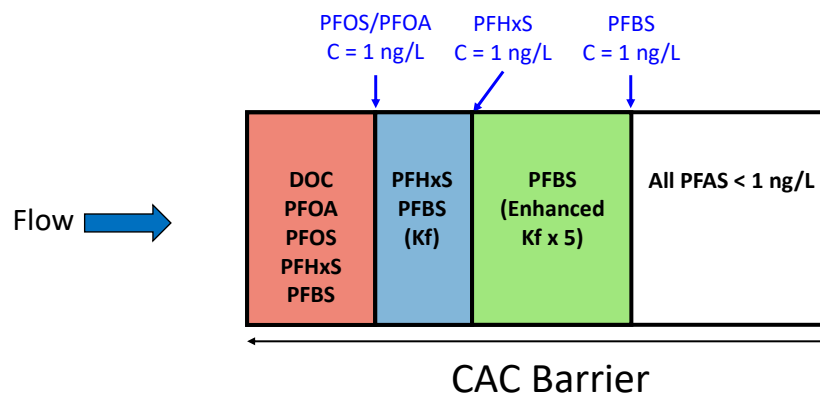


PFBS adsorption decreases substantially in the presence of long-chain PFAS.

Copyright (2025) Porewater Solutions

5-11

Front Positions in CAC Zone with Chromatographic Effect



Chromatographic Separation Effects with ISR Model

- Increased short-chain PFBS sorption in downgradient zone: Longevity 2x to 3x

Copyright (2025) Porewater Solutions

5-12

Model Results

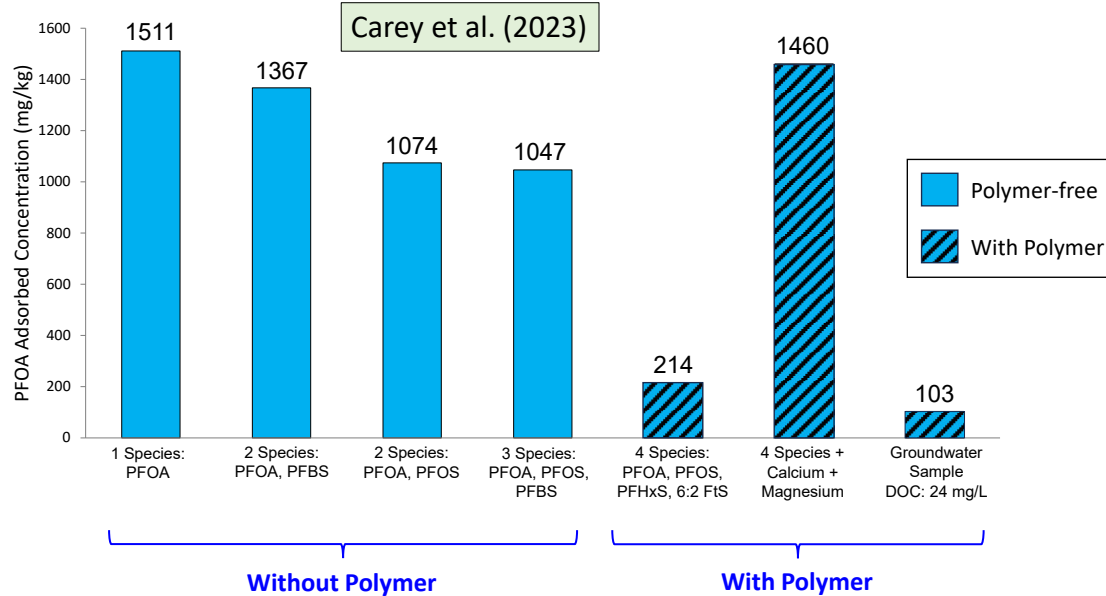
Model Description	CAC Longevity (years)			
	PFOA	PFOS	PFHxS	PFBS
Without chromatographic separation effects (uniform PFBS K _f)	19.5	21.8	18.0	5.6
Enhanced PFBS K _f 5 in advance of long-chain PFAA fronts	19.5	21.8	18.0	13.3

PFBS longevity is increased when model chromatographic separation in the CAC zone.

Copyright (2025) Porewater Solutions

5-13

Effects of Competitive Adsorption (C_w=1 ng/L)



Copyright (2025) Porewater Solutions

5-14

ESTCP ER24-8200: RemFluor Model Development

REMFluor-MD Model

- ◆ New 2nd generation, PFAS-centric version of **established ESTCP REMChlor Model**
- ◆ Mid-complexity groundwater model
- ◆ More sorption codes, less biodeg code
- ◆ Answers “How long, how far” plume questions

Existing REMChlor-MD User Interface

The screenshot displays the 'REMChlor-MD Data Input Screen' with the following sections:

- 1. STARTING INFORMATION:** Site Location and ID, Units (SI, English), and Model Type (Unconsolidated, Fractured Rock/Media).
- 2. MODEL CONFIGURATION:** Cell Size (20, 100, 200, 500, 1000, 2000, 5000, 10000), Model Size (2000, 2000, 2000), X-Direction (200), Y-Direction (200), Z-Direction (3), Observation Well Location (X-Value: 205.0, Y-Value: 23.0, Z-Value: 0.8), Starting Year of Simulation (1970), and Ending Year of Simulation (2070).
- 3. MEDIA CHARACTERISTICS:** Soil Type (Sand, Clay), Hydraulic Conductivity (1.25E+04, 1.00E+00), Porosity (0.33, 0.4), Tortuosity (0.70, 0.70), Transmissivity (1.00E+01, 4.00E+01), and T-Zone Groundwater Darcy Velocity (2.50E+03).
- 4. MATRIX DIFFUSION:** Average Darcy Velocity (1.00E+01), Transmissivity Zone Volume Fraction (4.00E+01), Average Diffusion Length (1.00E+01), and Surface Area of Low-k Interfaces (7.20E+02).
- 5. CONTAMINANTS AND SOURCE TERM:** Parent (PCE, TCE, cis-DCE, Vinyl Chloride), Initial Source Concentration (1.00E+03, 0.00E+00, 0.00E+00, 0.00E+00), Source Mass at Time of Release (1.82E+03, 0.00E+00, 0.00E+00, 0.00E+00), Retardation Factor in T-Zone (2, 2, 2, 2), Retardation Factor in Low-k (2, 2, 2, 2), Source Width (10, 3, 3, 3), Z-Value for Top of Source (0, 3, 3, 3), Z-Value for Bottom of Source (0, 3, 3, 3), and General Molecular Diffusion Coefficient for all Constituents (1.00E-09).

Copyright (2025) Porewater Solutions

5-15

Site-Specific PFAS Adsorption Isotherms

- Site-specific chemistry will influence CAC longevity
 - Relative PFAA concentrations
 - Precursors e.g., 6:2 FtS
 - Natural organic matter (NOM)
 - Other organic chemicals (e.g., DRO)
 - pH, ionic strength, divalent cations
- Site-specific isotherm testing – minor investment to increase confidence in CAC dose and remedy longevity



PFAS-Sorbent Isotherm Testing Services

Booth 211

Contact:

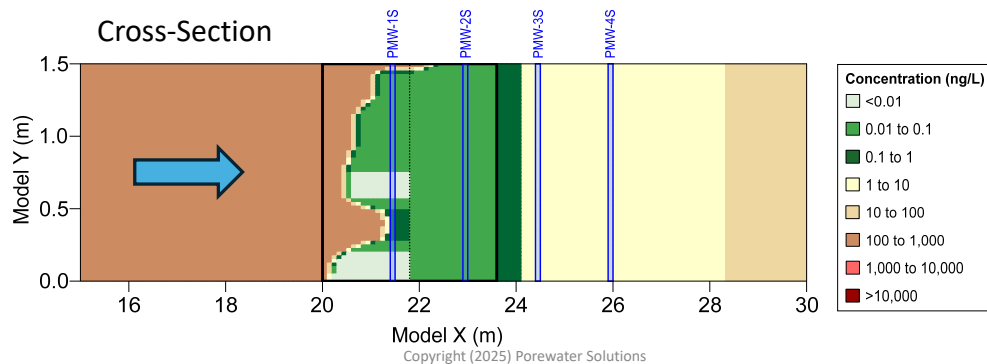
Jeff Roberts

JRoberts@SiREMLab.com

Copyright (2025) Porewater Solutions

5-16

Case Study #1: Navy Pilot Test



5-17

Acknowledgements



**Dr. Paul Hatzinger, Graig Lavorgna,
David Lippincott, Sarah Foxwell**
APTIM



Dr. Anthony Danko
NAVFAC EXWC

NESDI Project 569

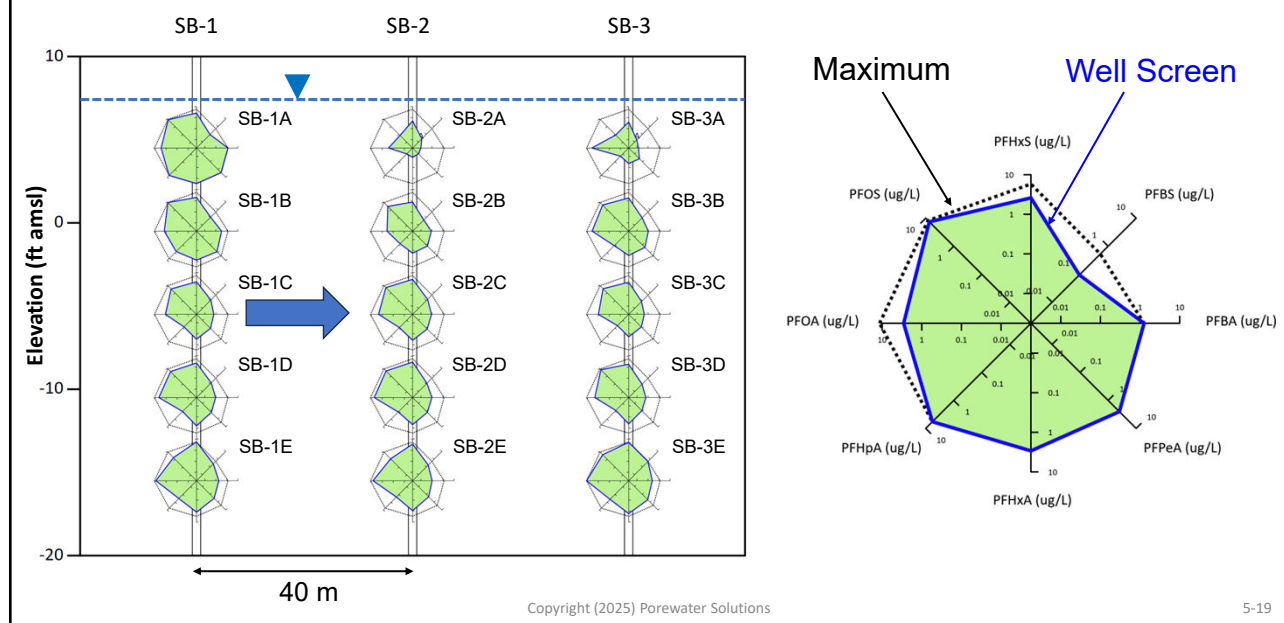


Dr. Brent Sleep
University of Toronto

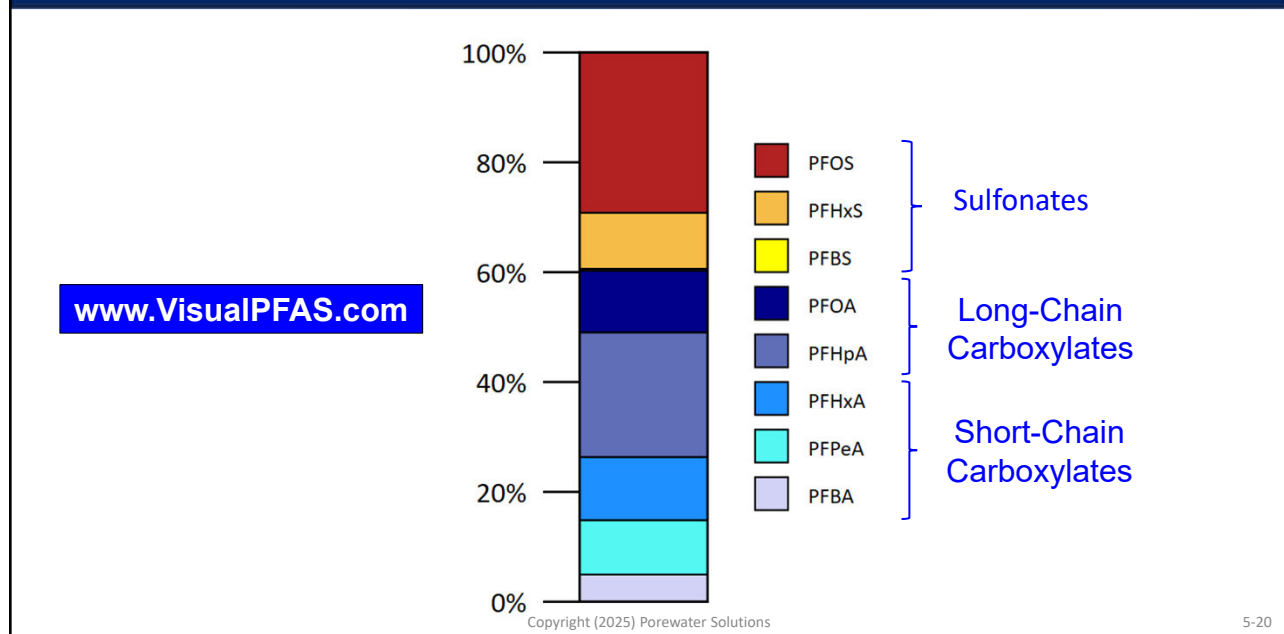
Copyright (2025) Porewater Solutions

5-18

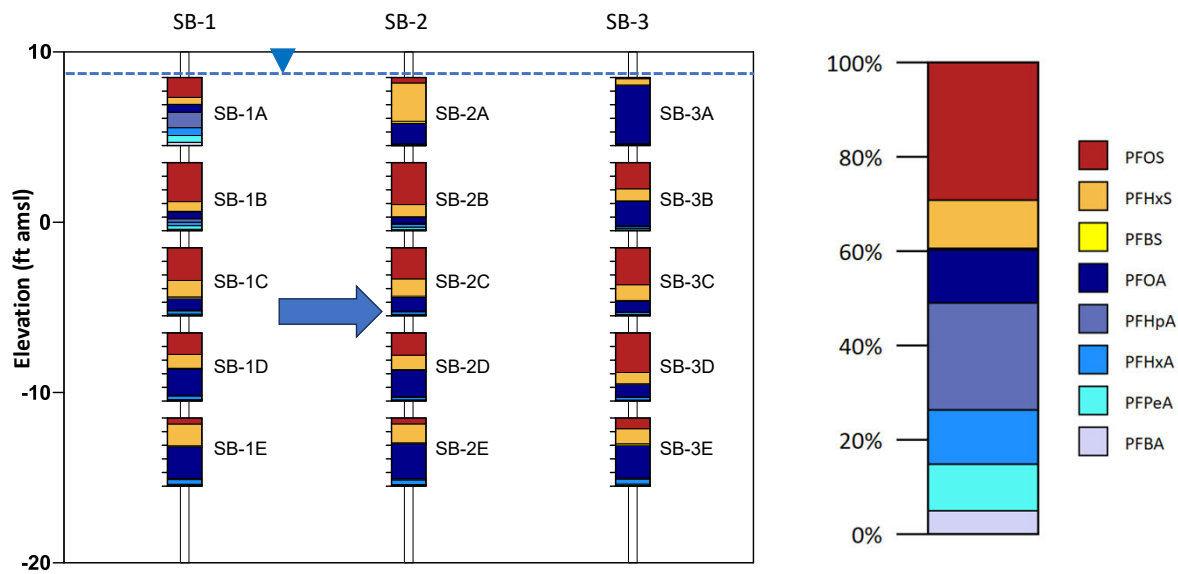
Pre-Remediation PFAS in Groundwater



Pre-Remediation PFAS in Groundwater



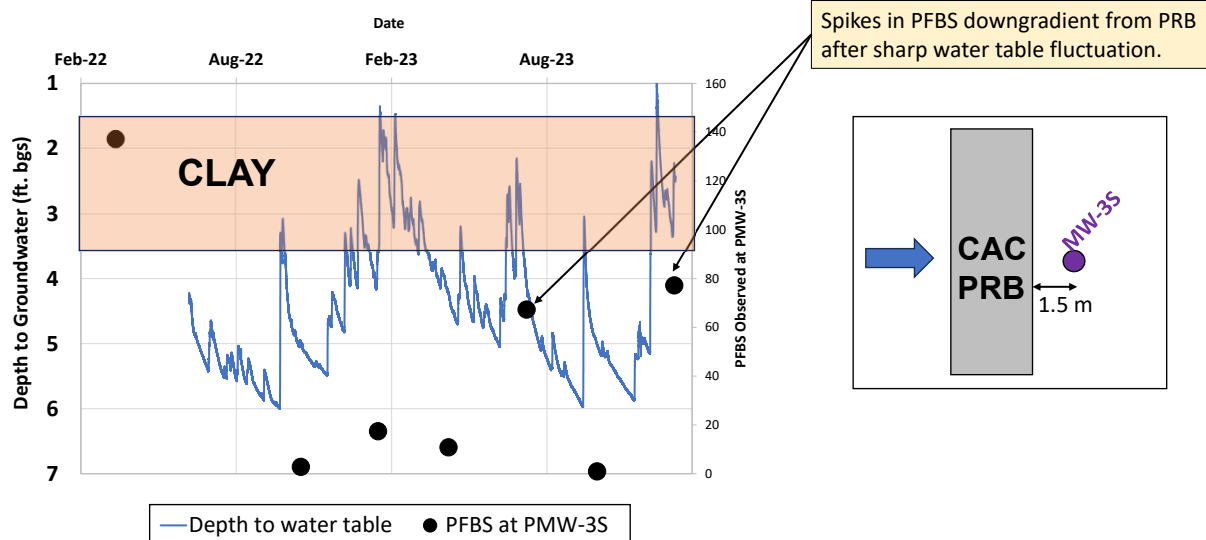
Pre-Remediation PFAS in Groundwater



Copyright (2025) Porewater Solutions

5-21

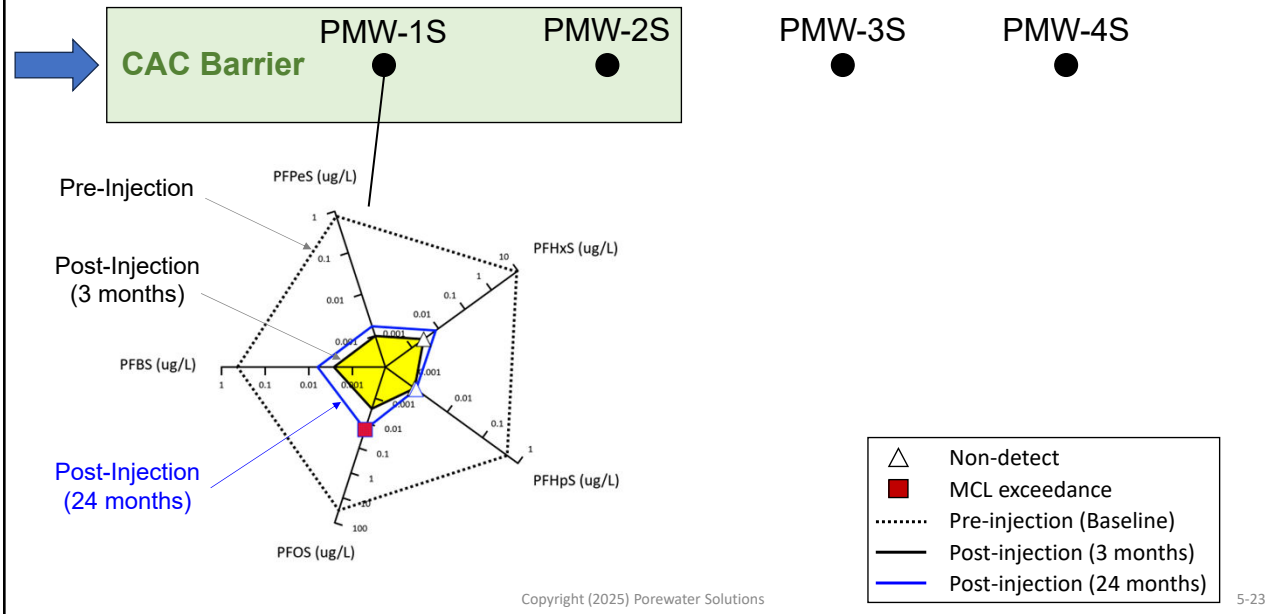
Downgradient Wells Influenced by Water Table



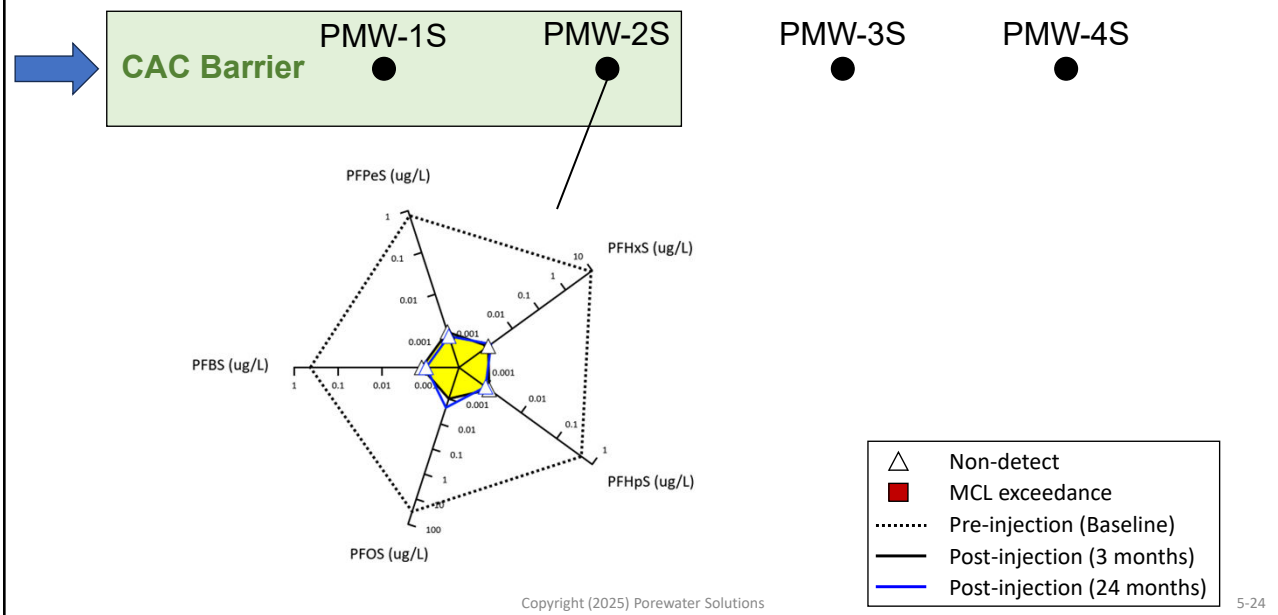
Copyright (2025) Porewater Solutions

5-22

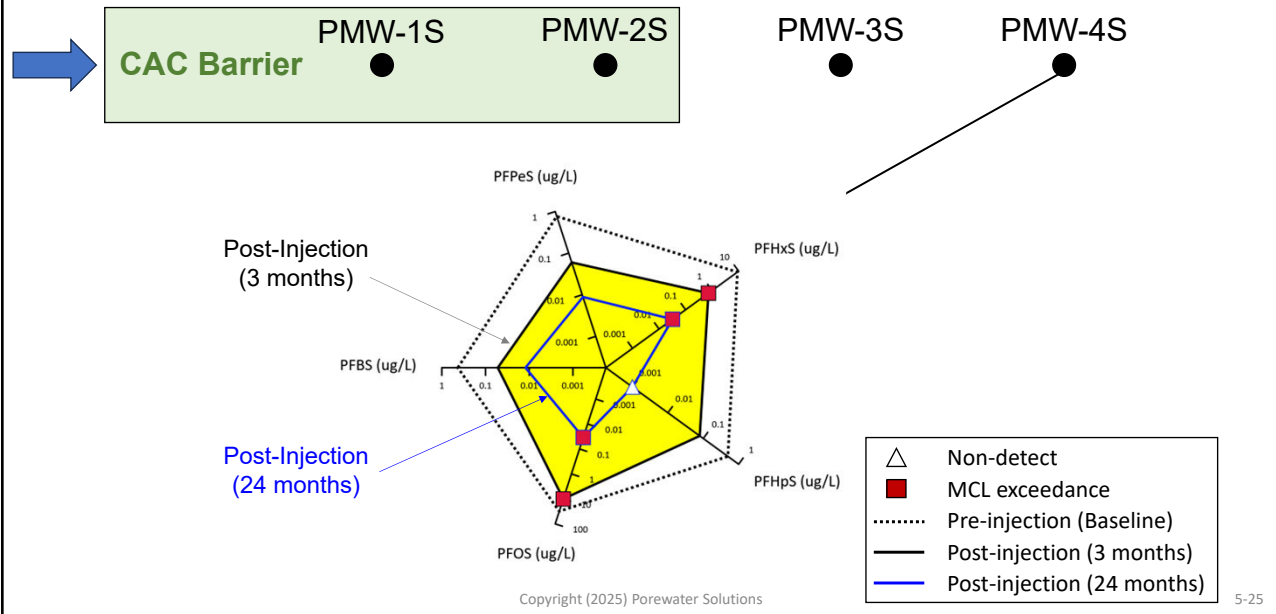
NESDI PRB Performance: PFSAs



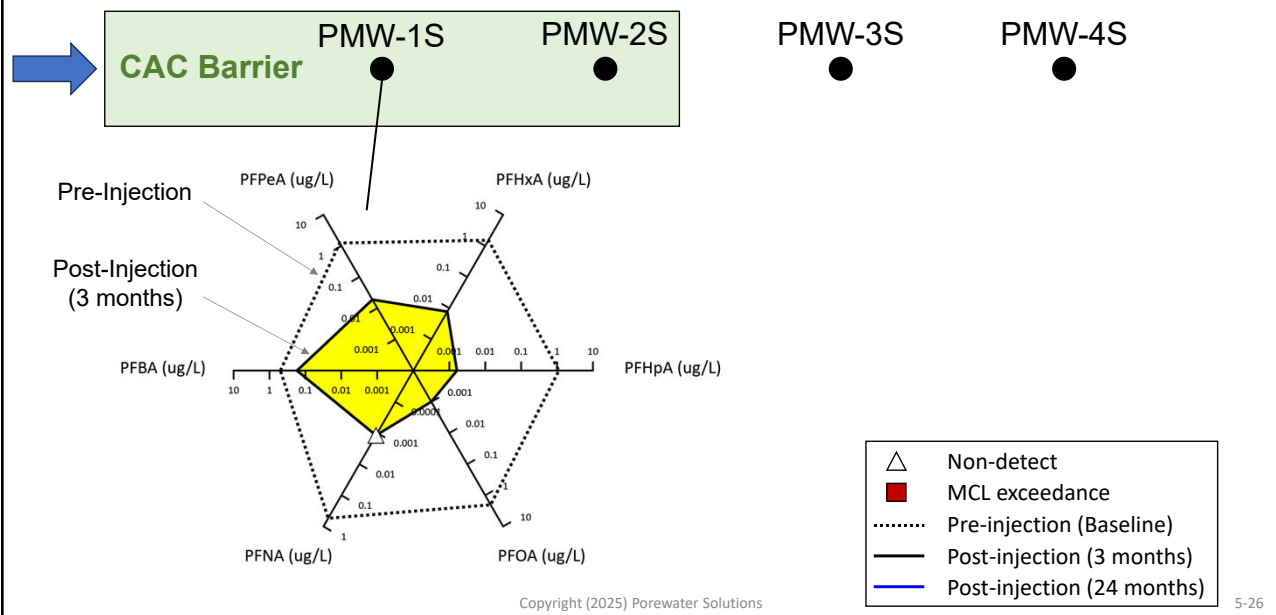
NESDI PRB Performance: PFSAs



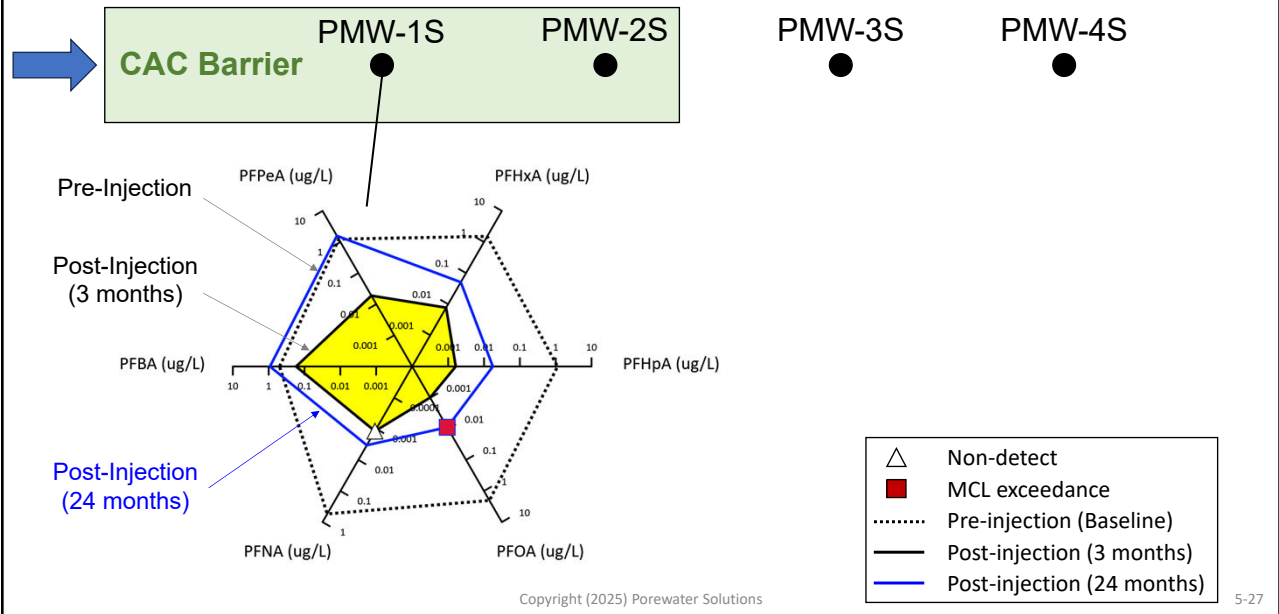
NESDI PRB Performance: PFSAs



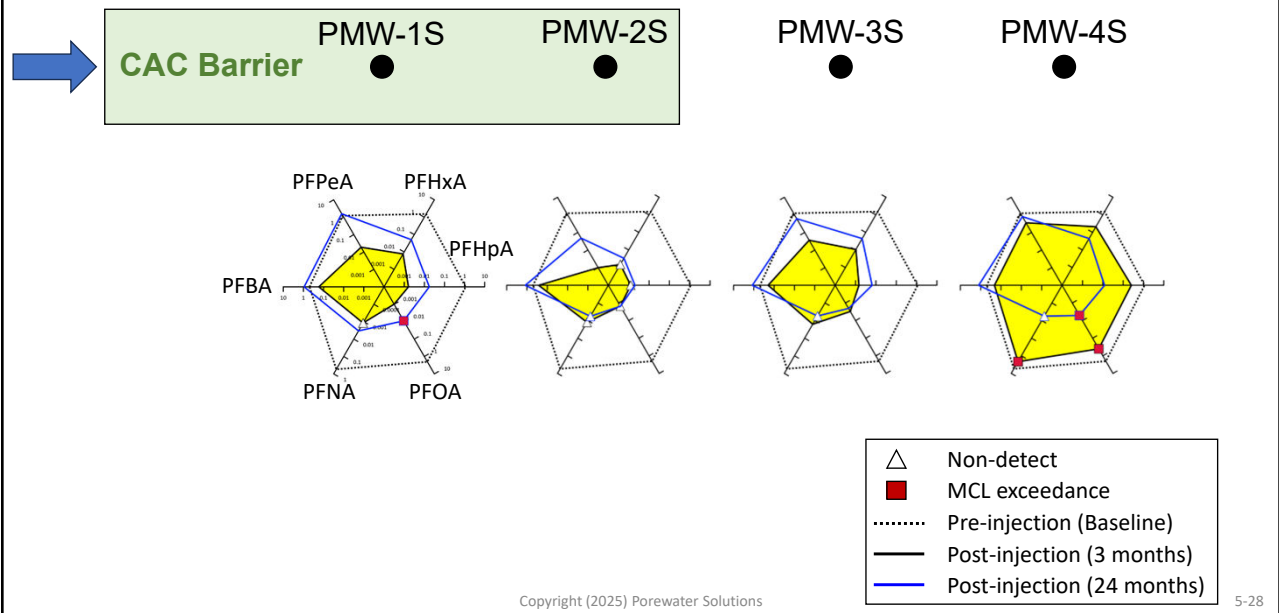
NESDI PRB Performance: PFCAs



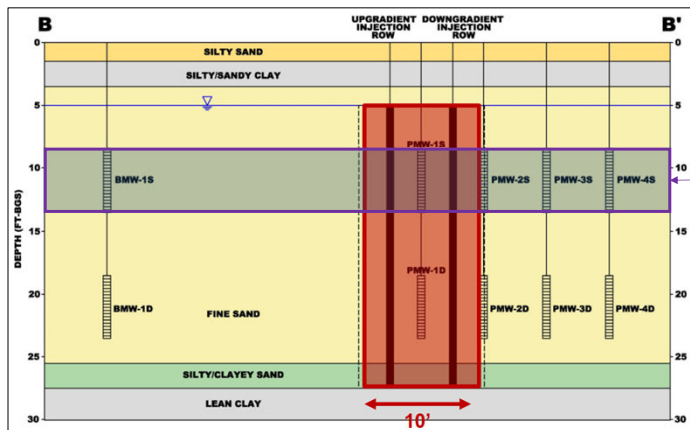
NESDI PRB Performance : PFCAs



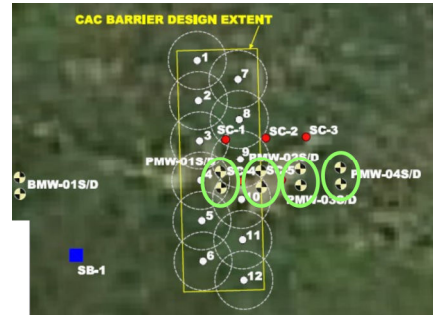
NESDI PRB Performance : PFCAs



CAC Layout



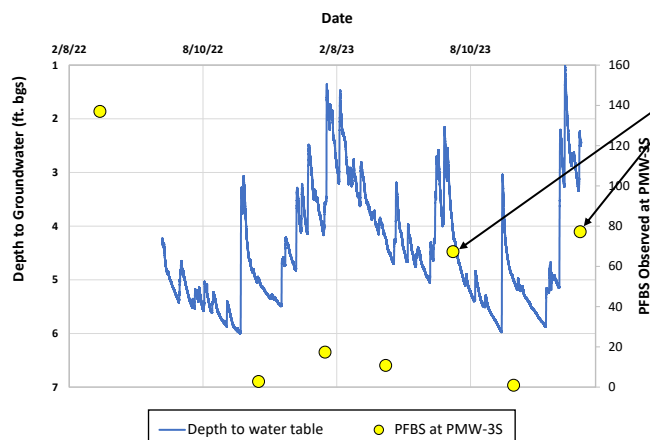
Model vertical extent includes the shallow well screen interval (5 ft thick).



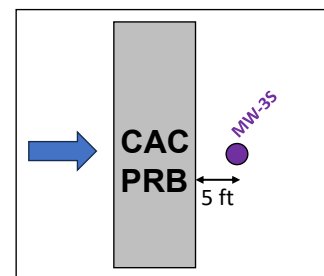
Copyright (2025) Porewater Solutions

5-29

Downgradient Wells Influenced by Water Table



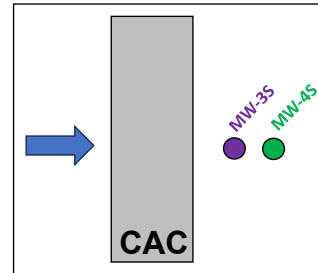
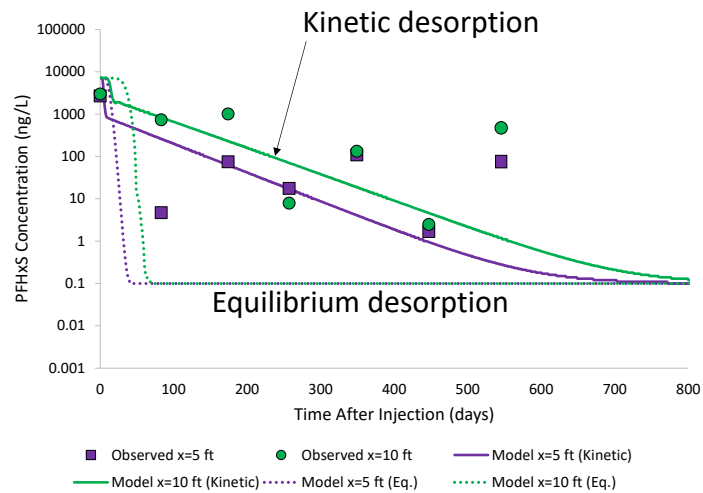
Spikes in PFBS downgradient from PRB after 2-3 ft rise and fall in water table.



Copyright (2025) Porewater Solutions

5-30

Downgradient: Equilibrium vs Kinetic Desorption

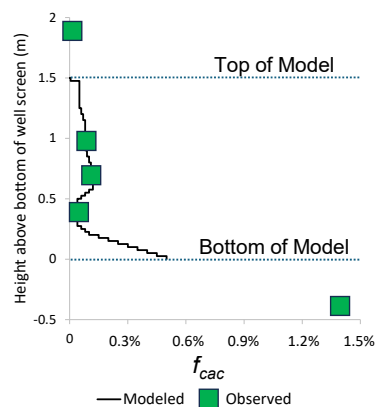


Copyright (2025) Porewater Solutions

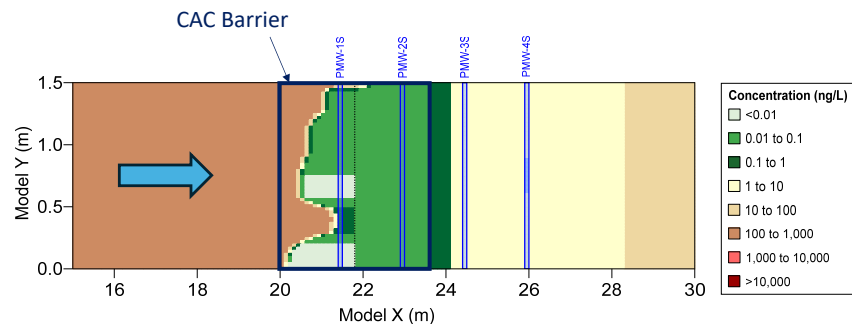
5-31

CAC Influence on PFAS Transport in Barrier

a) CAC Vertical Distribution at x = 5 ft



b) Modeled PFBS plume 400 days after CAC injection

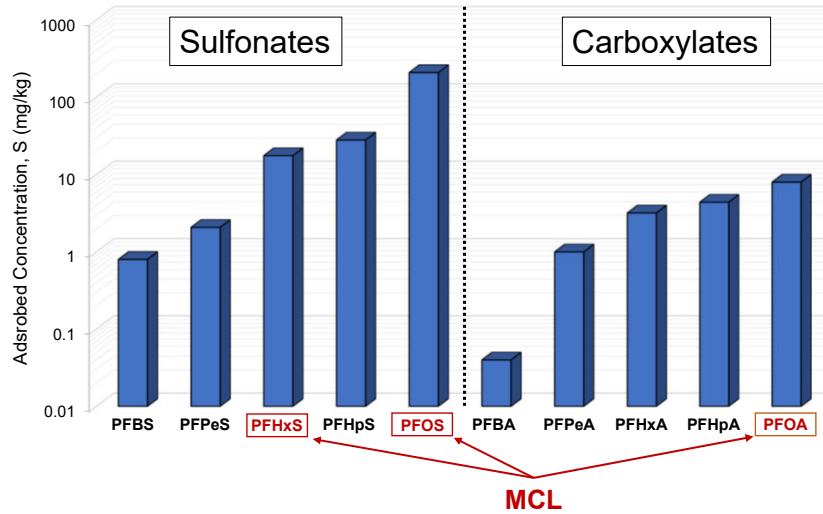


Copyright (2025) Porewater Solutions

5-32

Adsorbed Concentration Based on Calibrated Isotherms

DRAFT

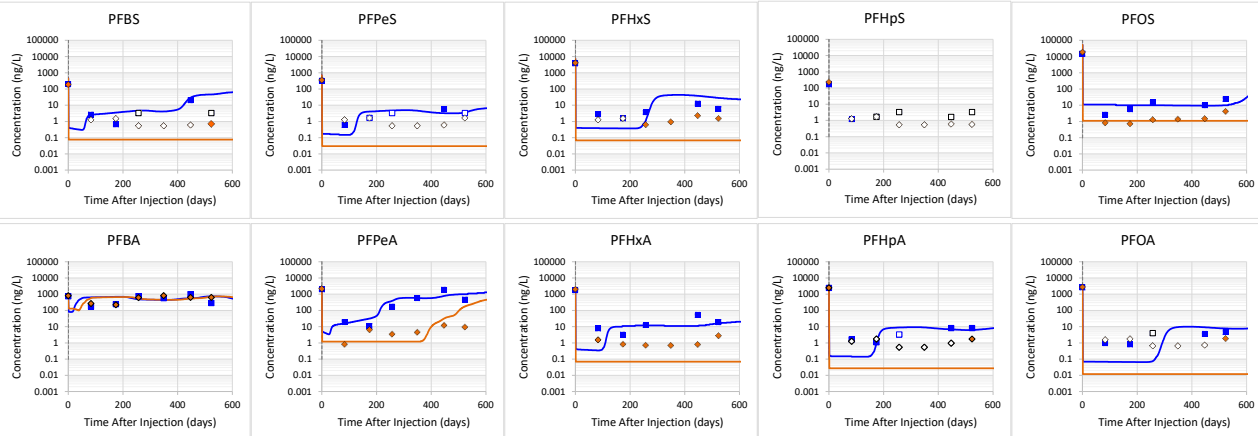
Adsorbed Concentration at Aqueous Concentration $C = 1$ ng/L

$$S = K_f C^a$$

Copyright (2025) Porewater Solutions

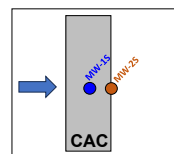
5-33

Preliminary Isotherm Calibration (First Six Quarters)



- Observed: PMW-1S ($x=5$ ft)
- ◆ Observed: PMW-2S ($x=10$ ft)
- Modeled: PMW-1S ($x=5$ ft)
- Modeled: PMW-2S ($x=10$ ft)

DRAFT



Copyright (2025) Porewater Solutions

5-34

South Dakota AFB: In-Situ Barrier Placement Alternatives

Carey et al. (2023)

Analysis of colloidal activated carbon alternatives for in situ remediation of a large PFAS plume and source area

Grant R. Carey^{1,2} | Richard H. Anderson³ | Paul Van Geel² | Rick McGregor⁴ |
Keir Soderberg⁵ | Anthony Danko⁶ | Seyfollah Gilak Hakimabadi⁷ |
Anh Le-Tuan Pham⁷ | Mia Rebeiro-Tunstall¹

¹Porewater Solutions, Ottawa, Ontario, Canada

²Department of Civil and Environmental Engineering, Carleton University, Ottawa, Ontario, Canada

³Air Force Civil Engineer Center, Joint Base, San Antonio, Texas, USA

⁴InSitu Remediation Services Limited, St. George, Ontario, Canada

⁵S.S. Papadopoulos & Associates, Rockville, Maryland, USA

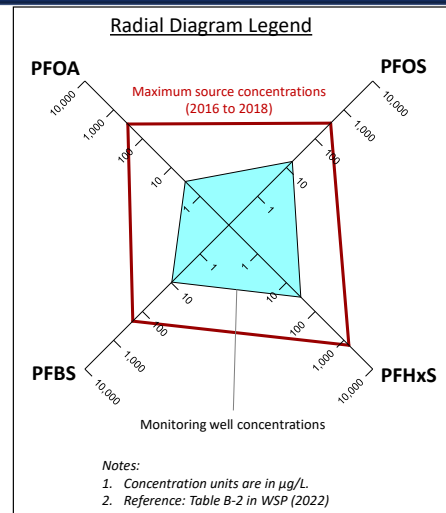
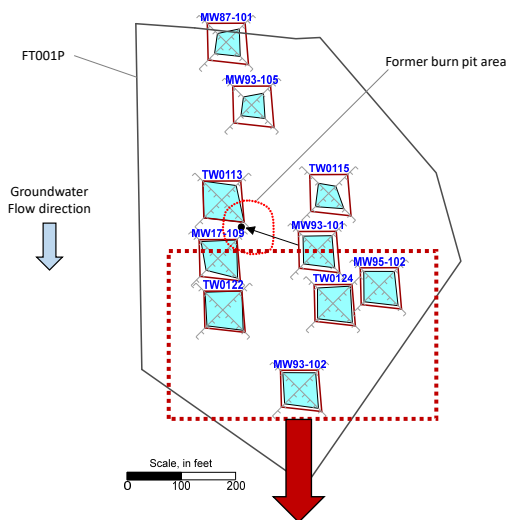
⁶Naval Facilities Engineering Command, Engineering and Expeditionary Warfare Center, Port Hueneme, California, USA

⁷Department of Civil and Environmental Engineering, University of Waterloo, Waterloo, Ontario, Canada

Copyright (2025) Porewater Solutions

5-35

PFOA Mass Discharge Estimates



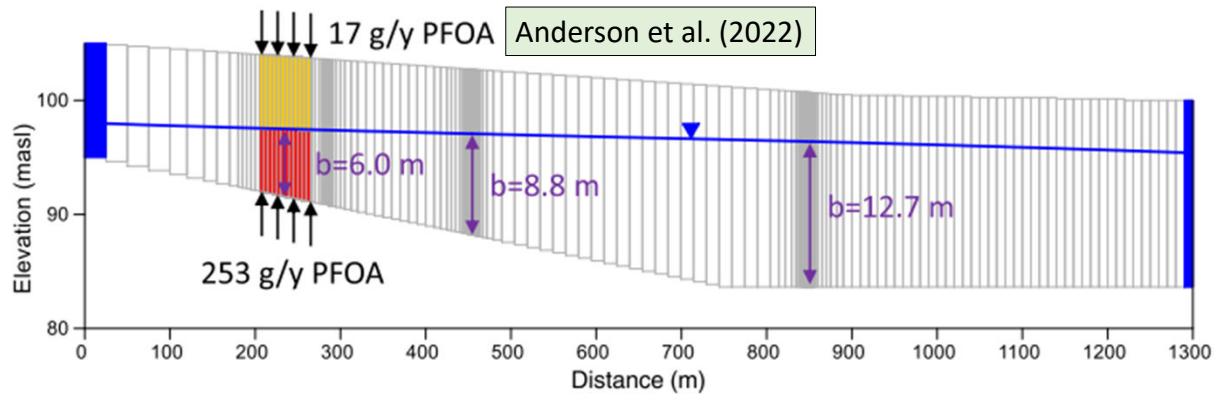
Copyright (2025) Porewater Solutions

5-36

PFOA Mass Discharge Estimates

PFOA mass discharge to GW plume:

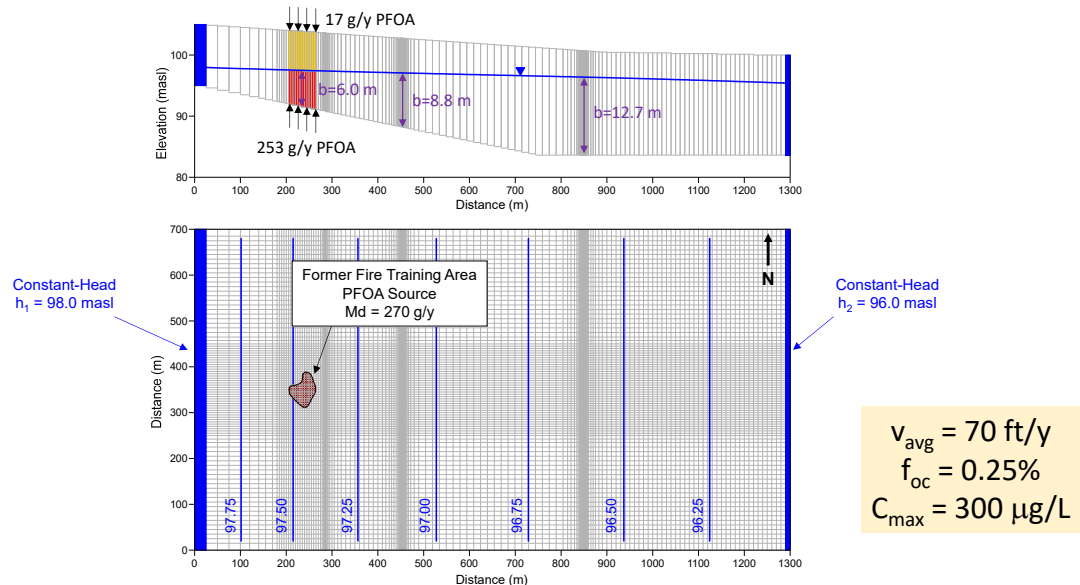
- 6% from vadose zone
- 94% from back-diffusion & desorption below water table



Copyright (2025) Porewater Solutions

5-37

2-D Model Domain and Grid

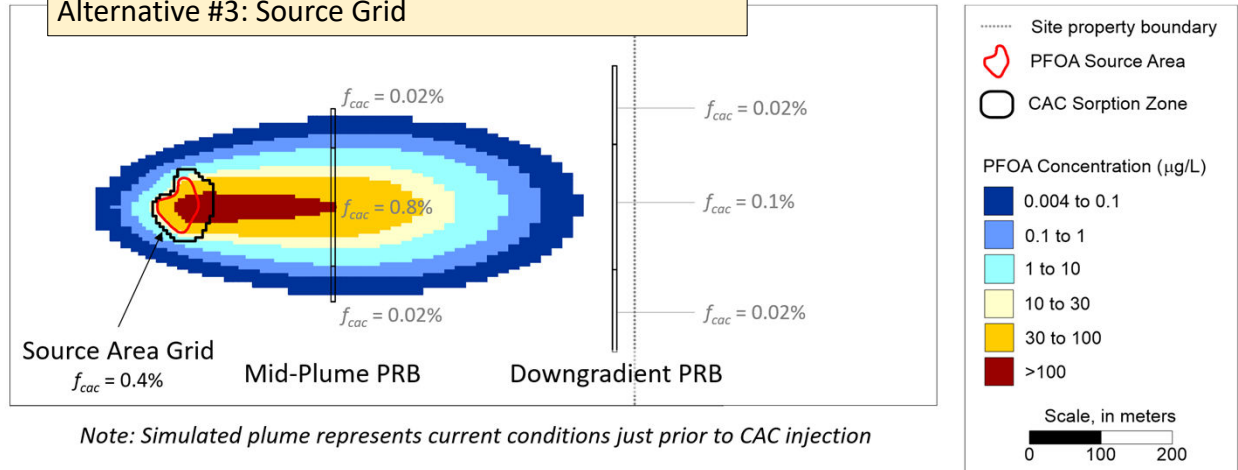


Copyright (2025) Porewater Solutions

5-38

CAC Barrier Placement Alternatives

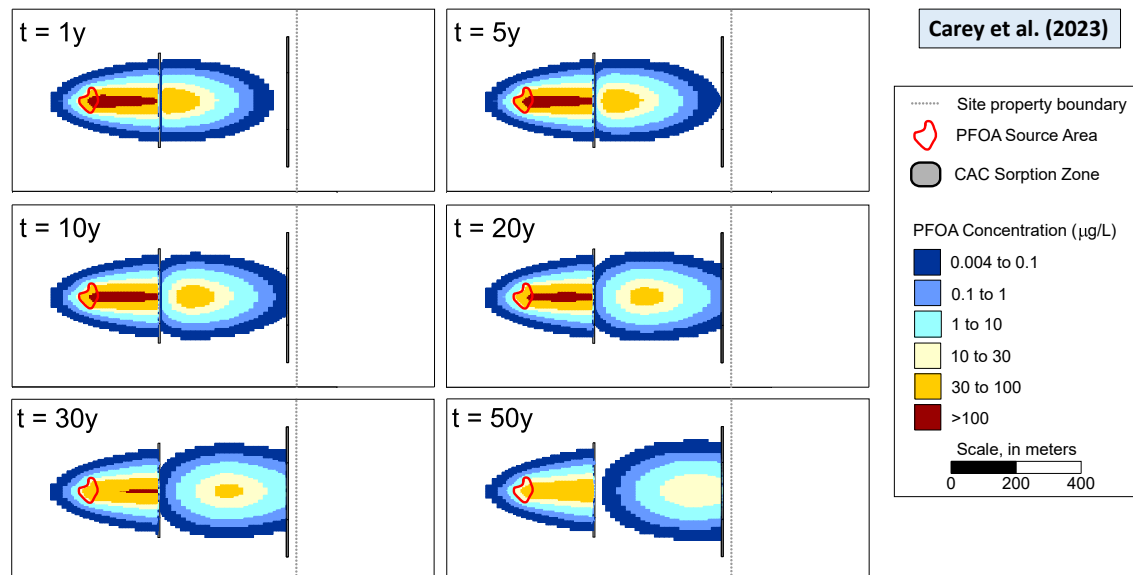
- Alternative #1: Downgradient PRB only
 Alternative #2: Downgradient PRB + Mid-plume PRB
 Alternative #3: Source Grid



Copyright (2025) Porewater Solutions

5-39

South Dakota Site: Integrated PRB Alternative



Copyright 2024 Porwater Solutions

40

Evaluating PlumeStop® Performance at Coastal Sites



Carey et al. (2024)

Tony Danko, Ph.D., P.E.
Environmental Engineer
NAVFAC EXWC/SH321
anthony.s.danko.civ@us.navy.mil

Grant Carey, Ph.D., P.Eng.
Environmental Engineer
Porewater Solutions
gcarey@porewater.com

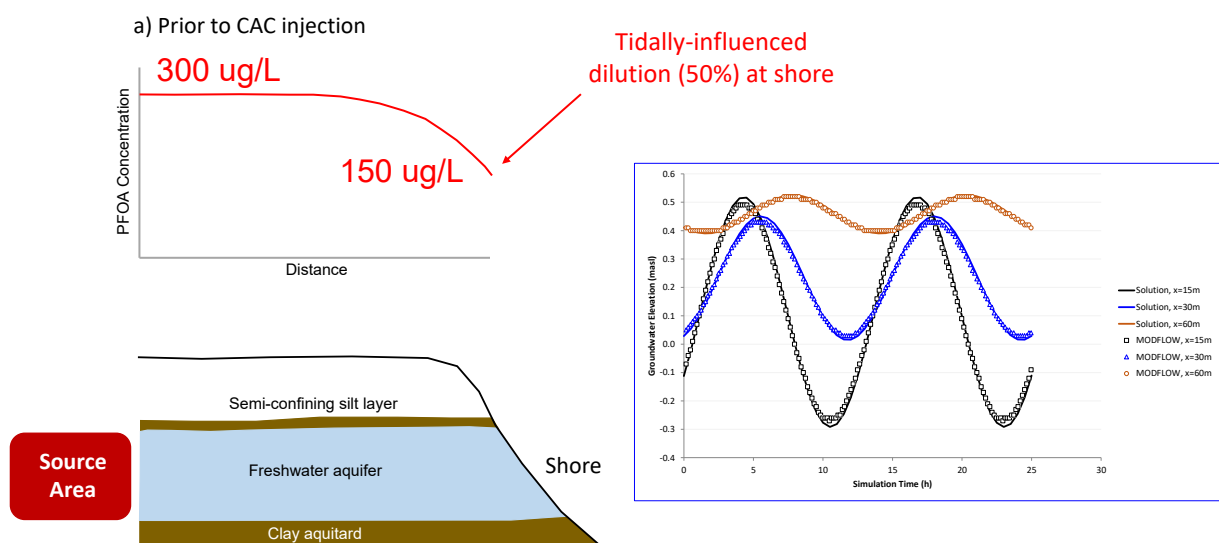


October 18, 2023

Copyright (2025) Porewater Solutions

5-41

Coastal Site Conceptual Model

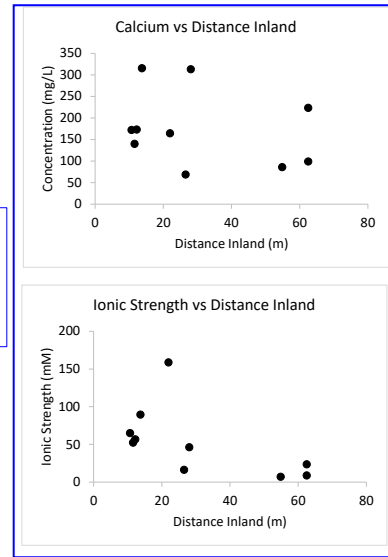
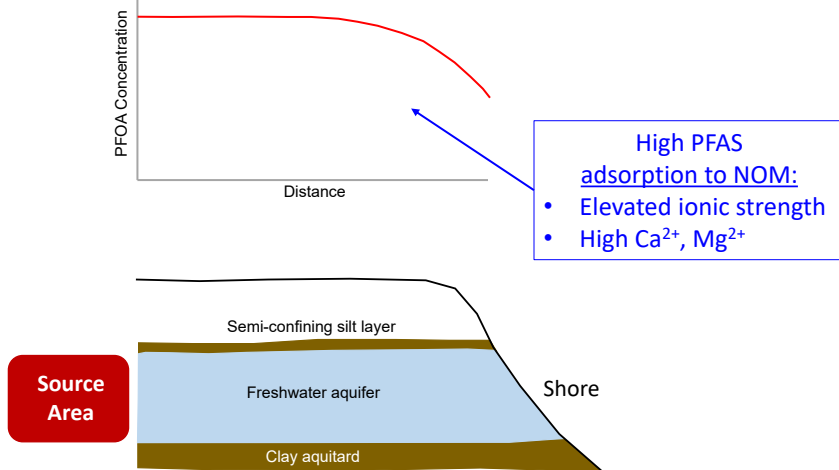


Copyright (2025) Porewater Solutions

5-42

Coastal Site Conceptual Model

a) Prior to CAC injection

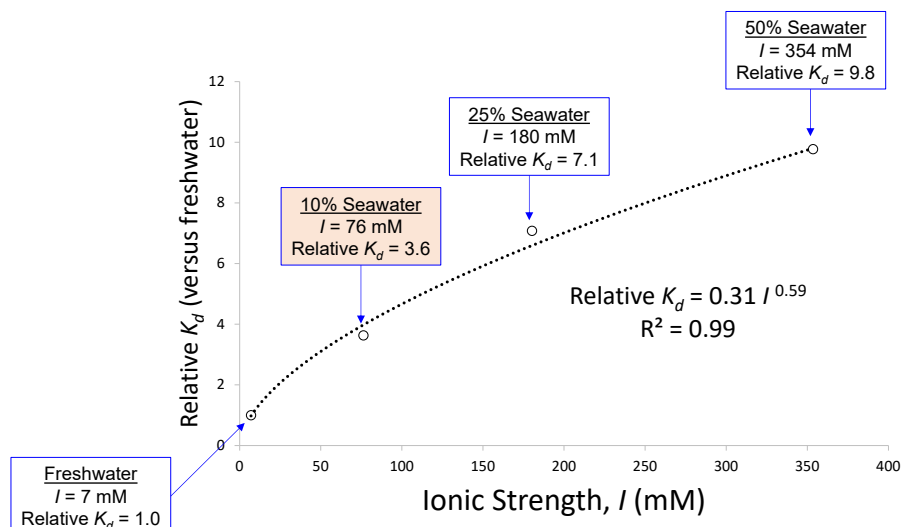


Copyright (2025) Porewater Solutions

5-43

PFAS Adsorption to NOM vs. Ionic Strength

Note: Chart prepared based on data presented in Chen et al. (2012)

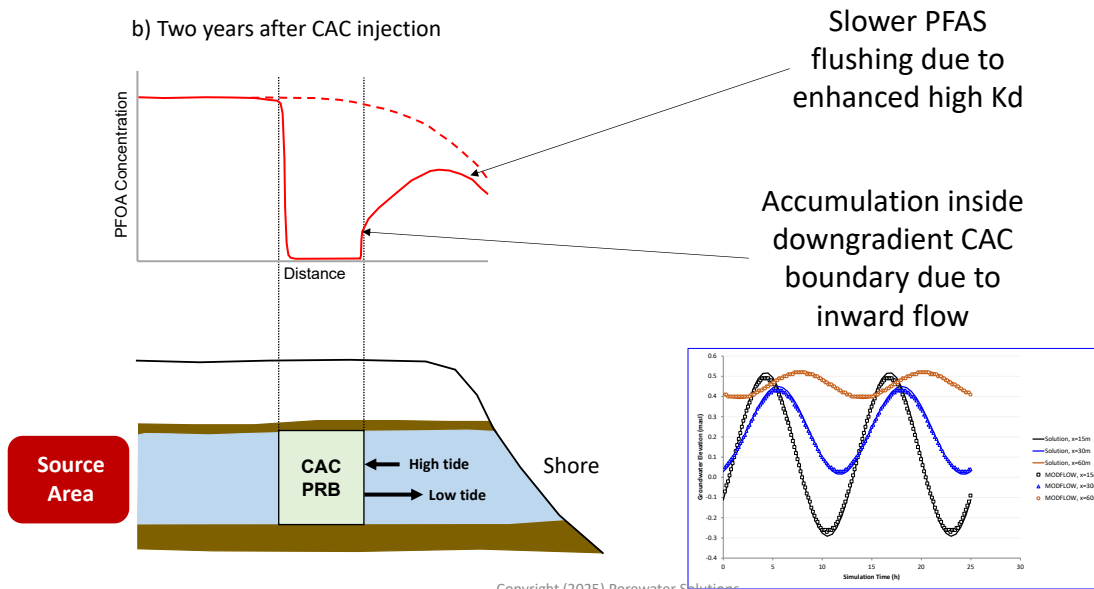


Copyright (2025) Porewater Solutions

5-44

Coastal Site Conceptual Model

b) Two years after CAC injection



Copyright (2025) Porewater Solutions

5-45

Long-Term Remediation Strategies

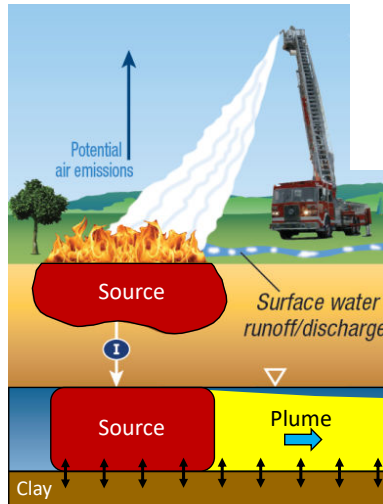
Copyright (2025) Porewater Solutions

5-46

Adsorption PRBs Recommendations



Modified from ITRC Fact Sheet, March 16, 2018 (Figure 1)



Downgradient PRB = Best bang for the buck

- Lower POCs, lower precursors & other organics
- Lower CAC dose needed
- Faster protection of downgradient receptors
- Interim goal: Mass Flux Reduction

Source Control + Downgradient PRB

- Evaluate cost-benefit with feasibility study

Implementation

- Modeling – expectation for downgradient flushing time
- Post-injection cores at one year – CAC distn
- Contingencies for re-injection
- Long-term plan

Copyright (2025) Porewater Solutions

5-47

Questions?

Grant R. Carey, Ph.D.

Porewater Solutions

gcarey@porewater.com



POREWATER SOLUTIONS

Expertise • Experience • Innovation

Copyright (2025) Porewater Solutions

5-48

APPENDIX A

Grant Carey Curriculum Vita

Profile Of Professional Activities

Dr. Carey has worked on projects across North America and Australia with a focus on:

- PFAS site characterization, transport, and remediation modeling
- Environmental forensics and data visualization
- Groundwater and soil vapor flow and transport modeling
- NAPL delineation and remediation
- Regulatory negotiations
- Expert witness and litigation support services

Dr. Carey has more than 30 years of experience, and is recognized as an industry leader in PFAS remediation. Dr. Carey also specializes in environmental forensics, NAPL delineation, contaminated site and sediment remediation, mining water management, and groundwater flow and transport modeling. Dr. Carey has worked on numerous projects across the United States, Canada, and Australia, providing regulatory and litigation support to various client sectors including law firms, the U.S. Department of Defense, chemical manufacturing, aerospace, and mining. Dr. Carey has also developed proprietary computer codes for PFAS modeling and visualization. Dr. Carey is currently involved with seven SERDP and ESTCP projects related to PFAS remediation. Dr. Carey is an Adjunct Research Professor at Carleton University and is an Adjunct Professor at the University of Toronto. Dr. Carey has published more than 100 short courses, seminars, and papers, and he has developed and delivered PFAS courses based on interactive classroom, e-learning, and web seminars. Dr. Carey was involved with the development of the ITRC PFAS Guidance manual and is currently participating in the development of the National Ground Water Association White Paper on PFAS Forensics. Dr. Carey also has experience and training as both a mediator and meeting facilitator.

PFAS QUALIFICATIONS

- Recognized industry leader in predicting the performance and longevity of in-situ sorbent technologies for PFAS remediation
- Widely published proprietary reactive transport model (The In-Situ Remediation Model, or ISR-MT3DMS) for evaluating the feasibility and design of PFAS remediation alternatives
- Proprietary forensic tools for visualizing PFAS source contributions, precursor transformations, redox geochemistry, and site background concentrations
- Expertise and experience gained through participation on industry-leading research teams studying PFAS adsorption to colloidal activated carbon

- 13 PFAS remediation peer-reviewed journal articles since 2019, including nine published, two in press, and two to be submitted in 2025
- U.S. Patent Pending for an innovative process to enhance PFAS ex-situ treatment
- Currently involved with seven SERDP-ESTCP projects related to PFAS remediation for the U.S. Department of Defense

SPECIALIZED PFAS CONSULTING SERVICES

In addition to standard site characterization, remediation, and litigation services, Dr. Carey is uniquely positioned to provide the following specialized PFAS services:

- Recommend site characterization methods that support the feasibility study or remedial design of in-situ sorbent alternatives
- Use proprietary reactive transport model (ISR-MT3DMS) to:
 - Predict future PFAS plume extents, and the potential for natural attenuation to reduce risk at downgradient receptors
 - Compare the performance and longevity of various in-situ sorbent technologies
 - Assess the effects of competitive adsorption on the long-term performance of in-situ sorbents
 - Conduct feasibility or remedial design studies including evaluation of integrated site-wide alternatives for source treatment and plume management
 - Evaluate the influence of rate-limited desorption or back-diffusion on the timing of the downgradient plume response to site remediation
- Apply commercial models including HYDRUS and the PFAS-LEACH Integrated Toolkit to quantify PFAS flux from the vadose zone to an underlying aquifer to support cost-benefit analyses of vadose zone remediation strategies.
- Forensic evaluation of PFAS source contributions in support of litigation

EDUCATION

- Ph.D. University of Guelph, Guelph, Ontario, 2015 (Part-time): Predicting Attainable Goals and Depletion Timeframes for DNAPL Source Zones
- M. Eng. Carleton University, Civil and Environmental Engineering, 2001 (Part-time): Development and Field-Validation of a Three-Dimensional, Redox-Dependent Biodegradation Transport Model
- 1997 One of two Canadian graduate students invited to a NATO Advanced Study Institute (Bioavailability of Organic Xenobiotics in the Environment) in the Czech Republic.

B.A.Sc. University of Waterloo, Civil Engineering, 1993: Thesis – Development and Validation of a Two-Dimensional, Density-Dependent Vapor Flow and Transport Model

EMPLOYMENT

2006-Present	President and CEO Porewater Solutions
2005-2006	Associate, and Director of Corporate Training Conestoga-Rovers & Associates
2002-2004	Senior Engineer and Training Developer Conestoga-Rovers & Associates
2000-2002	President and CEO Environmental Institute for Continuing Education (EICE)
1996-2002	President and CEO Environmental Software Solutions Inc. (ENSSI)
1997-1999	Carleton University Mediation Centre – Volunteer Mediator
1992-1996	Engineer, Conestoga-Rovers & Associates

PROFESSIONAL AFFILIATIONS

- California Groundwater Resources Association
- Professional Engineers Ontario

Site Remediation Projects

- Chemical manufacturing facility, Kentucky – Assessment of releases to subsurface soil and groundwater, including reviews of historical release documents, evaluation of leaks from tanks and from above-ground and underground utilities that correlated with observed impacts in groundwater. Provided technical expertise and supported regulatory negotiations at one of the largest NAPL-contaminated sites in North America, in a complex and contentious multiple-PRP project with litigation pending for a US\$300,000,000 remedy.
- Confidential Site, Saudi Arabia – Conducted soil vapor flow and transport modeling to support optimization of a soil vapor extraction system and to predict the timeframe for back-diffusion of methane and VOCs from bedrock.
- Cedar Chemical Site, Phillips County, Arkansas – Supported a PRP De Minimis evaluation for a chlorinated solvents site.
- Aeronautical Manufacturing Facility, San Diego – Providing expert support for the development of a final remedy involving both enhanced bioremediation and monitored natural attenuation of TCE in groundwater.
- San Fernando Valley Superfund Site (Area 2), Glendale, California – Expert peer review for implementation of a basin-scale investigation for delineation of hexavalent chromium, and groundwater modeling to evaluate capture zones for regional supply wells for VOCs (mainly PCE and TCE), 1,4-dioxane, hexavalent chromium, and other emerging chemicals.

- Former manufacturing facility, Glendale, California – Expert peer review for monitoring and remediation of hexavalent chromium and chlorinated solvents including PCE and TCE.
- Solvent Savers Superfund Site, Lincklaen Township, New York – DNAPL expert and supported regulatory negotiations for development of a TCE monitored natural attenuation remedy.
- Aerospace manufacturing facility, Phoenix, Arizona – Expert peer review for treatability pilot test analysis, and preparation of the corrective measures study and implementation plan for a TCE plume in bedrock.
- Former rocket manufacturing facility, Southern California – Conducted a detailed investigation of chemical fate (perchlorate and chlorinated solvents) including validation of a three-dimensional basin-wide groundwater flow model for the San Bernadino Basin.
- Seaspans Site, British Columbia – Calibrated a three-dimensional transient (tidal oscillation) freshwater groundwater flow model for a coastal site and evaluated remedial design alternatives and sediment cap performance based on groundwater flow and chemical transport modeling;
- Union Bay Site, British Columbia – Calibrated a three-dimensional transient (tidal oscillation) groundwater flow model based on seasonal positions of the freshwater-seawater interface, and used a one-dimensional groundwater flow and chemical transport model to compare remedial alternative performance based on mass discharge reductions;
- Sydney Tar Ponds, Nova Scotia – Directed three-dimensional groundwater flow model calibration and application to evaluate the Phase III feasibility of several remedial alternatives at a large former hazardous waste site.
- Savannah River National Laboratory (SRNL) – Conducted a reactive transport modeling study to evaluate the mass balance for a chlorinated solvent plume attenuation at Plattsburgh Air Force Base (New York) on behalf of SRNL's research efforts related to natural and enhanced attenuation
- Vandenberg Air Force Base, California - Modeled tracer tests and bioremediation pilot tests to evaluate remedial performance as part of a Department of Defense (ESTCP) project related to the design of soluble substrate injection systems

PFAS Projects

- Confidential Mine site, Western Australia – Modeled groundwater flow and PFAS transport to assess the feasibility and remedial design options for a colloidal activated carbon barrier to contain a PFAS plume which was preventing the dewatering of more than \$5 billion in metal ore.
- PFAS Manufacturer, Washington, D.C. – Previously retained by a large PFAS manufacturer in a matter related to the assessment of PFAS liability and various allocation methods.
- U.S. DoD Project ESTCP ER25-8483. "Demonstration of SERDP-ESTCP e-Learning Platform for Enhancing Technology Transition (PFAS In-Situ Remediation Modules)."
- U.S. DoD Project ESTCP ER25-8624. "Colloidal Activated Carbon for In Situ PFAS Remediation at Coastal Sites: Field Assessment and Modeling of Long-Term Efficacy."
- U.S. DoD Project ESTCP ER24-8875. "Evaluation of an Injected Surface Modified Clay Permeable Adsorptive Barrier for PFAS Sequestration."

- U.S. DoD Project ESTCP ER24-8200. “Two PFAS Remediation Models for Understanding and Managing PFAS in the Saturated Zone.”
- U.S. DoD Project ESTCP ER20-5182. “Validation of Colloidal Activated Carbon for Preventing the Migration of PFAS in Groundwater”.
- U.S. DoD Project SERDP ER21-3959. “An investigation of factors affecting in situ PFAS immobilization by activated carbon”.
- U.S. DoD Project SERDP ER21-1070. “Hydraulic, chemical, and microbiological effects of in situ activated carbon sorptive barrier for PFAS remediation in coastal sites”
- Mid-West Military Facility – Collaborating with the U.S. Air Force Civil Engineering Center to assess novel forensic methods for identifying PFAS source composition and evaluating PFAS precursor biodegradation to PFAAs in groundwater.
- Virginia Military Facility – Collaborating with the U.S. Navy to model the initial two years of performance of a colloidal activated carbon barrier, including estimation of field-scale adsorption isotherms for ten short- and long-chain PFAS.
- California Military Facility – Collaborating with the U.S. Navy to model the influence of tidal fluctuations and coastal site geochemistry on the performance of colloidal activated carbon for PFAS in-situ remediation adjacent to the coast.
- South Dakota Military Facility – collaborated with the U.S. Air Force to model the viability of colloidal activated carbon for in-situ remediation of PFAS at an AFFF-impacted site with high PFOS, PFHxS, and PFOA concentrations in groundwater.
- NGWA PFAS Forensics White Paper – Participating on a committee to prepare a comprehensive white paper on available PFAS forensic methods.
- NSERC Alliance Research Project – PFAS competitive adsorption to colloidal activated carbon and development and verification of several reactive transport model codes, in collaboration with the University of Waterloo, University of Toronto, and Carleton University.
- Ontario Center of Excellence Research Project – PFAS Adsorption isotherms with colloidal activated carbon and PFAS in-situ remediation model code development, in collaboration with the University of Waterloo and Carleton University.
- Central Canada site - Modeled PFAS transport and in-situ remediation performance based on colloidal activated carbon injections into the source zone.
- Former Solvent Processing Facility - Assessment of PFAS trends and remedy implications at a former waste disposal site in New York.

Litigation Projects

- Glendale, California – Retained by an aerospace corporation to provide litigation support involving the evaluation of relative source contributions to a commingled plume, including assessment of a basin-wide groundwater model (2024 to Present).
- North Hollywood, California – Retained by a site owner to provide litigation and regulatory support involving the evaluation of relative source contributions to a commingled plume (2024 to Present).
- Chemical Manufacturing Facility, Kentucky - Retained as an expert witness for a matter involving a large chemical manufacturing facility in Kentucky involving the remedial design

and construction of a \$200 million site remedy including a site-wide barrier wall, hydraulic containment, groundwater modeling, and onshore and offshore NAPL recovery (Expert witness retention, 2022 to Present; litigation consultant 2003 to 2019).

- Confidential site, California - Retained as a litigation consultant in a matter involving the forensic analysis of radiological soil and building remediation data, with multiple lawsuits including separate personal injury and property damage class action cases (2019 to Present).
- Washington, D.C. – Previously retained by a large PFAS manufacturer in a matter related to the assessment of PFAS liability and various allocation methods (2019-2020).
- Former aerospace facility, Pacoima, California – Expert support for due diligence investigation and pending litigation related to TCE and chromium (2015-2016).
- USA Petroleum site, San Jose, California – Retained as an expert witness regarding the fate of MTBE from a gas station release near a regional drinking water supply well (2013 to 2014).
- Manufacturing Facility, Phoenix, Arizona – Developed a regional groundwater flow and chemical transport model for litigation, to evaluate source release timing for a TCE plume in a multi-aquifer system with regional supply wells (2001 to 2004).

Mining and Water Resource Modeling Projects

- Vale Garson Mine, Sudbury, Ontario – Calibrated a large three-dimensional groundwater flow model based on current pumping rates for a 100-year old underground mine, and used the model to assess the potential influence of a future mine expansion on nearby streams and lakes.
- Impala Iron Ore Mine, Thunder Bay, Ontario – Constructed and calibrated a large three-dimensional groundwater flow model based on recent open pit and underground working pumping rates, and predicted life of mine conditions. Also constructed a three-dimensional transport model to assess potential receptors and steady-state attenuation rates for a future tailings management facility.
- Green Technology Metals Mine, Thunder Bay, Ontario – Constructed and calibrated a three-dimensional groundwater flow model to predict future dewatering rates for two large open pit mines, and evaluated the potential influence on dewater rates for two nearby water storage ponds.
- Clean Air Metals Mine, Thunder Bay, Ontario – Constructed and calibrated a three-dimensional groundwater flow model to evaluate the influence of an overlying lake on dewatering rates for planned underground workings.
- Sugar Gold Mine, Thunder Bay, Ontario – calibrated a large three-dimensional groundwater flow model to current conditions and simulated dewatering pumping rates for the underground workings in the life of mine scenario.
- Vale Copper Cliff Complex, Sudbury, Ontario – developed and calibrated a three-dimensional groundwater flow model to assist with remedial design for a pump-and-treat system and partial barrier wall.
- Schefferville Area Iron Ore Mine, Western Labrador – developed and calibrated a three-dimensional groundwater flow model, and developed a phased pumping scheme for dewatering during mine operations.

- Joyce Lake Orebody, Western Labrador – development and calibration of a three-dimensional groundwater flow model, and evaluation of dewatering schemes for the open pit mine.
- Former sand and gravel quarry, Maryland - Developed and calibrated a groundwater flow model to evaluate the range in dewatering pumping rates in support of a large excavation and bioremediation program
- Texas Central Gulf Coast Aquifer Groundwater Availability Model – calibrated a regional groundwater flow model that covered an area that represents more than 10% of the drinking water supply for Texas, and used this model to predict water supply resources over a 50-year period in the future.
- Pebble Project, Northern Dynasty Minerals Ltd., Alaska – developed and calibrated a multi-watershed, three-dimensional groundwater flow model for the world's largest undeveloped copper and gold resource, including a sophisticated representation of groundwater-surface water interactions and a transient water balance calibration for 14 sub-watersheds.

Modeling and Visualization Software Development

Dr. Carey has developed a variety of commercial and public domain software tools, including:

In-Situ Remediation (ISR-MT3DMS), 2023 – three-dimensional reactive transport model based on the MT3DMS framework, for simulating the performance of PFAS, chlorinated solvents, and metals in-situ remediation technologies, including adsorptive permeable reactive barriers, enhanced in-situ bioremediation (EISB) and in-situ chemical oxidation. Model includes an innovative local domain approach for modeling forward and back-diffusion, and also includes the reaction package from BioRedox.

Visual Bio, 2018 – radial diagram visualization tool for delineating biodegradation zones in groundwater and illustrating lines of evidence in support of MNA and EISB remedies.

NAPL Depletion Model, 2015 – semi-analytical screening model for simulating the depletion timeframe for LNAPL or DNAPL source zones.

BioRedox-MT3DMS, 1999 – a three-dimensional finite difference model for simulating multispecies contaminant transport, including advection, dispersion, sorption, and coupled biodegradation-redox reactions between electron donors and electron acceptors. BioRedox-MT3DMS can simulate oxidation, reduction, and co-metabolic reactions, and is capable of modeling sequential transformation pathways for chlorinated solvents and petroleum hydrocarbons. BioRedox-MT3DMS is also capable of simulating equilibrium or rate-limited dissolution of light or dense NAPL sources, and includes a leachate composition model to represent time-varying landfill constituent concentrations leaching to underlying aquifers. BioRedox-MT3DMS was previously available in the public domain.

SEQUENCE, 1999 – a visualization tool that uses a modified radial diagram approach to illustrate the effects of natural attenuation on groundwater redox conditions. SEQUENCE may also be used to evaluate spatial and temporal trends for chlorinated solvent species. The visual aids prepared using SEQUENCE provide convincing evidence for the effectiveness of remediation by natural attenuation. SEQUENCE

integrates these radial diagram tools with a comprehensive data management system is available. SEQUENCE was previously sold as a commercial product.

BioTrends, 1999 – a suite of tools for evaluating spatial and temporal trends using x-y charts with unique features that were specifically designed for evaluating chemical analytical data. Additional tools are provided for calculating first-order degradation rates between well pairs, or the average degradation rates along a flowpath based on a log-linear regression analysis, using the methods presented in the USEPA and AFCEE natural attenuation protocols. Another tool is provided to calculate the natural attenuation "score" for a site based on criteria presented in the USEPA protocol. BioTrends is integrated with a chemical properties database (CHEMbase), and the same project data management system used for the SEQUENCE visualization tool. BioTrends was previously sold as a commercial product.

BioTracker, 1999 – a one-dimensional screening model that is integrated with visualization tools for transport model calibration and documentation. BioTracker utilizes a one-dimensional version of the BioRedox finite difference model to simulate multispecies transport processes including advection, dispersion, sorption, and single or sequential transformation reactions with optional halogen accumulation. BioTracker incorporates a particle tracking tool that delineates flowpaths downgradient from one or more point source locations. The customized particle tracking routine utilizes Surfer contour maps of observed or simulated groundwater elevations as input. BioTracker is also integrated directly to the same project data management system used with BioTrends and SEQUENCE, and it is integrated with a chemical properties database (CHEMbase). BioTracker was previously sold as a commercial product.

Vapor-2D, 1992 – a two-dimensional finite element model that simulates multispecies, density-dependent vapor flow and transport. Vapor-2D was modified to predict the migration of gasoline vapors from a subsurface spill area, and includes a multicomponent NAPL source model. Vapor-2D was successfully validated by simulating laboratory experiments of vapor flow and transport of heptane in the vadose zone, and Vapor-2D has been used to assess density-dependent vapor migration at field sites. Vapor-2D is currently a proprietary model.

REPRESENTATIVE SHORT COURSES, WORKSHOPS, AND TRAINING SEMINARS

- Invited instructor for a half-day short course for the Canadian Federal PFAS Working Group: PFAS In-Situ Remediation Using Colloidal Activated Carbon, May 2025.
- Invited instructor for an internet seminar entitled: PFAS In-Situ Remediation Case Studies and Long-term Strategies, organized by Regenesys, late May, 2024
- Instructor for the 8-hour short course entitled "In Situ Management of PFAS in Groundwater", including recent SERDP-ESTCP research advancements, presented at the Battelle 2024 Chlorinated Conference in Denver on June 2, 2024
- Lead Instructor for the 4-hour short course entitled "Radial Diagram Visualization to Improve Conceptual Models and Communication for Sites Impacted with PFAS or Chlorinated solvents", to be presented at the Battelle 2024 Chlorinated Conference in Denver on June 4, 2024

- Invited instructor for an internet seminar with 1,500 registrations entitled “Longevity of PFAS Remediation Using Colloidal Activated Carbon at AFFF-Impacted Sites”, organized by Regenesys, January 26, 2023.
- Invited instructor for an internet seminar with 1,200 registrations entitled “Longevity of PFAS Remediation Using Colloidal Activated Carbon”, organized by Regenesys, November 19, 2020.
- Invited instructor for a PFAS short course entitled “Managing PFAS at Your Site: Key Technical and Regulatory Issues Associated with PFAS”, International Cleanup Conference, Adelaide, Australia, September 12, 2019.
- Invited instructor for a workshop entitled: “PFAS Remedial Strategies”, at the RPIC 2018 Federal Contaminated Sites Workshop, Toronto, Ontario, June 13, 2018.
- Invited instructor for a workshop entitled: “Innovative Methods for Optimizing Remediation Efficiency”, at the 2018 Battelle Conference on Remediation of Chlorinated and Recalcitrant Compounds, Palm Springs, CA, April 10, 2018.
- Instructor for a Learning Lab presentation entitled: “Visualizing Biodegradation Zones in Groundwater”, to be presented at the 2018 Battelle Conference on Remediation of Chlorinated and Recalcitrant Compounds, Palm Springs, CA, April 10, 2018.
- Invited instructor for an internet seminar with between 500 and 1,000 participants entitled: “In-Situ Remediation Modeling and Visualization Tools”, organized by Regenesys on October 26, 2017.
- Invited instructor for a workshop entitled “Innovative Visualization, Modeling, and Optimization Tools for Improving Remediation Efficiency”, presented at the 2017 Cleanup Conference, Melbourne, Australia, September 10, 2017.
- Invited Instructor for the ITRC webinar entitled "Remediation of Contaminated Sediments" offered from 2014 through 2016.
- Invited Instructor for the ITRC webinar entitled "Use and Measurement of Mass Flux and Mass Discharge" offered from 2010 through 2016.
- Invited Instructor for a 1.5-hour short course entitled “Mass Flux/Discharge: DNAPL and Back-Diffusion” at the 24th Annual NAPRM Training Program, United States Environmental Protection Agency, Pittsburgh, Pennsylvania.
- Instructor for a 4-hour short course entitled “Using the NAPL Depletion Model for Estimating Timeframes for Natural and Enhanced Attenuation”, presented at the Third International Symposium on Bioremediation and Sustainable Environmental Technologies, Miami, Florida, May 18, 2015.
- Invited Instructor for 2015 Smart Remediation short course with presentation entitled “A New Paradigm for Managing Chlorinated Solvent Sites” in Ottawa, Ontario February 12, 2015.
- Senior Instructor for the following seminars which were delivered by webcast or on CD-ROM to clients in North America, Europe, Australia, and Africa:
 - Application of SEQUENCE Radial Diagrams for Visualizing Natural Attenuation Trends for Chlorinated Solvents and Redox Indicators;
 - Avoiding Common Mistakes when Estimating First-Order Biodegradation Rates;
 - Arsenic Mobilization during Natural Attenuation of Organic Compounds;

- Biodegradation Process and Biodegradability of Petroleum Hydrocarbons and Chlorinated Solvents;
- Case Study of Innovative Techniques for Evaluating In-Situ Remediation;
- Introduction to Biogeochemical Processes;
- Overview of Bioremediation Transport Models for Evaluating Natural and Enhanced Bioremediation;
- Overview of Monitored Natural Attenuation: Key Concepts and Regulatory Issues;
- Overview of the Remediation ToolKit: Trend Analysis, Visualization, and Modeling Tools;
- Reactive Transport Modeling for Evaluating Natural and Enhanced Bioremediation;
- Visualizing the Effectiveness of MNA and Enhanced Attenuation Remedies Using SEQUENCE;
- Visual Trend Analysis Methods for Evaluating Monitored Natural Attenuation Trends
- Senior instructor for a half-day short course “Evaluating the Effectiveness of Monitored Natural Attenuation and Enhanced Attenuation Remedies, delivered to the New Jersey Department of Environmental Protection, Trenton, New Jersey, June 28, 2006.

PUBLICATIONS

Refereed Journal Papers

- Carey, G.R., P. Hatzinger, A. Danko, B. Sleep, D. Lippincott, G. Lavorgna, 2025, Modeling the Performance of a Field-Scale PFAS In-Situ Adsorption Barrier, in preparation.
- Carey, G.R., R. Krebs, G.T. Carey, M. Rebeiro-Tunstall, J. Duncan, G.N. Carey, and K. Rooney, 2025, Visualizing PFAS Trends at a South Dakota AFFF-Impacted Site, *Remediation Journal*, 35(3): E70023.
- Newell, C.J., W.B. Smith, K. Kearney, S. Clay, H. Javed, G.R. Carey, S. Richardson, C. Werth, 2025, Tool and Database for Estimating Potential Longevity of Colloidal Activated Carbon Barriers for PFAS in Groundwater, *Remediation Journal*, 35(3): e70017.
- Jiang, L., X. Chen, G. Carey, X. Liu, G. Lowry, D. Fan, A. Danko, and G. Li, 2025, Effects of Physical and Chemical Aging of Colloidal Activated Carbon on the Adsorption of Per- and Poly-fluoroalkyl Substances, *Environmental Science & Technology*, 59(7): 3691-3702.
- Carey, G.R., Danko, A., Pham, A.L-T., Soderberg, K., Hoagland, B., 2025, Modeling the influence of coastal site characteristics on PFAS In Situ Remediation, *Ground Water*, 63(2): 175-191.
- Singh, M., S.G. Hakimabadi, P.J. Van Geel, G.R. Carey, A.L. Pham, 2024, Modified Competitive Langmuir Model for Prediction of Multispecies PFAS Competitive Adsorption Equilibria on Colloidal Activated Carbon, *Separation and Purification Technology*, 345, 127368: 1-12.

- Mole, R., C. de Velosa, G. Carey, X. Liu, G. Li, D. Fan, A. Danko, G. Lowry, 2024, Groundwater Solutes Influence the Adsorption of Short-Chain Perfluoroalkyl Acids (PFAA) to Colloidal Activated Carbon and Impact Performance for In Situ Groundwater Remediation, *Journal of Hazardous Materials*, 474, 134746, 1-10.
- DiGuseppi, W.H., C.J. Newell, G.R. Carey, P.R. Kulkarni, Z. Xia, J. Stults, T.L. Maher, E.F. Houtz, R. Mora, R. Wice, P.W. Tomiczek, S.D. Richardson, J. Xiong, J. Hale, J.P. Hnatko, R. McGregor, J.T. McDonough, A. Oka, R. Thomas, J. Fenstermacher, J. Hatton, 2024, Available and emerging liquid treatment technologies for PFASs, *Remediation Journal*, 34:e21782.
- Carey, G.R., R.H. Anderson, P. Van Geel, R. McGregor, K. Soderberg, A. Danko, S.G. Hakimabadi, A.L.T. Pham, M. Rebeiro-Tunstall, 2023, Analysis of colloidal activated carbon alternatives for in situ remediation of a large PFAS plume and source area. *Remediation Journal*, 34(1): e21772.
- Carey, G.R., S.K. Hakimabadi, M. Singh, R. McGregor, C. Woodfield, P. Van Geel, A.L. Pham, 2022, Longevity of Colloidal Activated Carbon for In-Situ PFAS Remediation at AFFF-Contaminated Airport Sites, *Remediation Journal*, 33(1): 1-21.
- Bryant, J.D., R. Anderson, S.C. Bolyard, J.T. Bradburne, M.L. Brusseau, G. Carey, D. Chiang, R. Gwinn, B.R. Hoyer, T.L. Maher, A.E. McGrath, M. Schroeder, B.R. Thompson, D. Woodward, 2022, PFAS Experts Symposium 2: Key Advances in PFAS Characterization, Fate and Transport, *Remediation Journal*, 32(1-2): 19-28.
- Carey, G.R., R. McGregor, A. Pham, and B. Sleep, and S. Hakimabadi, 2019, Evaluating the Longevity of a PFAS In-Situ Colloidal Activated Carbon Remedy, *Remediation Journal*, Winter 2019.
- McGregor, R. and G.R. Carey, 2019, The In-Situ Treatment of Synthetic Musk Fragrances in Groundwater, *Remediation Journal*, Spring 2019.
- Carey, G.R., E.A. McBean, and S. Feenstra, 2018, Estimating Transverse Dispersivity Based on Hydraulic Conductivity, *Environmental Technology & Innovation*, 10(5): 36-45.
- Carey, G.R., E.A. McBean, and S. Feenstra, 2016, Estimating Tortuosity Coefficient based on Hydraulic Conductivity, *Ground Water*, 54(4): 476-487.
- Carey, G.R., S.W. Chapman, B.L. Parker, and R. McGregor, 2015, Application of an Adapted Version of MT3DMS for Modeling Back-Diffusion Remediation Timeframes, *Remediation Journal*, Autumn 2015, p. 55-79.
- Carey, G.R., E.A. McBean, and S. Feenstra, 2014, DNAPL Source Depletion: 1. Predicting Rates and Timeframes, *Remediation Journal*, Summer 2014, p. 21-47.
- Carey, G.R., E.A. McBean, and S. Feenstra, 2014, DNAPL Source Depletion: 2. Attainable Goals and Cost-Benefit Analyses, *Remediation Journal*, Autumn 2014, p. 79-106.
- Schreiber, M., G.R., D. Feinstein, G.R. Carey, and J. Bahr, 2004, Mechanisms of Electron Acceptor Utilization, *Journal of Contaminant Hydrology*, 73(1-4), p. 99-127.

Carey, G.R., P.J. Van Geel, T.H. Wiedemeier, and E.A. McBean, 2003, A Modified Radial Diagram Approach for Evaluating Natural Attenuation Trends for Chlorinated Solvents and Inorganic Redox Indicators, *Ground Water Monitoring and Remediation*, 23(4): 75-81.

Carey, G.R., T.H. Wiedemeier, P.J. Van Geel, E.A. McBean, J.R. Murphy, and F.A. Rovers, 1999, Visualizing Natural Attenuation Trends: Petroleum Hydrocarbons Attenuation at the Hill Air Force Base, *Bioremediation Journal*, 3(4): 379-393

Book Contributions

Carey, G.R., P.J. Van Geel, E.A. McBean, and F.A. Rovers, 1999, Application of a Biodegradation-Redox Model for Predicting Bioremediation Performance, in P. Baveye, J.C. Block, and V.V. Goncharuk, (Eds.), *Bioavailability of Organic Xenobiotics in the Environment: Practical Consequences for the Environment*, Kluwer Academic Publishers, pp. 73-77.

Farquhar, G.J. and G.R. Carey, 1991, An Overview of Landfill Practices Now and in the Future, *Municipal Solid Waste Management: Making Decisions in the Face of Uncertainty*, University of Waterloo Press, Waterloo, Ontario, pp. 77-92.

Software Manuals

Carey, G.R., 2017, Visual Bio: Radial Diagrams for Visualization Natural and Enhanced Chemical Degradation Trends, Porewater Solutions, Ottawa, Ontario, Canada.

Carey, G.R., 2015, NAPL Depletion Model (NDM): User's Guide, Porewater Solutions, Ottawa, Ontario, Canada.

Carey, G.R., P.J. Van Geel, and J.R. Murphy, 1999, BIOREDOX-MT3DMS: A Coupled Biodegradation-Redox Model for Simulating Natural and Enhanced Bioremediation of Organic Pollutants – V2.0 User's Guide, Conestoga-Rovers & Associates, Waterloo, Ontario, Canada

Carey, G.R., P.J. Van Geel, and J.R. Murphy, 1999, BIOREDOX-MT3DMS: A Coupled Biodegradation-Redox Model for Simulating Natural and Enhanced Bioremediation of Organic Pollutants – V2.0 Verification Manual, Conestoga-Rovers & Associates, Waterloo, Ontario, Canada

Carey, G.R., 1999, BIOREDOX-MT3DMS Tutorial Guide: Modeling Natural Attenuation at the Plattsburgh Air Force Base, Conestoga-Rovers & Associates, Waterloo, Ontario, Canada

Carey, G.R., 1999, The Remediation ToolKit (SEQUENCE, BioTrends, BioTracker) – User's Guide, Conestoga-Rovers & Associates, Waterloo, Ontario, Canada

Conference Presentations and Workshops

- Carey, G.R., M. Vanderkooy, A. Schneider, P. Erickson, K. Gaskill, B. Sleep, 2024, Lessons Learned for Increasing PFAS Remediation Effectiveness, poster presented at the 2024 SERDP-ESTCP Symposium in Washington, D.C., December 4, 2024.
- Carey, G.R., R. Krebs, G.T. Carey, M. Rebeiro-Tunstall, J. Duncan, G.N. Carey, and K. Rooney, 2025, PFAS Visualization for Site Characterization, Remediation, and Forensic Analysis, poster presented at the 2024 SERDP-ESTCP Symposium in Washington, D.C., December 4, 2024.
- Carey, G.R., 2024, PFAS In-Situ Remediation Using CAC: Modeled Field Performance and Cost-Benefit Analysis, presented at The REMTEC Summit, Denver, Colorado, October 14, 2024.
- Carey, G.R., A. Danko, R. Anderson, P. Hatzinger, and K. Soderberg, 2024, Case Studies and Long-Term Strategies for PFAS In-Situ Remediation Using Colloidal Activated Carbon, Battelle 2024 Chlorinated Conference in Denver on June 4, 2024.
- Pennel, K., M. Vanderkooy, A. Pham, N. Thomson, B. Sleep, G. Carey, 2024, Novel Research on PFAS Adsorptive Technologies, 90-minute webinar organized by SERDP-ESTCP, February 22, 2024.
- Vanderkooy, M., A. Pham, N. Thomson, B. Sleep, G. Carey, 2023, Opportunities, Issues, and Ideas for Activated Carbon at PFAS Sites, platform presentation at the 2023 SERDP-ESTCP Symposium in Washington, D.C., November 3, 2023.
- Carey, G.R., S. Hakimabadi, M. Singh, R. McGregor, C. Woodfield, P. Van Geel, A. Pham, 2022, Longevity of Colloidal Activated Carbon for In-Situ PFAS Remediation at AFFF-Contaminated Airport Sites, poster presentation at the 2022 SERDP-ESTCP Symposium in Washington, D.C., November 30, 2022.
- Carey, G.R., P. Van Geel, M. Singh, 2022, New Empirical Model for Predicting PFAS Breakthrough in Granular Activated Carbon, poster presentation at the 2022 SERDP-ESTCP Symposium in Washington, D.C., November 30, 2022.
- Carey, G.R., 2022, Radial Diagram Visualization and Semi-Quantitative Forensic Methods for PFAS Site Characterization, poster presentation at the 2022 SERDP-ESTCP Symposium in Washington, D.C., November 30, 2022.
- Bryant D. and G.R. Carey, 2022, invited expert participant in the PFAS Experts Webinar entitled USEPA's Health Advisory Levels Explained: What, Why, and When, presentation on Background PFAS Concentrations, organized by the Remediation Journal, July 19, 2022.
- Carey, G.R., 2021, Invited expert participant in the PFAS Experts Symposium 2, organized by the Remediation Journal, June 29, 2021.
- Carey, G.R., 2019, State of PFAS Remediation, Invited Panelist at the PFAS Research Symposium organized by CRC Care, Adelaide, Australia, September 2019.
- Carey, G.R., 2019, In-Situ PFAS Remediation Using Colloidal Activated Carbon, Invited Keynote address at the International CleanUp Conference, Adelaide, Australia, September 9-11, 2019.
- Carey, G.R., 2018, Modeling LNAPL Depletion at a Former Xylene Processing Facility (Germany), accepted for platform presentation at the 2018 Battelle Conference on Remediation of Chlorinated and Recalcitrant Compounds, Palm Springs, CA, April 9, 2018.

- Carey, G.R., 2018, Innovative Visualization Method for Demonstrating Natural and Enhanced Attenuation, presented at the 2018 SmartRemediation conference in Ottawa, Ontario, February 15, 2018.
- Carey, G.R., 2017, Innovative Visualization Method for Delineating Biodegradation Zones in Groundwater, presented at the 2017 Cleanup Conference, Melbourne, Australia, September 12, 2017.
- Carey, G.R., R. McGregor, and J. Birnstingl, 2017, In-Situ Remediation of a PFOS/PFOA Plume In Ontario, presented at the 2017 Cleanup Conference, Melbourne, Australia, September 12, 2017.
- Carey, G.R., 2016, In-Situ Remediation (ISR-MT3DMS) For Modeling Back-Diffusion Timeframes, platform presentation at the 10th International Conference on Remediation of Chlorinated and Recalcitrant Compounds, Battelle, Palm Springs, California, May 22-26, 2016.
- Carey, G.R., 2016, Forensic Analysis of NAPL Architecture at a Field Site using the NAPL Depletion Model (NDM), poster presentation at the 10th International Conference on Remediation of Chlorinated and Recalcitrant Compounds, Battelle, Palm Springs, California, May 22-26, 2016.
- Carey, G.R., 2015, Using the NAPL Depletion Model (NDM) for Forensic Analysis of NAPL Architecture at a Field Site, presented at the 30th Biennial Groundwater Conference, Sacramento, California, October 6-7, 2015.
- Carey, G.R., 2015, Using In-Situ Remediation (ISR-MT3DMS) to Model Back-Diffusion Timeframe for Thin Silts and Clays, presented at the 30th Biennial Groundwater Conference, Sacramento, California, October 6-7, 2015.
- Carey, G.R., 2015, Invited to Chair the Fractured Rock Session at Cleanup 2015 Conference, organized by CRC Care, Melbourne, Australia, September 13-16, 2015.
- Carey, G.R., 2015, Review of Characterization Methods for NAPL Source Zone Delineation and Mass Estimation, Invited Keynote presentation at Cleanup 2015 Conference, organized by CRC Care, Melbourne, Australia, September 13-16, 2015.
- Carey, G.R., 2015, ISR-MT3DMS for Modeling Back-Diffusion Timeframe, invited platform presentation at Cleanup 2015 Conference, organized by CRC Care, Melbourne, Australia, September 13-16, 2015.
- Carey, G.R., 2015, Modeling LNAPL Depletion at a Former Xylene Processing Facility (Germany), invited platform presentation at Cleanup 2015 Conference, organized by CRC Care, Melbourne, Australia, September 13-16, 2015.
- Carey, G.R., 2015, ISR-MT3DMS for Modeling Back-Diffusion Timeframe, presented at REMTEC Summit, Westminster, Colorado, March 3, 2015.
- Carey, G.R. and E.A. McBean, 2013, Predicting Achievable Mass Discharge Goals, Timeframes, and Back-Diffusion Contributions, invited platform presentation at REMTEC Summit, Westminster, Colorado, March 4-6, 2013.
- Carey, G.R., M. King, J. Christensen, and C. Pattersen, 2013, Modeling the Influence of Tidal Pumping on Naphthalene Transport through an AquaBlok Cap, presented at Battelle's Conference on Remediation of Contaminated Sediments, Dallas, Texas, February 4-7, 2013.

- Carey, G.R. and E.A. McBean, 2010, Uses, Benefits, and Limitations of Mass Flux and Mass Discharge: A Case Study Review, presented at Consoil 2010, Salzburg, Austria, September 22-24, 2010.
- Carey, G.R. and E.A. McBean, 2010, NAPL Depletion Model (NDM) for Predicting Remediation Timeframe, presented at Consoil 2010, Salzburg, Austria, September 22-24, 2010.
- Carey, G.R. and E.A. McBean, 2010, Validation of a Mass Balance Approach for Estimating DNAPL Remediation Timeframe, presented at Battelle 2010 Remediation of Chlorinated and Recalcitrant Compounds, Monterey, California, May 24-27, 2010.
- Carey, G.R. and E.A. McBean, 2010, A Mass Balance Approach for Estimating DNAPL Source Remediation Timeframe, presented at the 2010 RPIC Federal Contaminated Sites National Workshop in Montreal, QC May 10-13, 2010.
- Carey, G.R. and E.A. McBean, 2010, Back-Diffusion and Discount Rate Implications for DNAPL Remediation Strategies, presented at the 2010 RPIC Federal Contaminated Sites National Workshop in Montreal, QC May 10-13, 2010.
- Stroo, H. and G.R. Carey, 2010, Use and Measurement of Mass Flux and Mass Discharge, invited platform presentation at the AFCEE Technology Transfer Workshop in San Antonio, Texas, April 6-9, 2010.
- Carey, G.R., 2006 Plattsburgh Mass Balance Modeling Case Study, invited to submit to Savannah River National Laboratory, 2006.
- Carey, G.R., J. Vaillancourt, M.G. Mateyk, and J. Maude, 2006, Case Study Feasibility Study for an In Situ Oxygen Curtain, presented at the Fifth International Conference on Remediation of Chlorinated and Recalcitrant Compounds, Monterey, California, May 22-25, 2006.
- Carey, G.R., 2006, "Overview of Monitored Natural Attenuation", excerpt from the "ITRC MNA and Enhanced Attenuation Resource Guide", available online in 2006.
- Kean, J., K. Wilson, J. Doyon, K.M. Vangelas, and G. Carey, 2006, Monitored Natural Attenuation and Enhanced Attenuation – A National Overview: Results of an ITRC Survey, in Proceedings of the Fifth International Conference on Remediation of Chlorinated and Recalcitrant Compounds, Monterey, California, May 22-25, 2006.
- Kean, J., K.M. Vangelas, K. Wilson, G.R. Carey, D. Green, J. Doyon, and P. Harrington, 2005, Monitored Natural Attenuation and Enhanced Attenuation – A National Overview: Results of an ITRC Survey, presented at the SERDP conference, Seattle, Washington, November 2005.
- Carey, G.R., "Visualizing the Effectiveness of MNA and Enhanced Attenuation Remedies Using SEQUENCE ", presented at the ITRC EACO team meeting, October 2005.
- Carey, G.R., D. Major, D. Verret, and M. Roworth, 2003, Visualization and Modeling of Bioaugmentation at Kelly Air Force Base, presentation at the Seventh International Symposium on In Situ and On-Site Bioremediation, Orlando, Florida, June 2-5, 2003
- Carey, G.R. and M. Roworth, 2003, Evaluating Remediation Timeframe for Combined Source Containment-MNA Remedies, presentation at the Seventh International Symposium on In Situ and On-Site Bioremediation, Orlando, Florida, June 2-5, 2003.
- King, M., G. Carey, D. Abbey and F. Baechler, 2003, Groundwater and Contaminant Transport Modelling at the Sydney Tar Ponds, in Proceedings of the 2003 IAH Conference, Winnipeg, Canada.

- Carey, G.R., 2001, Case Study of New Techniques for Calculating Biodegradation Rates, presented at the Sixth International Symposium on In Situ and On-Site Bioremediation, San Diego, California, 2001.
- Carey, G.R., Derivation of Multi-Dimensional Inverse Models for Estimating First-Order Biodegradation Rates, Technical Note published online by the Environmental Institute for Continuing Education, July 17, 2001.
- Carey, G.R. and P.J. Van Geel, 2000, Calibration of a Leachate Natural Attenuation Model for the Vejen Landfill (Denmark), in Proceedings of the Groundwater 2000 Conference, Copenhagen, Denmark, June 2000.
- Van Geel, P.J., K. Britton, and G.R. Carey, 1999, Impact of Biodegradation Rates on the Redox Zones Generated below Landfills, Proceedings of the 52nd Canadian Geotechnical Conference, Regina, Saskatchewan, October 24-27, 1999.
- Carey, G.R., P.J. Van Geel, J.R. Murphy, E.A. McBean, and F.A. Rovers, 1999, Modeling Natural Attenuation at Plattsburgh Air Force Base, Presented at the Fifth International Symposium on In Situ and On-Site Bioremediation, San Diego, California, April 19-22, 1999.
- Carey, G.R., E.A. McBean, and F.A. Rovers, 1999, Visualizing Natural Attenuation Trends, in Proceedings of the Fifth International Symposium on In Situ and On-Site Bioremediation, San Diego, California, April 19-22, 1999.
- Carey, G.R., E.A. McBean, and F.A. Rovers, 1999, Risk Management Using Natural Attenuation Processes, presented at the 1999 Risk Management Symposium, Air Force Space Command, February 1999.
- Carey, G.R., P.J. Van Geel, J.R. Murphy, E.A. McBean, and F.A. Rovers, 1998, Full-Scale Field Application of a Coupled Biodegradation-Redox Model (BIOREDOX), in Proceedings of the First International Conference on Remediation of Chlorinated and Recalcitrant Compounds, Monterey, California, May 18-21, 1998.
- P.J. Van Geel, G.R. Carey, E.A. McBean, and F.A. Rovers, 1998, An Integrated Landfill Modeling System (ILMS) for Evaluating Remediation Alternatives, in Proceedings of the First International Conference on Remediation of Chlorinated and Recalcitrant Compounds, Monterey, California, May 18-21, 1998.
- Harris, S.M., S. Day, E. Roberts, F.A. Rovers, and G.R. Carey, 1998, Applications of an Innovative Method for Visualizing Natural Attenuation, in Proceedings of the First International Conference on Remediation of Chlorinated and Recalcitrant Compounds, Monterey, California, May 18-21, 1998.
- Carey, G.R., P.J. Van Geel, J.R. Murphy, E.A. McBean, and F.A. Rovers, 1998, Coupled Biodegradation-Redox Modeling to Simulate Natural Attenuation Processes at the Plattsburgh Air Force Base (New York), in Proceedings of MODFLOW'98, Golden, Colorado, October 5-7, 1998.
- Carey, G.R., P.J. Van Geel, J.R. Murphy, and E.A. McBean, 1998, An Efficient Screening Approach for Modeling Natural Attenuation, in Proceedings of MODFLOW'98, Golden, Colorado, October 6-8, 1998.
- Carey, G.R., P.J. Van Geel, E.A. McBean, and F.A. Rovers, 1997, An Innovative Modeling and Visualization Approach for Demonstrating the Effectiveness of Natural Attenuation, presented at the IBC Natural Attenuation '97 Conference, December 8-10, Scottsdale, Arizona.

- Carey, G.R., P.J. Van Geel, E.A. McBean, F.A. Rovers, and G.T. Turchan, 1997, Modeling Landfill Cap Influence on Natural Attenuation, in Sardinia'97, Proceedings of the Sixth International Landfill Symposium, October 13-17, Cagliari, Italy.
- Carey, G.R., P.J. Van Geel, E.A. McBean, F.A. Rovers, 1997, Effect of Landfill Cap Permeability on the Natural Attenuation of Chlorinated Solvents Below a Landfill, in 1997 Canadian Geotechnical Conference Proceedings, October 20-22, Ottawa, Ontario.
- Carey, G.R., M.G. Mateyk, G.T. Turchan, E.A. McBean, F.A. Rovers, J.R. Murphy, and J.R. Campbell, 1996, Application of an Innovative Visualization Method for Demonstrating Intrinsic Remediation at a Landfill Superfund site, Proceedings of API/NGWA Petroleum Hydrocarbons and Organic Chemicals in Groundwater Conference, Houston, Texas.
- Carey, G.R., M.G. Mateyk, E.A. McBean, G.T. Turchan, J.R. Campbell, and F.A. Rovers, 1996, Multiple Lines of Evidence for Evaluating Intrinsic Remediation at a Landfill Site, Proceedings of the Nineteenth International Madison Waste Conference, Madison, Wisconsin.


APPENDIX B

2025 PFAS Visualization Journal Paper

Carey, G.R., R. Krebs, G.T. Carey, M. Rebeiro-Tunstall, J. Duncan, G.N. Carey, and K. Rooney, 2025, Visualizing PFAS Trends at a South Dakota AFFF-Impacted Site, *Remediation Journal*, 35(3): E70023.

RESEARCH ARTICLE OPEN ACCESS

Visualizing PFAS Trends at a South Dakota AFFF-Impacted Site

Grant R. Carey^{1,2}  | Rita K. Krebs³ | Gabriel T. Carey¹ | Mia Rebeiro-Tunstall¹ | Jeremiah Duncan⁴ | Gillian N. Carey¹ | Kiera Rooney¹

¹Porewater Solutions, Ottawa, Ontario, Canada | ²Carleton University, Ottawa, Ontario, Canada | ³Air Force Civil Engineer Center (AFCEC), Ellsworth AFB, South Dakota, USA | ⁴GZA GeoEnvironmental Inc., Meredith, New Hampshire, USA

Correspondence: Grant R. Carey (gcarey@porewater.com)

Received: 26 December 2024 | **Revised:** 10 May 2025 | **Accepted:** 28 May 2025

Keywords: AFFF | forensic | PFAS | radial diagram | stacked bar | visualization

ABSTRACT

Various visualization alternatives are demonstrated for evaluating per- and polyfluoroalkyl substances (PFAS) trends at an aqueous film forming foam- (AFFF-) impacted site in South Dakota, including the use of radial diagrams, stacked bar maps, and pie charts. The purpose of this study was to compare and contrast visualization methods which may be used for PFAS site characterization or forensic assessments. PFAS groundwater concentration trends are first visualized based on site-wide wells with maximum perfluorosulfonic acid (PFOS) plus perfluorooctanoic acid (PFOA) concentrations in AFFF source areas. Then a more detailed analysis of trends, including the potential for precursor transformations to perfluoroalkyl acids (PFAAs), is presented for a smaller portion of the site where former fire training activities were conducted. The advantages of using radial diagram reference series, such as maximum source or background concentrations, to better illustrate changes along a flow path are discussed. The benefits of including symbols on radial diagram maps to illustrate where PFAS are non-detect or are in exceedance of site cleanup criteria, particularly in support of a PFAS plume delineation, are demonstrated. Radial diagrams and stacked bar maps are used to illustrate the relative proportion of perfluoroalkyl sulfonates and carboxylates in groundwater, which may help to identify relative contributions of AFFF products derived from electrochemical fluorination versus telomerization manufacturing processes. The benefit of using select PFAS ratios on radial diagram axes to support a combined assessment of precursor transformation and PFAA production along a flow path is demonstrated. Stacked bar maps are shown to have significant advantages over pie charts for PFAS forensic analyses.

1 | Introduction

Per- and polyfluoroalkyl substances (PFAS) are widespread in the environment, and some PFAS are both resistant to degradation and are toxic at very low concentrations. PFAS that are regulated due to toxicity in groundwater and drinking water are typically a subset of constituents within the perfluoroalkyl acids (PFAAs) class. PFAAs may be further subdivided into two groups: perfluoroalkyl carboxylates (*carboxylates*) and perfluoroalkyl sulfonates (*sulfonates*). Precursors are parent PFAS species which may biodegrade, predominantly under aerobic

conditions in groundwater, to PFAAs, which are recalcitrant due to the strength of the carbon-fluorine bond.

The US Environmental Protection Agency (USEPA; 2024) recently introduced new maximum contaminant levels (MCLs) including for the following PFAAs, which are typically present at AFFF-impacted sites: perfluorooctane sulfonate (PFOS) at 0.004 µg/L, perfluorohexane sulfonate (PFHxS) at 0.010 µg/L, perfluorooctanoate (PFOA) at 0.004 µg/L, and perfluorononanoate (PFNA) at 0.010 µg/L. These low MCLs pose a challenge to site remediation because PFAS concentrations in

This is an open access article under the terms of the [Creative Commons Attribution](https://creativecommons.org/licenses/by/4.0/) License, which permits use, distribution and reproduction in any medium, provided the original work is properly cited.

© 2025 The Author(s). *Remediation Journal* published by Wiley Periodicals LLC.

groundwater are often orders of magnitude higher than these criteria.

USEPA also included perfluorobutane sulfonate (PFBS) in a hazard index calculation when at least one of two other PFAS are present in a “mixture” at AFFF-impacted sites: PFHxS and PFNA. EPA also included hexafluoropropylene oxide dimer acid, or HFPO-DA (in the Gen-X class) in this hazard index calculation, and with a separate MCL of 0.010 µg/L; however, our experience has been that the majority of AFFF-impacted sites do not have HFPO-DA present, so this compound is not considered further in this present study.

If PFBS is present in a mixture with PFHxS and/or PFNA, then the health-based water concentration (HBWC) used for PFBS in the hazard index calculation is 2 µg/L, which is orders of magnitude higher than the long-chain PFAA MCLs. Even when PFBS is present in a mixture, its concentration is often below the HBWC, and PFHxS and/or PFNA in a plume are likely to exceed the respective low MCL criteria. Therefore, PFBS is typically not a regulatory driver compared to the regulated long-chain species.

Aqueous film-forming foam (AFFF) containing PFAS has been used to support fire fighting activities at military and civilian airport sites starting in the late 1960s (Yan et al. 2024). There are two types of processes used to manufacture AFFF products: electrochemical fluorination (ECF) and telomerization. Each of these manufacturing processes use different types of ingredients in the AFFF formulation, resulting in markedly different PFAS fingerprints in AFFF-impacted groundwater.

Impacts to groundwater associated with the ECF-based AFFF, which was almost exclusively used by 3 M (Yan et al. 2024), typically includes higher concentrations of sulfonates, such as PFOS and PFHxS, and lower concentrations of PFBS. Impacts from this type of AFFF product may also include secondary precursors such as perfluoroalkane sulfonamides (FASAs), including perfluorooctane sulfonamide (FOSA), which may biodegrade to PFOS, and perfluorohexane sulfonamide (FHxSA), which may biodegrade to PFHxS.

Yan et al. (2024) indicate that impacts to groundwater from telomerization-based AFFF include precursors such as $n:2$ fluorotelomer sulfonates (e.g., 6:2 FtS, 8:2 FtS, and/or 4:2 FtS). Each of these fluorotelomer sulfonates will degrade to carboxylates having n , $n - 1$, and $n - 2$ carbon atoms. For example, 6:2 FtS is commonly found at relatively high concentrations at AFFF-impacted sites, and this may biodegrade to perfluorobutanoate (PFBA), perfluoropentanoate (PFPeA), and perfluorohexanoate (PFHxA), which contain 4, 5, and 6 carbon atoms, respectively.

Carey et al. (2022) and Molé et al. (2024) present statistical analyses of the maximum groundwater concentrations at 96 AFFF-impacted sites that include PFOS, PFHxS, PFBS, PFOA, and PFNA. This analysis determined that the two sulfonates with MCLs (PFOS and PFHxS) typically have higher concentrations than the two carboxylates with MCLs (e.g., PFOA and PFNA). PFNA was also shown to typically have groundwater concentrations at AFFF-impacted sites that are at least an order of magnitude lower than PFOA.

A number of PFAS-impacted sites are either at or will soon be reaching the remedial investigation (or equivalent) phase. Laboratory analysis of PFAS in groundwater and soil samples will include results for up to 40 PFAS (i.e., precursors and PFAAs) when the analysis is conducted using EPA Method 1633. The large number of analytes associated with each soil and groundwater sample poses a major challenge for data analysis, and for communicating the results of site characterization to a nontechnical audience.

Visualization techniques may be used to support these PFAS site characterization efforts, including assessment of:

- Source zone and groundwater plume delineation;
- Precursor biotransformation to corresponding PFAAs along a flow path;
- Redox zone delineation (e.g., aerobic, moderately anaerobic, and strongly anaerobic) to support a precursor biotransformation analysis;
- Total oxidizable precursor (TOP) assay results along a flow path to determine the maximum potential for PFAA increases due to future precursor transformations;
- Temporal changes due to remediation or non-stable plume transport;
- Source differentiation and forensic analysis of contributions from multiple sites to a commingled plume; and,
- Visual comparison of background levels to PFAS at various site monitoring wells.

Visual aids that are capable of illustrating spatial and/or temporal distributions of multiple PFAS species on a single map are particularly useful, given the need to assess both intra-well and inter-well trends for PFAS in the source area and within a downgradient plume. Carey et al. (1996, 1999, 2003) demonstrate several case study examples of how radial diagrams may be used to support analogous applications for chlorinated solvents and petroleum hydrocarbons. Radial diagrams were used to provide a temporal analysis of pre- and post-remediation PFAS concentrations for a PlumeStop barrier based on in-barrier and down-gradient monitoring wells (Carey 2024). Pie charts have been applied to assess relative proportions of PFAS constituents within a group on site maps (e.g., Reinikainen et al. 2022). The use of stacked bars to visualize PFAS trends is not typically conducted with site maps, although this method may have some advantages over pie chart maps as discussed below.

The purpose of this study is to evaluate the benefits and limitations associated with a range of visualization alternatives for an AFFF-impacted site in South Dakota, including the use of radial diagrams, stacked bar maps, and pie charts. Two data sets were used for this case study analysis: site-wide groundwater samples collected during a 2019 PFAS Site Inspection at AFFF source areas; and local groundwater samples collected in 2012 at a former fire training area in a smaller portion of the site. Different types of data were available with each data set, which facilitated a review of multiple visualization alternatives between the two study areas. The advantages and disadvantages of each visualization alternative are discussed, and key findings

from each of the two studies at this AFFF-impacted site are presented.

2 | Site Setting

The 5400-acre site used for this case study contains an airfield which has been in use since the 1940s. A site-wide screening level study (Site Inspection) identified 13 AFFF source areas (AFFF-1, AFFF-2A, AFFF-2B, and AFFF-3 through AFFF-12). The general location and size of each AFFF area is shown on Supporting Information S1: Figure SI-1. These AFFF source areas were identified based on the location of current fire training activities (AFFF-1), the former site wastewater treatment plant which received discharges from areas with AFFF spills or drainage (AFFF-10), known AFFF spills, and AFFF applications at historical crash sites and a nozzle test area (see Supporting Information S1: Table SI-1).

Multiple groundwater monitoring wells were sampled for PFAS at each of these AFFF areas (Aerostar 2019). The monitoring well at each AFFF area with the highest sum of PFOS and PFOA concentrations was used in the Site Inspection data set for this visualization study. One of the objectives with visualizing the Site Inspection data was to compare the maximum PFAS groundwater concentrations across these 13 AFFF source areas.

In addition to these AFFF areas, a former fire training area (FTA) with a known AFFF source area was contained in a distinct operable unit (OU-1) in the southwest portion of the site. McGuire (2013) and McGuire et al. (2014) present details on the history of AFFF use at this former FTA, and the hydrogeologic setting for OU-1. In this portion of the site, the groundwater direction is southward. The location of OU-1, which is approximately 8 acres in size, is shown in the southwest portion of Supporting Information S1: Figure SI-1. The former FTA at OU-1 is adjacent to the current FTA (AFFF-1). McGuire et al. (2014) presented 2012 groundwater sample results for temporary and permanent monitoring wells, with analytes including carboxylates, sulfonates, and three precursors (6:2 FtS, 8:2 FtS, and FHexSA). This 2012 monitoring event also included TOP assay results (Δ PFBA, Δ PFPeA, Δ PFHxA, Δ PFHpA, and Δ PFOA). This 2012 combined data set was used for evaluating alternative visualization approaches not considered in the site-wide AFFF area analysis.

3 | PFAS Visualization at Site-Wide AFFF Areas

3.1 | Components of a Radial Diagram

Figure 1a shows an example radial diagram that includes axes to represent three sulfonates (PFOS, PFHxS, and PFBS); and FHexSA which is a precursor that may biodegrade to PFHxS under aerobic conditions. The PFAA axes are sequenced in order of chain length which facilitates a relatively quick visual comparison of long versus short-chain concentrations at each well location. In this example, a *reference* series is shown on Figure 1a to represent the maximum source zone concentrations, and a single *monitoring event* series representing sample

results at a downgradient well is shown as the data series with blue fill. When these radial diagrams are plotted at individual well locations on a site map, the well-specific monitoring event series will change at each well location. The reference series (e.g., maximum source zone concentrations) will be uniform across all well radial diagrams.

The distance between one pair of tick marks on an axis represents an order of magnitude change in concentration when the axis is plotted using a logarithmic scale. So changes in concentration with radial diagrams may be visually estimated by counting the number of tick marks between the reference and monitoring event series. The purpose of including a reference series on the radial diagram, in addition to the well-specific concentrations for a specific monitoring event, is to allow for more effective visualization of changes in well concentrations with distance downgradient from a source zone. It is easier to visualize the size of the gap by counting the number of tick marks between the reference series and the well-specific monitoring event series, than trying to visually measure changes in the size of well-specific series in radial diagrams overlaid onto a site map. This will be demonstrated further in the radial diagram map discussion below.

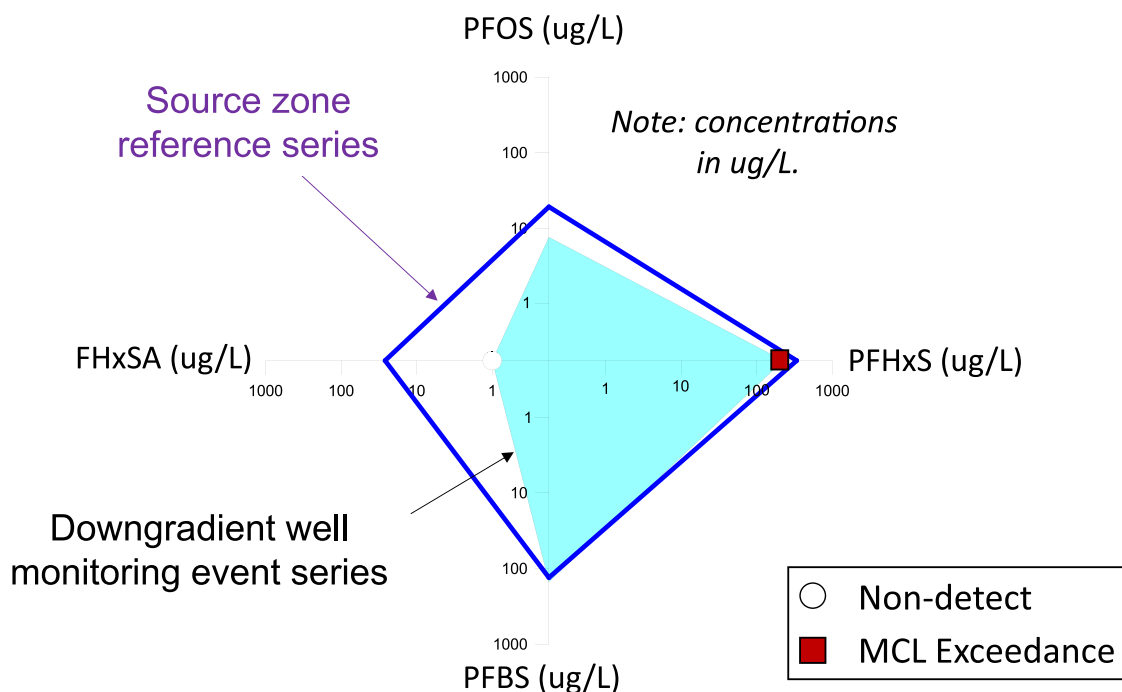
For this example, inspection of Figure 1a reveals that the FHexSA concentration at the downgradient well has declined about 1.5 orders of magnitude relative to the maximum source zone concentration, and PFOS has declined close to half an order of magnitude. In this example, there has been relatively little change in PFHxS and PFBS concentrations between the source zone and the downgradient well location.

Figure 1a also demonstrates the use of symbols for representing MCL or other cleanup criteria exceedances, and to represent non-detect results. Including symbols to identify cleanup criteria exceedances, with multiple regulated PFAS constituents shown on a site radial diagram map, facilitates delineation of the extent of exceedances and the corresponding plume boundary.

The radial diagram figures included with this study were prepared using Visual PFAS (Porewater Solutions, 2024). Visual PFAS provides the option of plotting non-detect values on radial diagram axes: (i) at the minimum axis range; (ii) at the detection limit; or (iii) at one-half of the detection limit. For the site-wide AFFF radial diagram maps prepared for this study, the detection limits associated with non-detects were available, and thus non-detects were plotted at the corresponding detection limit for each sample result. If a non-detect is recorded for a PFAS species and the detection limit is below the minimum axis range for that species, then the data series line and non-detect symbol will be plotted at the minimum range on the axis. For the OU-1 area in the southwest portion of the site, detection limits associated with non-detects were not available, and thus non-detects for this localized portion of the site were plotted on radial diagrams at the minimum axis range.

Figure 1b shows another example of a PFAS radial diagram for a hypothetical site, this time with nine PFAAs (three sulfonates and six carboxylates). The reference series in this example represents background concentrations for each of the nine

a) Sulfonates and precursor radial diagram for a downgradient monitoring well with source zone reference series



b) PFAAs radial diagram for a site monitoring well with a background reference series

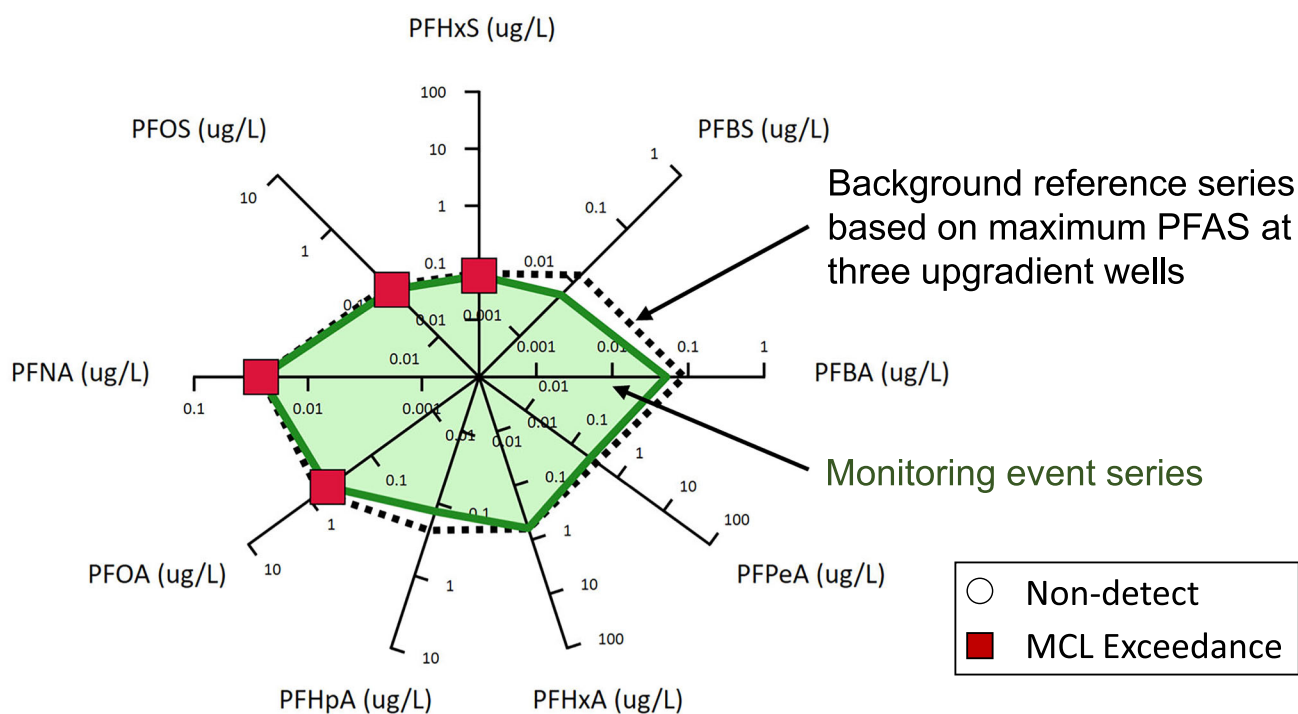


FIGURE 1 | Components of a PFAS radial diagram. [Color figure can be viewed at [wileyonlinelibrary.com](https://onlinelibrary.wiley.com/doi/10.1002/rem.70023)]

PFAS species based on upgradient background wells, which is in contrast to the prior example that used maximum source concentrations as the reference series. The well-specific monitoring event series on Figure 1b represents PFAS concentrations at a downgradient site well. Using this type of example, a

single radial diagram map can be used to visually compare background levels to site-wide monitoring well concentrations for up to 5 to 10 PFAS species. This provides a simple qualitative approach for evaluating which site wells (if any) indicate the influence of site-derived PFAS impacts.

Selection of the minimum and maximum values for each PFAS axis is typically based on two potential approaches:

- Uniform axis limits for all PFAS axes (e.g., Figure 1a), which facilitates the rapid intra-well visualization of differences in concentrations between each PFAS at individual well locations; or,
- Varying axis limits (e.g., Figure 1b) based on PFAS-specific concentration ranges at the site, which more easily facilitates inter-well comparisons of how individual PFAS concentrations change between well locations.

3.2 | Radial Diagram Maps

Figure 2 shows a radial diagram map for PFAS of Concern (POCs), that is, EPA-regulated PFAS, with axes sequenced in the following order: PFOS, PFHxS, PFBS, PFNA, and PFOA. The radial diagram legend shows that all axes range from 0.01 to 1000 $\mu\text{g/L}$. Some minor detections at AFFF areas are less than 0.01 $\mu\text{g/L}$, but it helps the visualization process to use fewer tick marks on an axis, so the axis minimum was chosen to be 0.01 $\mu\text{g/L}$, which is at or only slightly above applicable MCLs. In this example, all axes have the same minimum and maximum range to facilitate intra-well comparison of PFAS concentrations. All axes are shown with a logarithmic scale given that PFAS concentrations vary by orders of magnitude between AFFF areas. A reference series is shown with the maximum source area concentrations, which correspond to the AFFF-1 monitoring well for all five POCs. AFFF-2A and AFFF-4 radial diagrams have been offset from the actual well locations to avoid overlap with radial diagrams at nearby well locations.

The relative size of monitoring event series (orange fill) shown on Figure 2 varies for each AFFF area; the size and shape of this data series depends on the relative PFAS concentrations at each location. Inspection of Figure 2 indicates that it is sometimes difficult to determine which wells have higher and lower PFAS concentrations for AFFF areas by inspecting only the monitoring event series at each well location in Figure 2. Visualization of concentration changes between wells is more effectively conducted by visually measuring the gap between the reference series and the monitoring event series at each well location.

Inspection of this radial diagram map reveals the following trends:

- The current FTA (AFFF-1) has the highest concentrations for all five POCs out of the 13 AFFF areas.
- AFFF-8 (2006 Marten crash) and AFFF-10 (former wastewater treatment plant) have the lowest groundwater concentrations out of all AFFF areas, with no MCL exceedances at AFFF-8 and only low-level MCL exceedances at AFFF-10 for PFHxS, PFOS, and PFOA.
- PFBS exceeded the HBWC at only two AFFF areas: AFFF-1 and AFFF-12. The PFBS concentration at AFFF-12 is proportionally larger than other POC concentrations, relative to trends at AFFF-1. This suggests that a different formulation

of ECF-based AFFF may have been used at AFFF-12 (and possibly also AFFF-1) compared to the ECF-based product variations used at other areas.

- PFNA exceeded the EPA MCL at six of 13 AFFF areas (AFFF-1, AFFF-2B, AFFF-3, AFFF-4, AFFF-6, and AFFF-12), and PFNA is typically lower than PFOA across the site.

Another option with radial diagrams is to use each axis to represent a ratio of select PFAS concentrations to another PFAS species. For example, Figure 3 shows a radial diagram map where all POC axes represent the ratio of the respective POC concentration to the PFOS concentration at the same well location. A ratio of 1.0 indicates that the POC and PFOS have the same concentration at the well. As expected, the PFOS:PFOS axis shows a ratio of 1 for all well locations.

Inspection of Figure 3 indicates that PFHxS is significantly higher than PFOS at four AFFF areas (AFFF-4, AFFF-7, AFFF-11, and AFFF-12). One potential explanation for this trend is that enhanced precursor biotransformation to PFHxS (relative to potential precursor transformation to PFOS) may be occurring at these four locations. Figure 2 indicates that PFOS, PFHxS, and PFBS are at least one order of magnitude higher than PFOA at AFFF-12, which suggests that ECF-based AFFF was predominantly used in this source area. Given that ECF-based AFFF typically contains ten times higher concentrations of PFOS than PFHxS (Interstate Technology Regulatory Council ITRC 2024), the high PFHxS concentrations at AFFF-12 further suggests this has been caused by precursor biotransformation to PFHxS.

Inspection of Figure 3 also indicates that:

- PFBS concentrations at the site are typically one or more orders of magnitude lower than PFOS, with PFOS to PFBS ratios greater than 10. This is consistent with many other AFFF sites (Carey et al. 2022; Molé et al. 2024), as well as with the relative ratios of PFOS to PFBS in ECF- and fluorotelomer-based AFFF products (Interstate Technology Regulatory Council ITRC 2024). Three AFFF areas have ratios of PFOS to PFBS between 1 and 5 (AFFF-4, AFFF-7, AFFF-11), and AFFF-12 has a PFBS concentration 2.5 times higher than PFOS, indicating that precursor transformation to PFBS may have been significant in these four source areas. (Note that differential transport may influence the ratio of PFBS:PFOS in a long plume; however, it is not expected to influence this ratio directly in a source area where conditions are more likely to be stable.)
- PFOA is one-half to one order of magnitude lower than PFOS at six AFFF areas and is similar to PFOS concentrations at the remaining AFFF areas. This indicates that a mixture of ECF- and fluorotelomer-based AFFF products have been used at the site over time.
- PFNA is one to two orders of magnitude lower than PFOS at 10 of 13 monitoring locations. This is consistent with a statistical analysis of PFAS trends at 96 AFFF-impacted sites (Carey et al. 2022).

Non-detect symbols plotted for the AFFF-8 radial diagram on Figure 2 indicate that the only POC detected at this southern-most

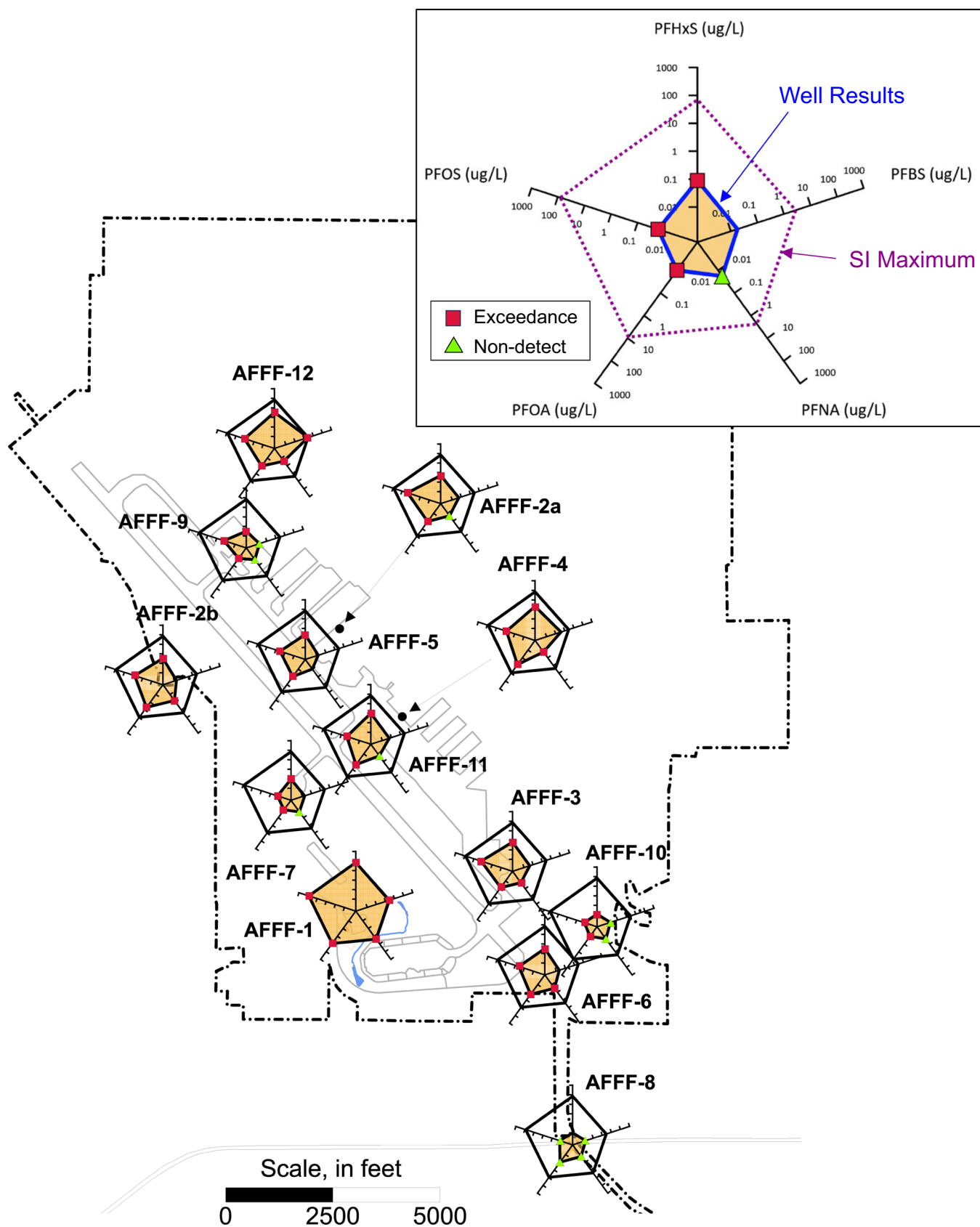


FIGURE 2 | PFAS of Concern (POCs) radial diagrams at AFFF source areas with PFASs in the upper portion (PFOS, PFHxS, and PFBS) and carboxylates in the lower portion (PFNA and PFOA). Exceedance symbols are based on EPA maximum contaminant levels (MCLs), or EPA health-based water concentrations for PFBS. Non-detects are plotted at detection limits. [Color figure can be viewed at [wileyonlinelibrary.com](https://onlinelibrary.wiley.com/doi/10.1002/rem.70023)]

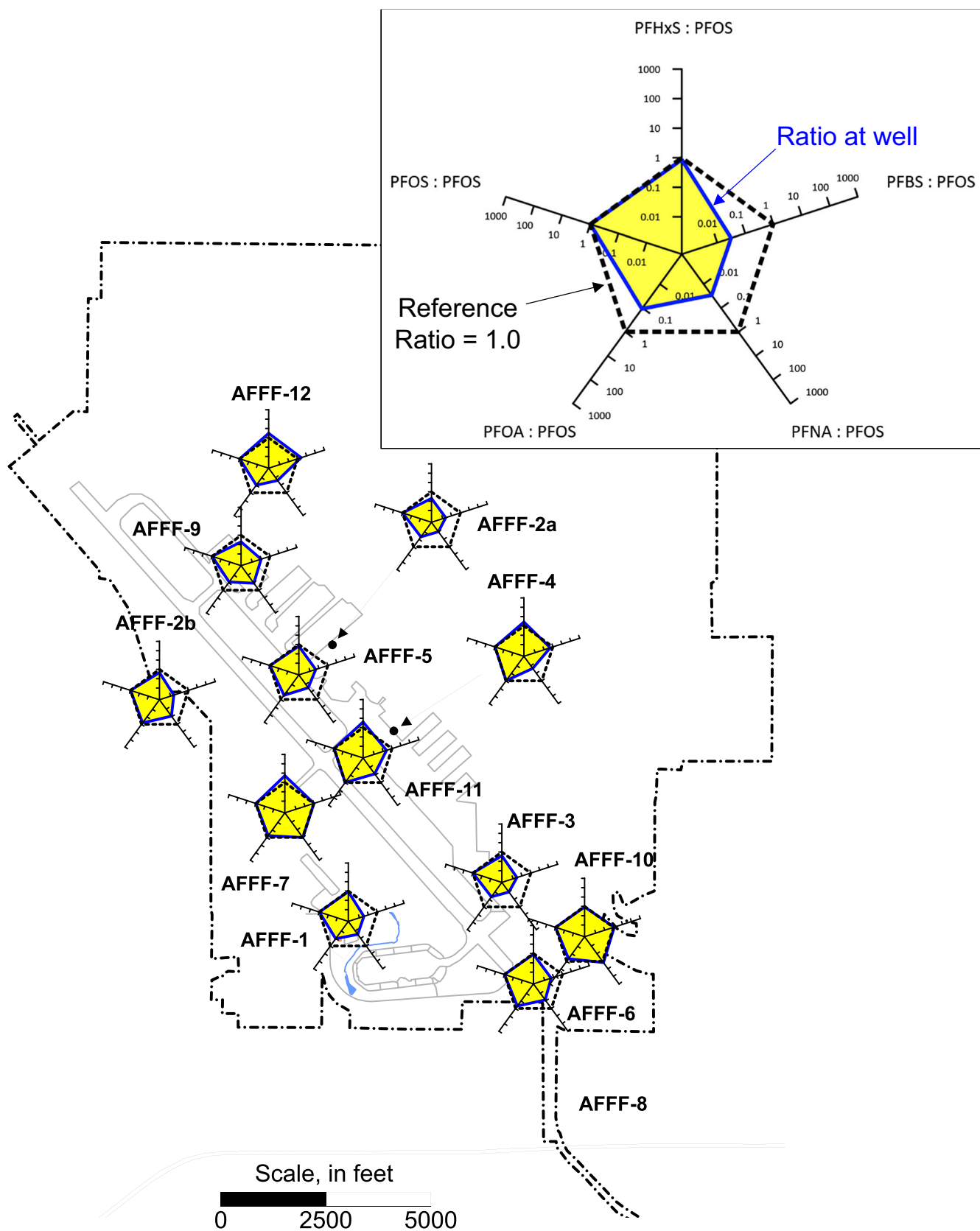


FIGURE 3 | PFAS of Concern (POC) radial diagrams at AFFF source areas with ratios to PFOS. Sulfonates are in the upper portion (PFOS, PFHxS, and PFBS), and carboxylates are in the lower portion (PFNA and PFOA). Non-detect POC ratios are based on detection limits. [Color figure can be viewed at [wileyonlinelibrary.com](https://onlinelibrary.wiley.com/doi/10.1002/rem.70023)]

AFFF area was PFHxS at a low concentration (0.0089 $\mu\text{g/L}$) which is below the MCL. Figure 3 does not include a ratio radial diagram for AFFF-8, because POC ratios at this location with respect to the detection limit for PFOS would not be meaningful.

Another option with radial diagrams is to show all applicable PFAA data for the most commonly detected PFAS at AFFF-impacted sites. For example, Supporting Information S1: Figure SI-2 shows a radial diagram map with nine radial diagram axes to represent three sulfonates and six carboxylates. Such figures may be more useful for internal data analysis because they show more data than may be necessary when communicating with a nontechnical audience.

3.3 | Stacked Bar Maps and Pie Charts

Stacked bars represent the proportion of a select series of chemicals relative to the total concentration for the corresponding group of chemicals. For example, a stacked bar may include six intervals representing the proportion of six carboxylates (C4 through C9 to represent PFBA through PFNA, inclusive). The proportion of each carboxylate is calculated based on the ratio of the individual carboxylate concentration at a well location, to the sum of the six carboxylates in the group at that same well location. For example, if PFBA was 1 $\mu\text{g/L}$ and the sum of the six carboxylates was 10 $\mu\text{g/L}$, then the proportion of PFBA in the stacked bar for this example would be 10%, and the remaining five carboxylates account for the remaining 90% of the group total.

Supporting Information S1: Table SI-2 presents the six carboxylate concentrations (C4 to C9) for the 13 AFFF source areas, as well as the calculation of the proportion of each carboxylate (in %) for each of these areas. Similarly, Supporting Information S1: Table SI-3 presents the three sulfonate concentrations (C4, C6, and C8) and proportions of the total sulfonates for the AFFF source areas. Figure 4 illustrates a stacked bar map showing the C4 through C9 proportion at each AFFF area. The total carboxylate concentrations (based on the sum of C4 to C9 carboxylates) are shown in brackets at each bar location. In this representation, all bars have uniform height and width. It would be difficult to use a proportional bar height based on the total carboxylates concentration because it spans up to three orders of magnitude over the 13 AFFF areas. It is also not practical to use a log-scale to represent the proportional height of stacked bars, because this will adversely affect the ability to visually estimate relative proportions based on the thickness of each chemical interval in the bar.

As explained by the legend at the top right of Figure 4, the stacked bar represents a total proportion of 0% to 100%, where 100% represents the sum of all six carboxylates at the well location. Tick marks at intervals of 20% are shown to the left of the bar to assist with visual estimation of the thickness of each carboxylate proportion. For this figure, two sets of colors were used to represent the short- and long-chain carboxylates. Shades of green were used to represent the three shortest chain carboxylates, where the lightest green represents the shortest chain (PFBA) and the darkest green represents the longer chain (PFHxA) of these three species. Shades of yellow to orange were used to represent the longer chain carboxylates, with yellow

representing the shorter chain (PFHpA) and dark orange representing the longer chain (PFNA) of these three species. Using only two general types of color shades allows for more rapid visualization of the relative proportion of short- and long-chain carboxylates.

The stacked bar in the legend of Figure 4 illustrates that the three shortest-chain carboxylates (PFBA, PFPeA, and PFHxA) represent a cumulative 80% of the total carboxylates for the AFFF-1 area. This indicates that there may have been relatively high biodegradation of 6:2 FtS in the AFFF-1 (current FTA) source area.

The stacked bar map shown on Figure 4 illustrates that there are AFFF areas with similar “signatures” of carboxylate proportions, where a signature is defined as the relative proportion of C4 to C6 (short-chain) versus C7 to C9 (long-chain) species. There are six AFFF areas (AFFF-1, AFFF-2B, AFFF-3, AFFF-5, AFFF-6, and AFFF-9) where the cumulative concentrations of C4 to C6 carboxylates represent approximately 50% to 60% of the total carboxylates. The remaining AFFF areas have distinctly different signatures where the cumulative C4 to C6 carboxylates represent 80% or more of the total carboxylates. The cause of these different signatures may be related to the use of different AFFF products in each area, or they may suggest that AFFF applications (e.g., during crashes) or spills may have occurred during different periods of time. For example, telomerization-based AFFF products used earlier in time may result in higher proportions of long-chain carboxylates in groundwater, whereas products used later in time may result in a greater proportion of short-chain PFAS in groundwater (Interstate Technology Regulatory Council [ITRC] 2024).

The use of pie charts is a common approach for mapping this type of proportional relationship (e.g., see Reinikainen et al. 2022). To facilitate a comparison between stacked bar maps and pie charts, Supporting Information S1: Figure SI-3 illustrates the use of pie charts to represent the relative proportion of C4 to C9 carboxylates. The colors used to represent each carboxylate in the pie charts corresponds to the same colors used in the stacked bar map on Figure 4. Side-by-side comparison of Figure 4 and Supporting Information S1: Figure SI-3 indicates that there are three advantages associated with the use of stacked bars to represent this proportional distribution:

1. It is easier to estimate the relative proportion of individual carboxylates with stacked bars at each AFFF area, particularly when tick marks are shown to the left of the stacked bars. (There are no corresponding tick marks available to help with estimating the proportion of each species in the pie charts.)
2. The stacked bars better convey the linear progression in chain length from C4 to C9 (i.e., from bottom-up in each stacked bar). The pies also show a progression in chain length in a clockwise direction, although the change in chain length concentrations is less evident in pie charts when compared to the stacked bar representation.
3. The stacked bars are also more effective for visualizing relative similarities and differences in PFAS concentrations between well locations.

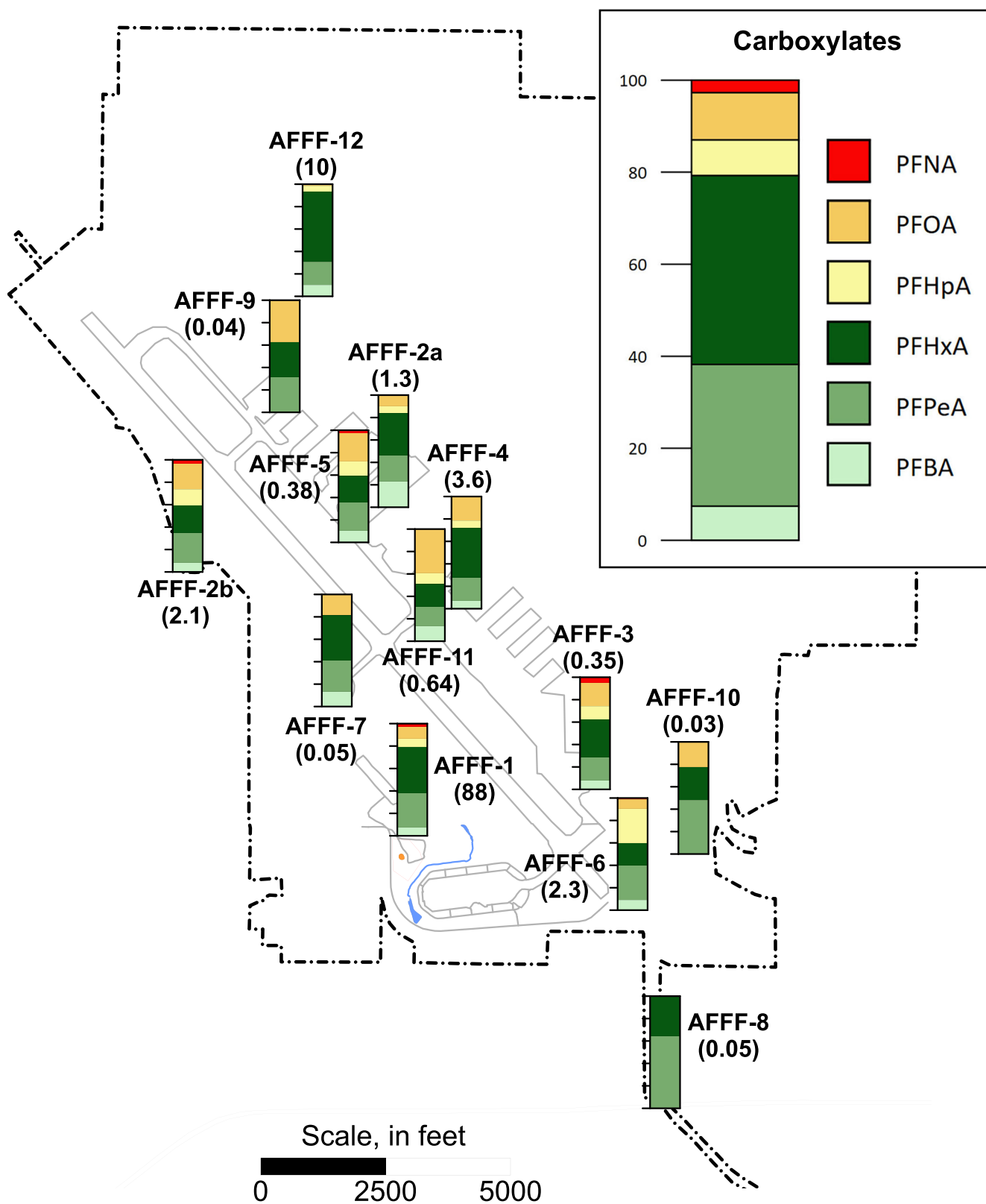


FIGURE 4 | Stacked bar map representing carboxylates at AFFF source areas. Shaded bar intervals represent the proportion of PFBA, PFPeA, PFHxA, PFHpA, PFOA, and PFNA to the sum of these six carboxylates. Values in brackets below each source area label represent the sum of these carboxylates in units of $\mu\text{g/L}$. [Color figure can be viewed at [wileyonlinelibrary.com](https://onlinelibrary.wiley.com)]

Supporting Information S1: Figure SI-4a shows another example of a stacked bar map which illustrates the relative proportion of total carboxylates (yellow) to total sulfonates (orange) based on the sum of C4, C6, and C8 sulfonates. This stacked bar

map clearly shows a distinction in AFFF areas, where seven of the 13 AFFF areas have a higher proportion of sulfonates, and the remaining six AFFF areas have a higher proportion of carboxylates. This suggests that some AFFF areas had greater

groundwater impacts from the ECF-based AFFF products, and other AFFF areas appear to have had higher impacts from telomerization-based products.

Supporting Information S1: Figure SI-4b provides an example of a stacked bar map to show relative concentrations of the three sulfonates with available data from the Site Inspection (PFBS, PFHxS, and PFOS). The stacked bar map on Supporting Information S1: Figure SI-4b better conveys the relative relationship between PFBS and PFOS that was discussed above based on the radial diagram showing ratios of POCs to PFOS (i.e., Figure 3).

4 | PFAS Visualization at OU-1 Former Fire Training Area

McGuire et al. (2014) and McGuire (2013) describe historical remedial activities in the vicinity of the former FTA at OU-1. Initially, groundwater remediation efforts were focused on petroleum hydrocarbons and chlorinated solvents. This involved the use of a pump-and-treat system from 1996 to 2011, although PFAS were not monitored during the operation of the on-site granular activated carbon treatment system. A dissolved oxygen (DO) infusion system (iSOC) was used from 2008 to 2015 to enhance aerobic bioremediation of hydrocarbons within and directly downgradient of the source area. McGuire et al. (2014) evaluated a PFHxS:PFOS ratio contour map in combination with FHxSA concentrations (and absence), based on the 2012 OU-1 data set. McGuire et al. demonstrated that enhanced aerobic biodegradation of precursors such as FHxSA in the vicinity of these DO infusion wells may have resulted in increased PFHxS concentrations relative to PFOS in this downgradient area.

4.1 | Radial Diagrams Based on PFAS Concentrations

Figure 5 shows a radial diagram map for the OU-1 source area and immediately downgradient monitoring wells, with representation of concentrations for FHxSA, PFBS, PFHxS, and PFOS. Radial diagrams for 18 monitoring wells are shown on Figure 5. Radial diagrams for GW22 and MW108-02 have been offset from the original locations to avoid overlap with nearby well locations. A reference series is included on the radial diagrams at the OU-1 maximum PFAS concentrations based on the 2012 monitoring event (FHxSA, 52.7 µg/L; PFBS, 150 µg/L; PFHxS, 338 µg/L; and PFOS, 74.9 µg/L). (Note that additional investigations have been conducted since this 2012 event, so these concentrations do not necessarily represent the maximum concentrations in this area when future investigations are considered.) Historical DO infusion well locations are indicated with symbols on the site map shown on Figure 5, both within and downgradient of the OU-1 source area. Symbols are also plotted on the radial diagrams to represent MCL or HBWC exceedances, and non-detect results.

Monitoring well MW89-105 is located near the south boundary of the OU-1 source area and is also situated adjacent to a DO infusion well. Groundwater flow at OU-1 is generally toward the south. The two nearest upgradient wells to MW89-105 are

MW07-101 and GW04 (see Figure 5). FHxSA concentrations at the two upgradient wells were 8.5 and 3.54 µg/L, respectively; and FHxSA was non-detect at the downgradient monitoring well MW89-105 adjacent to the DO infusion well. PFHxS concentrations at the two upgradient wells were 143 and 70.8 µg/L; respectively, and the PFHxS concentration at the downgradient monitoring well was 224 µg/L.

The radial diagram map shown on Figure 5 shows a substantial reduction in FHxSA concentrations as well as significant increases in PFBS and PFHxS concentrations between these two upgradient wells and the downgradient monitoring well. (Note that the radial diagram axes are plotted with a logarithmic scale). The increase in PFHxS is much greater than would be expected based on the relatively low FHxSA concentrations observed at the two upgradient wells, which indicates that other precursors may have been also been degrading to PFHxS as a result of DO infusion into the aquifer.

This single radial diagram map illustrates the same trend observed by McGuire et al. (2014) using several contour maps, which is one of the advantages of using radial diagrams. A single radial diagram map may be used to visualize trends for up to 5 to 10 PFAS species between wells along a flow path, and between PFAS species at individual well locations. Radial diagram maps may be an effective alternative to using multiple contour maps which are time-consuming to prepare and are not as efficient for comparing trends between multiple species at one or more well locations.

Supporting Information S1: Figure SI-5 shows a similar plot for C4 to C9 carboxylates (PFBA through PFNA) with two precursors: 6:2 FtS and 8:2 FtS. There is a general decline in 6:2 FtS concentration between one upgradient well (MW07-101) and the downgradient well. The 6:2 FtS concentration at the other upgradient well (GW04) is similar to the downgradient well, so the extent to which DO infusion caused a decrease in 6:2 FtS is not as clear. The C4 to C6 carboxylates (PFBA, PFPeA, and PFHxA) are all shown as having increased concentrations at the downgradient well relative to the two upgradient wells, indicating that precursor degradation was likely enhanced by DO infusion. Supporting Information S1: Figure SI-5 also illustrates that 8:2 FtS is much lower in concentration than 6:2 FtS. This demonstrates that the fluorotelomer-based AFFF used in or upgradient of this area is predominantly modern (C6) relative to the legacy (C8) telomerization-based product. This is based on the modern fluorotelomer-based AFFF developed in response to the USEPA 2010/2015 voluntary PFOA Stewardship, where modern fluorotelomer-based AFFF contains limited to no long-chain PFAS (Interstate Technology Regulatory Council [ITRC] 2024).

4.2 | Radial Diagrams Based on PFAS Ratios

Yan et al. (2024) showed that 6:2 FtS will biodegrade aerobically to PFBA, PFPeA, and PFHxA. To visualize the influence of enhanced aerobic degradation of 6:2 FtS to these three daughter products, a ratio approach was developed for this study. Figure 6 shows a radial diagram map with three axes to represent the ratios of 6:2 FtS:PFBA, 6:2 FtS:PFPeA, and 6:2 FtS:PFHxA. Ignoring the effects of differential adsorption (which is a

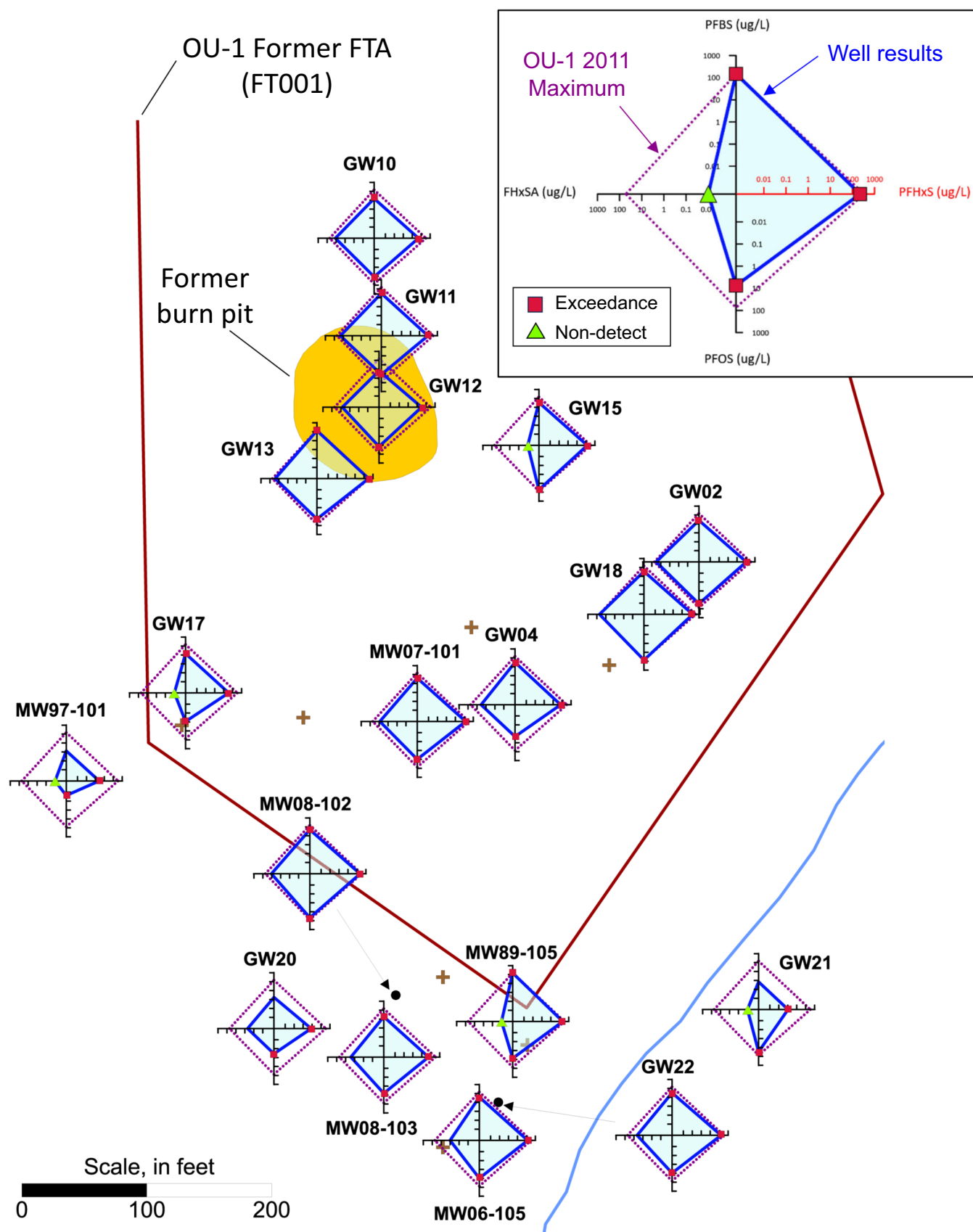


FIGURE 5 | OU-1 radial diagrams with sulfonates (PFBS, PFHxS, PFOS) and the precursor FHxSA which may biodegrade to PFHxS in aerobic environments. Brown “+” symbols represent the former locations of dissolved oxygen infusion wells. [Color figure can be viewed at [wileyonlinelibrary.com](https://onlinelibrary.wiley.com)]

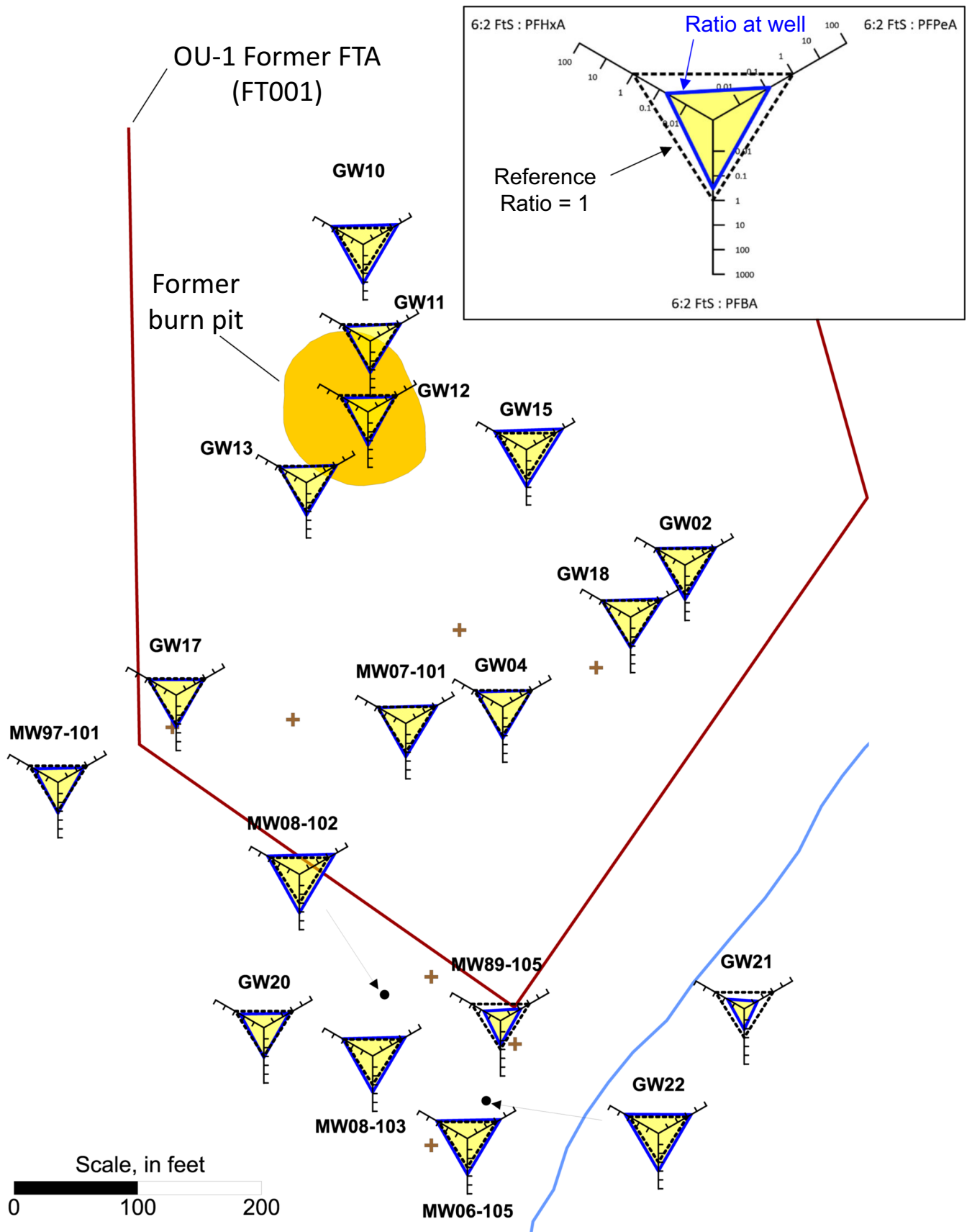


FIGURE 6 | OU-1 radial diagrams with ratios of 6:2 FtS to PFHxA, PFPeA, and PFBA. Brown “+” symbols represent the former locations of dissolved oxygen infusion wells. [Color figure can be viewed at [wileyonlinelibrary.com](https://onlinelibrary.wiley.com/doi/10.1002/rem.70023)]

reasonable approach if the plume is stable in time), these ratios will decrease during degradation of 6:2 FtS to these three daughter products. A reference series is plotted on each radial diagram corresponding to a ratio of 1.0 to help illustrate changes in these ratios along the southerly groundwater flow path.

Figure 6 shows that all three ratios at the two upgradient wells (GW04 and MW07-101) are close to the reference ratio of 1.0, meaning that the concentrations of PFBA, PFPeA, and PFHxA are similar to the concentration of 6:2 FtS at the two upgradient wells. The downgradient well MW89-105 shows a marked reduction in these ratios relative to the upgradient wells: approximately one order of magnitude reduction in the 6:2 FtS:PFHxA ratio, about half an order of magnitude reduction in the 6:2 FtS:PFPeA ratio, and a little less for the 6:2 FtS:PFBA ratio. This provides evidence that transformation of 6:2 FtS (and potentially other precursors) to these three daughter products has occurred near the DO infusion well, and that PFHxA may have had the largest yield of the three daughter products. The greater insight into 6:2 FtS degradation gained from inspection of Figure 6 relative to Supporting Information S1: Figure SI-5 demonstrates the advantage of plotting ratios to help with site characterization and forensic assessments.

Gamlin et al. (2024) suggested the use of four different ratios to assess the combined effects of precursor biotransformation to PFAAs and/or differential adsorption (i.e., assuming an unsteady plume). Three ratios are expected to decrease along a groundwater flow path: PFOS:PFHxS, PFOA:PFHxA, and PFOS:PFOA. Gamlin et al. identified a fourth ratio, PFHxS:PFOA, which is expected to increase along a flow path. Figure 7 shows a radial diagram map based on these four ratios. The legend at the top right of Figure 7 indicates that the direction of the PFHxS:PFOA axis is reversed, so the ratio increases when moving from the outer to the inner portion of the axis (i.e., toward the origin of the radial diagram), so that all four ratio axes are expected to trend toward the center of the radial diagram when moving in the downgradient direction along a flow path.

The radial diagram map on Figure 7 shows that the ratios are close to 1.0 at the former burn pit location in the OU-1 source area, where PFAS concentrations are generally the highest. There is a reduction in the size of the well-specific ratios with distance downgradient, although the trend is not clear beyond the immediate vicinity of the former burn pit. This may be because the plume was under relatively stable conditions in 2012, which would violate some of the assumptions by Gamlin et al. (2024) regarding how differential adsorption should affect ratios along a flow path. (A stable plume is not affected by differential adsorption between shorter- and longer-chain PFAS.)

4.3 | Visualizing TOP Assay Results With Radial Diagram and Stacked Bar Maps

TOP assays are conducted using oxidation to determine the potential for future in-situ transformation of precursors to terminal PFAAs (Houtz et al. 2013). While all of the oxidation daughter products are carboxylates in the TOP assay, some of these daughter products could be of the same chain length but in sulfonate form if aerobic degradation were to drive the

precursor transformation in situ. This test essentially shows the potential for future PFAA production through a laboratory oxidation test; it does not indicate that all of this mass will actually be transformed in situ.

The post-oxidation results were presented as concentrations for Δ PFBA, Δ PFPeA, Δ PFHxA, Δ PFHpA, and Δ PFOA, where Δ represents the increase in these carboxylates after oxidation. Using the graphical tools presented herein, two ways to visualize these TOP assay results on a site map are:

- i. Compare the pre- (C_n) and post-oxidation (C_n plus ΔC_n) concentrations using a radial diagram map, where $n = 4$ to 8; or
- ii. Assess the relative proportion of C4 to C8 carboxylate concentrations produced at each well location using a stacked bar map.

One objective with reviewing TOP assay results is to assess the relative proportion of short- and long-chain carboxylates produced, to determine if regulated PFAAs (which are typically long-chained) may be produced during future in-situ transformations under natural or active remediation conditions. TOP assays may also help with a forensic source differentiation analysis, or to assess where significant precursor transformations may have already occurred historically.

A TOP assay radial diagram is shown in Figure 8. The radial diagram in the top right of this figure shows that the inner data series (gray fill) represents the pre-oxidation carboxylate concentrations (C_n), while the outer data series (red line) represents the total post-oxidation concentrations (i.e., sum of the pre-oxidation carboxylate concentrations [C_n] and the change in concentration due to oxidation [ΔC_n] concentrations), where n ranges from 4 to 8 for PFBA through PFOA. (Δ PFNA results from the TOP assay were not available.) Unlike previous figures, an arithmetic scale was used for the radial diagram axes because the changes are relatively small. In the case of TOP assay results, the main focus on visualization is the post-oxidation increase in concentrations relative to the pre-oxidation concentrations.

Inspection of the radial diagram map indicates that all locations have negligible post-oxidation Δ C7 and Δ C8 concentrations, which indicates that there is little likelihood that PFOA (which is typically regulated) will be produced as a result of aerobic transformation in situ. Although the downgradient monitoring well MW89-105 shows a post-oxidation increase in C4 concentrations of about 50% relative to the pre-oxidation PFBA concentration, there was no apparent change in C5 or C6 concentrations post-oxidation. This is in contrast to increases in C5 and C6 concentrations in nearly all of the upgradient wells, suggesting that significant precursor transformation has already occurred in the vicinity of this well, presumably due to the historical DO infusion well nearby.

Results from another monitoring well (MW08-102) situated on the downgradient boundary of the OUOU-1 source area indicated that relatively high amounts of C4 to C6 are produced during oxidation, suggesting there are still precursors present to support

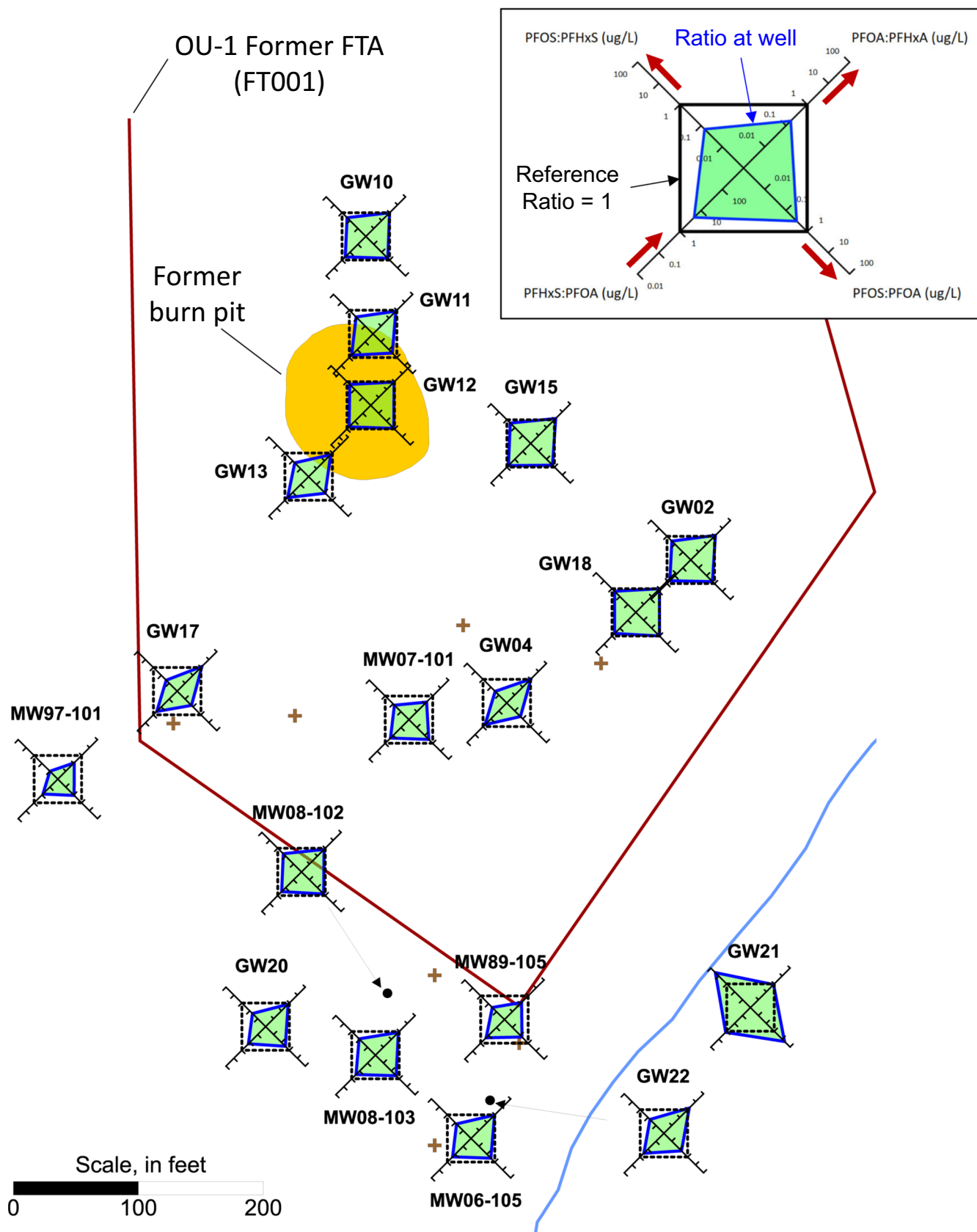


FIGURE 7 | OU-1 radial diagrams with ratios of PFOS:PFHxS, PFOA:PFHxA, PFOS:PFOA, and PFHxS:PFOA. Brown “+” symbols represent the former locations of dissolved oxygen infusion wells. [Color figure can be viewed at [wileyonlinelibrary.com](https://onlinelibrary.wiley.com/doi/10.1002/rem.70023)]

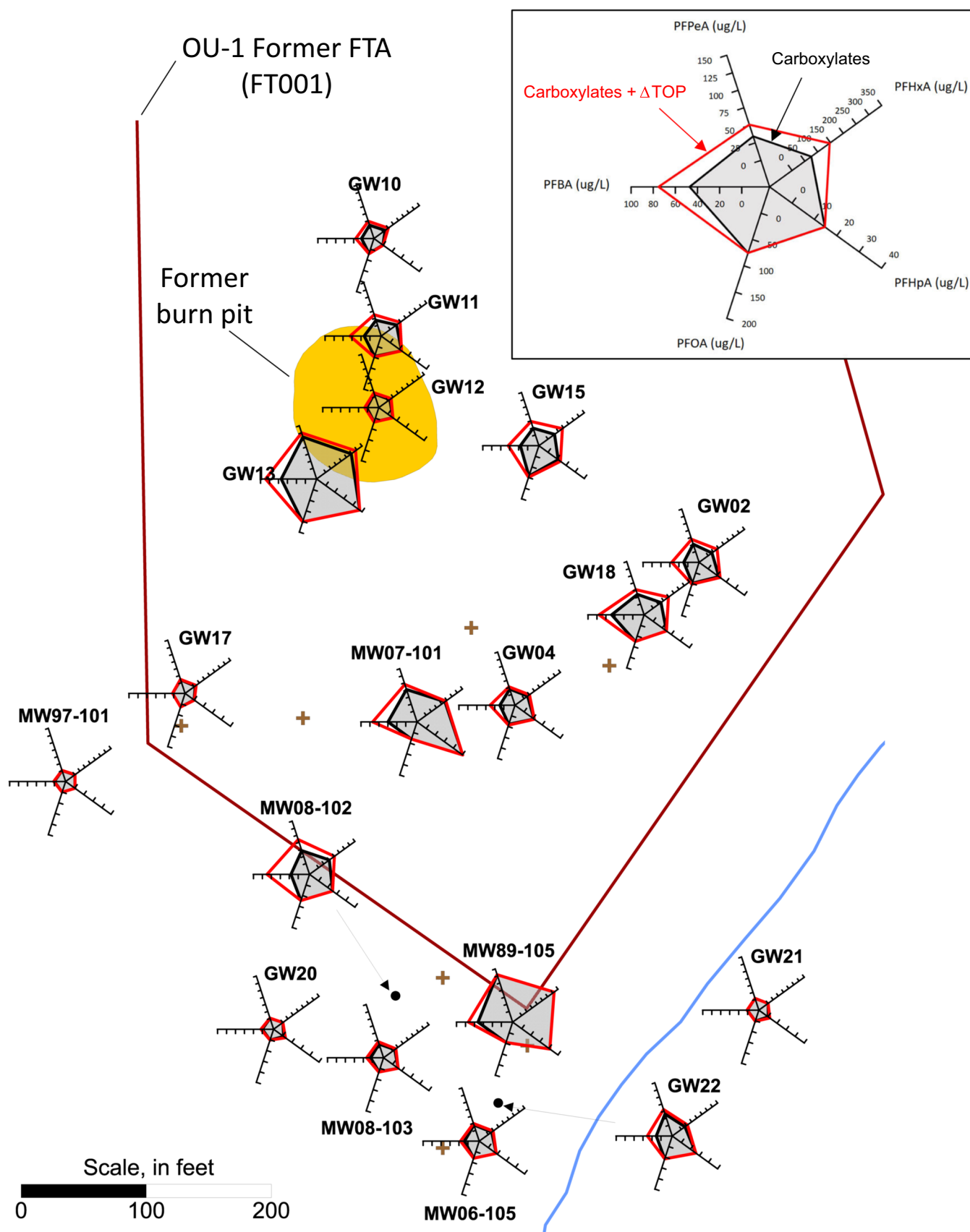


FIGURE 8 | OU-1 radial diagrams with 2011 carboxylates and the sum of carboxylates with the results from TOP assays. Brown “+” symbols represent the former locations of dissolved oxygen infusion wells. [Color figure can be viewed at [wileyonlinelibrary.com](https://onlinelibrary.wiley.com)]

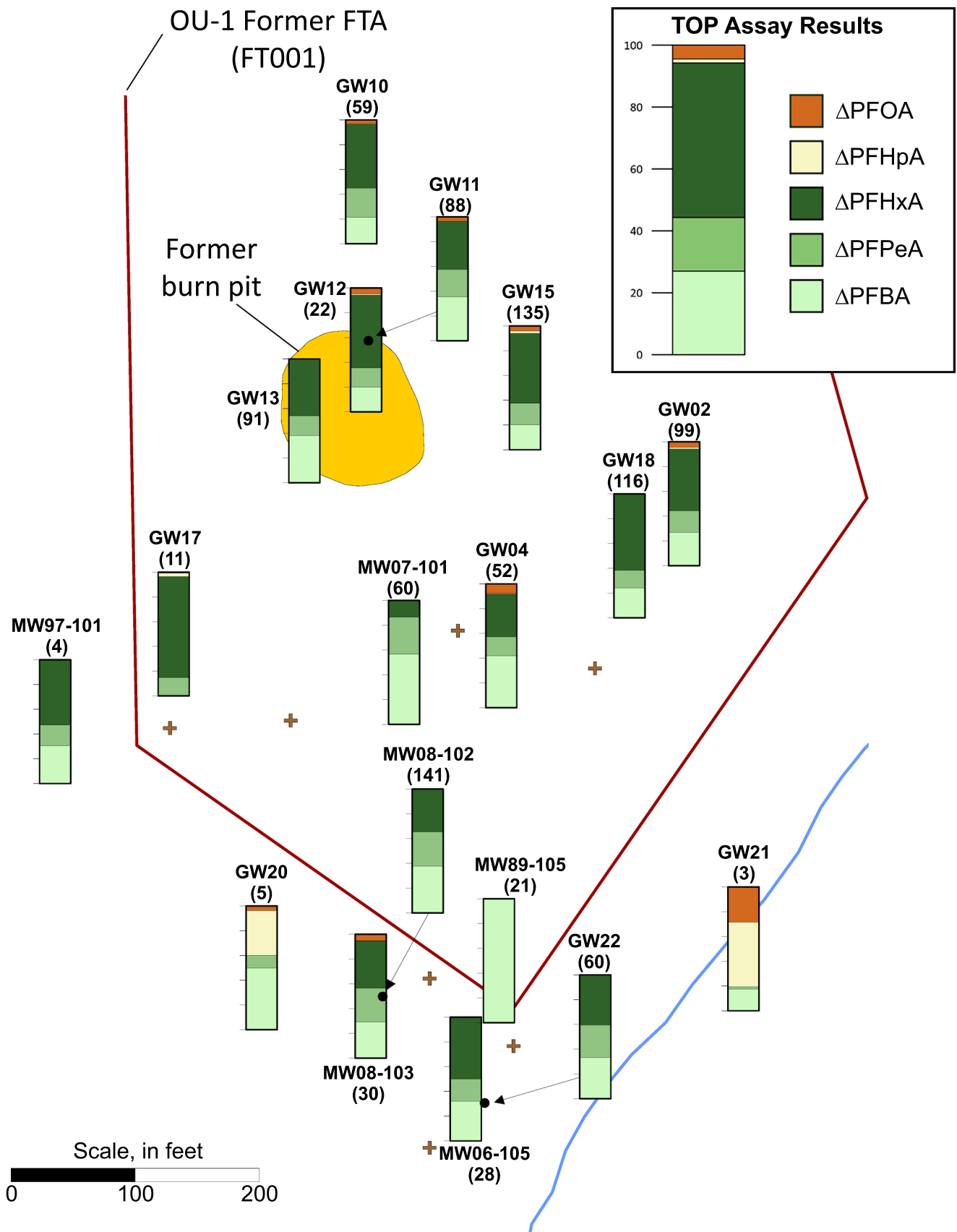


FIGURE 9 | Stacked bar map representing TOP assay results for C4 to C9 carboxylates at OU-1. Shaded bar intervals represent the proportion of ΔPFBA, ΔPFPeA, ΔPFHxA, ΔPFHpA, and ΔPFOA to the sum of these five ΔPFAS. Values in brackets below each label represent the sum of these ΔPFAS in units of μg/L. Stacked bars were offset for monitoring wells GW11, GW12, and MW08-102 to avoid overlap with nearby wells. [Color figure can be viewed at [wileyonlinelibrary.com](https://onlinelibrary.wiley.com)]

future potential transformations to short-chain PFAAs in situ. A similar trend with C4 to C6 production is observed at various monitoring wells in the source area. Other downgradient wells (GW-20, MW08-103, MW06-105, GW22, and GW21) show relatively low concentrations both for pre-oxidation carboxylates and post-oxidation daughter products, confirming that precursors available for transformation downgradient of the DO infusion wells are in relatively low supply.

Figure 9 shows an alternative approach for visualizing TOP assay results using a stacked bar map. The bar intervals represent the post-oxidation ΔCn concentrations for C4 through C8. The stacked bar map shows more clearly than Figure 8 that the post-oxidation daughter products are predominantly in the C4 to C6 range downgradient from the OU-1 source area, with some exceptions noted in wells with relatively low total PFAS concentrations. For example, MW89-105 had only C4 daughter products in the post-oxidation sample, indicating that long-chain precursors have already been degraded at this well due to the DO infusion well nearby. Most of the monitoring wells have the highest increase in C6, then C4, followed by C5 post-oxidation. This signature is relatively easy to identify when inspecting the stacked bar map. Figure 9 also shows that a small amount of C7 and a little more C8 are produced post-oxidation in the source area, although the sum of C7 and C8 is typically less than 10% of the total carboxylates produced.

5 | Conclusions and Recommendations

The utilization of PFAS radial diagram and stacked bar maps will facilitate an improved understanding of the conceptual site model during site characterization, will enhance the evaluation of groundwater remediation performance, and will also help to support forensic assessments such as contributions from different PFAS-containing products or source areas. These visualization methods will also improve communication with project stakeholders.

Radial diagram maps were used to represent between 3 and 9 PFAS species concentrations or ratios. The value of representing multiple PFAS species on a single map was demonstrated, including being able to assess inter-species trends at individual well locations (e.g., precursor vs. short-chain and long-chain PFAAs); and the increased efficiency of being able to review multiple PFAS trends on a single map. This will provide a more efficient approach at some sites when compared to the alternative of preparing separate concentration contour maps for each species; although in some cases both types of visual aids may be warranted.

Another beneficial feature demonstrated with radial diagrams in this study is the use of symbols to identify non-detect results, and locations where PFAS exceed applicable cleanup criteria. Inclusion of symbols on radial diagrams adds another layer of information which helps to delineate the overall PFAS plume during site characterization, and to visualize post-remediation monitoring results.

The use of ratios on radial diagrams are shown to be effective for evaluating the effects of precursor transformation to PFAAs along a groundwater pathway, or for evaluating the relative

concentrations of sulfonates versus carboxylates across different AFFF source areas. Plotting ratios of 6:2 FtS versus PFBA, PFPeA, and PFHxA was particularly successful at showing the influence of 6:2 FtS degradation at a monitoring well situated adjacent to a DO infusion well.

Stacked bar maps were demonstrated to be effective for visualizing signatures related to the relative proportion of chemicals within a group. For example, it was fairly simple to identify AFFF areas across the site where short-chain (C4 to C6) carboxylate concentrations predominated over long-chain (C7 to C9) carboxylates. Stacked bar charts were also useful for evaluating the relative proportion of short- versus long-chain carboxylates produced during a TOP assay.

Comparison of a stacked bar map to a pie chart representing the same characteristics indicates that it is easier to estimate the relative proportion of chemicals in a stacked bar map, which is a major advantage for this visual approach over pie charts. The stacked representation of short- to long-chain PFAS also provided more intuitive visualization compared to pie charts where the chain length was oriented in a clockwise progression. It was also easier to visualize changes in PFAS concentrations along a groundwater flow path using a stacked bar map instead of pie charts.

The following are recommendations for the use of radial diagrams or stacked bar maps for evaluating PFAS trends:

- PFAS radial diagram axes should use a log scale when groundwater concentrations are orders of magnitude higher than cleanup criteria.
- Including a reference series, such as maximum source concentrations or background concentrations, helps with visualizing spatial trends between upgradient and downgradient monitoring wells.
- Including tick marks on stacked bar maps (from 0% to 100%) makes it easier to estimate the proportion of each chemical represented in the stacked bar at an individual monitoring well location.
- Including symbols on radial diagrams to identify MCL exceedances and non-detect results supports groundwater plume delineation and identification of areas with concentrations above regulatory standards.

References

- Aerostar. 2019. "Final Site Inspection Report of Aqueous Film Forming Foam Areas at South Dakota Air Force Base." Prepared for Air Force Civil Engineering Center, March 2019.
- Carey, G. R. 2024. "PFAS Remediation Using CAC: Field Performance and Cost-Benefit Analysis." Presented at REMTEC & Emerging Contaminants Summit, October 14-16, 2024, Westminster, Colorado.
- Carey, G. R., P. J. Van Geel, T. H. Wiedemeier, and E. A. McBean. 2003. "A Modified Radial Diagram Approach for Evaluating Natural Attenuation Trends for Chlorinated Solvents and Inorganic Redox Indicators." *Groundwater Monitoring & Remediation* 23, no. 4: 75-84. <https://ngwa.onlinelibrary.wiley.com/doi/abs/10.1111/j.1745-6592.2003.tb00697.x>.

Carey, G. R., S. G. Hakimabadi, M. Singh, et al. 2022. "Longevity of Colloidal Activated Carbon for In Situ PFAS Remediation at AFFF-Contaminated Airport Sites." *Remediation Journal* 33, no. 1: 3–23.

Carey, G. R., M. G. Mateyk, G. T. Turchan, E. A. McBean, F. A. Rovers, and J. R. Murphy. 1996. "Application of an Innovative Visualization Method for Demonstrating Intrinsic Remediation at a Landfill Superfund Site." In *Proceedings of the API/NGWA Petroleum Hydrocarbons and Organic Chemicals in Groundwater Conference, Houston, Texas, November 1996*. https://porewater.com/Case_Studies/Carey-1996-Michigan_Landfill_Visualization.pdf.

Carey, G. R., T. H. Wiedemeier, P. J. V. Geel, E. A. McBean, J. R. Murphy, and F. A. Rovers. 1999. "SEQUENCE Visualization of Natural Attenuation Trends at Hill Air Force Base, Utah." *Bioremediation Journal* 3, no. 4: 379–393.

Gamlin, J., C. J. Newell, C. Holton, et al. 2024. "Data Evaluation Framework for Refining PFAS Conceptual Site Models." *Groundwater Monitoring & Remediation* 44, no. 4: 53–66. <https://ngwa.onlinelibrary.wiley.com/doi/10.1111/gwmr.12666>.

Houtz, E. F., C. P. Higgins, J. A. Field, and D. L. Sedlak. 2013. "Persistence of Perfluoroalkyl Acid Precursors in AFFF-Impacted Groundwater and Soil." *Environmental Science & Technology* 47, no. 15: 8187–8195.

Interstate Technology Regulatory Council (ITRC). 2024. "PFAS Technical and Regulatory Guidance Document." Washington, DC. <https://pfas-1.itrcweb.org/>.

McGuire, M. 2013. "An In-Depth Site Characterization of Poly- and Perfluoroalkyl Substances at an Abandoned Fire Protection Training Area." Master of Science thesis, Colorado School of Mines, Golden.

McGuire, M. E., C. Schaefer, T. Richards, et al. 2014. "Evidence of Remediation-Induced Alteration of Subsurface Poly- and Perfluoroalkyl Substance Distribution at a Former Firefighter Training Area." *Environmental Science & Technology* 48: 6644–6652.

Molé, R. A., A. C. Velosa, G. R. Carey, et al. 2024. "Groundwater Solutes Influence the Adsorption of Short-Chain Perfluoroalkyl Acids (PFAA) to Colloidal Activated Carbon and Impact Performance for In Situ Groundwater Remediation." *Journal of Hazardous Materials* 474: 134746.

Reinikainen, J., N. Perkola, L. Äystö, and J. Sorvari. 2022. "The Occurrence, Distribution, and Risks of PFAS at AFFF-Impacted Sites in Finland." *Science of the Total Environment* 829: 154237.

Yan, P. F., S. Dong, K. D. Pennell, and N. L. Cápiro. 2024. "A Review of the Occurrence and Microbial Transformation of Per- and Polyfluoroalkyl Substances (PFAS) in Aqueous Film-Forming Foam (AFFF)-Impacted Environments." *Science of the Total Environment* 927: 171883.

Supporting Information

Additional supporting information can be found online in the Supporting Information section.

Supporting Information

Visualizing PFAS Trends at a South Dakota AFFF-Impacted Site

**Grant Carey^{a,b,*}, Rita Krebs^c, Gabriel T. Carey^a, Mia Rebeiro-Tunstall^a,
Jeremiah Duncan^d, Gillian N. Carey^a, Kiera Rooney^a**

^a Porewater Solutions, Ottawa, ON, Canada

^b Carleton University, Ottawa, ON, Canada

^c Air Force Civil Engineer Center, Joint Base San Antonio, TX, USA

^d GZA GeoEnvironmental, Inc., New Hampshire

* Corresponding Author; 2958 Barlow Crescent, Ottawa, Ontario, Canada
K0A 1T0. Email: gcarey@porewater.com

Figure SI-1. Base-wide AFFF Source Areas. *AFFF: Aqueous film-forming foam; FTA: Fire training area*

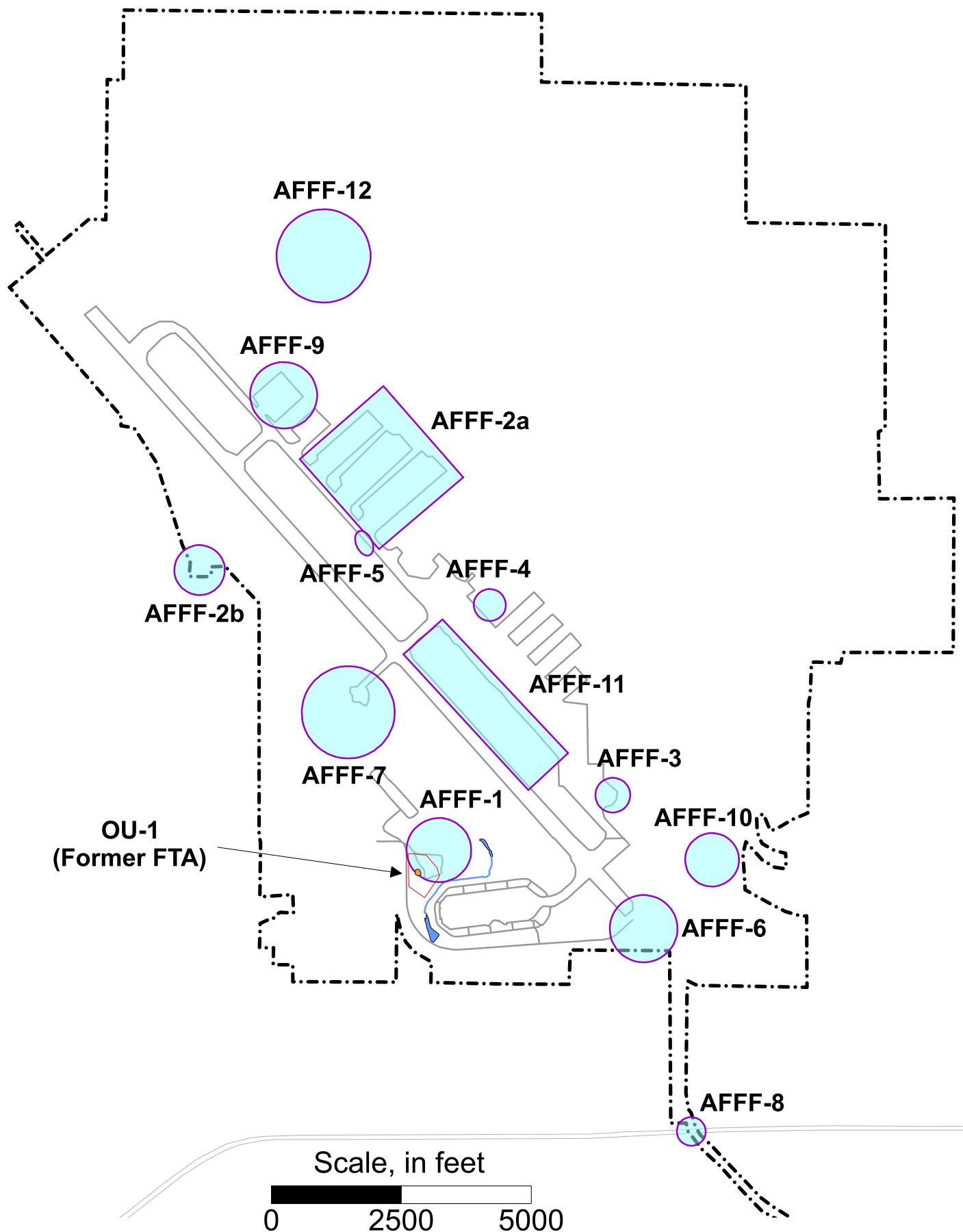


Table SI-1. Description of AFFF Areas Based on Aerostar (2019).

AFFF Area	Location	Rationale
AFFF-1	Current FTA	In operation since 1993, including all nozzle spray testing and flushing; most AFFF was contained within the retention pond, but some AFFF may have been released to adjacent soils.
AFFF-2a AFFF-2b	70, 80, 90 Rows; and Outfall #3	Known AFFF releases in eight of 10 hangars
AFFF-3	Building 618	Prior AFFF spills noted at this location
AFFF-4	Former Fire Station (Building 7506)	Overhead AFFF tanks, prior AFFF spill (5 gallons), several engines/trailer contained AFFF, and AFFF has been observed on fire station driveways in the past.
AFFF-5	B-52 Crash (1972)	AFFF use is unknown, but possible.
AFFF-6	B-1 Crash (1988)	Unknown amount of AFFF used during emergency response.
AFFF-7	Delta Taxiway West Crash (2000)	100 gallons of AFFF spilled; likely migrated to adjacent soils.
AFFF-8	Marten Crash (2006)	Based on crash photos, AFFF was applied at the crash location.
AFFF-9	Crash 4 (2001)	10 gallons of AFFF released from fire truck.
AFFF-10	Wastewater Treatment Plant	WWTP received discharge from several locations which had AFFF releases such as the diversion tank at 70 row, Building 618, and fire station floor drains
AFFF-11	Spray Nozzle Test Area	During nozzle testing, AFFF was sprayed on a grassed area for up to 20 years in the 1970s and 1980s.
AFFF-12	Building 88240	Formerly contained an AFFF fire suppression system
OU-1	Former Fire Training Area	AFFF use with PFAS started in early 1970s

Figure SI-2. PFAA radial diagrams at AFFF source areas with sulfonates in the upper portion (PFOS, PFHxS, and PFBS) and carboxylates in the lower portion (PFBA, PFPeA, PFHxA, PFHpA, PFOA, and PFNA).

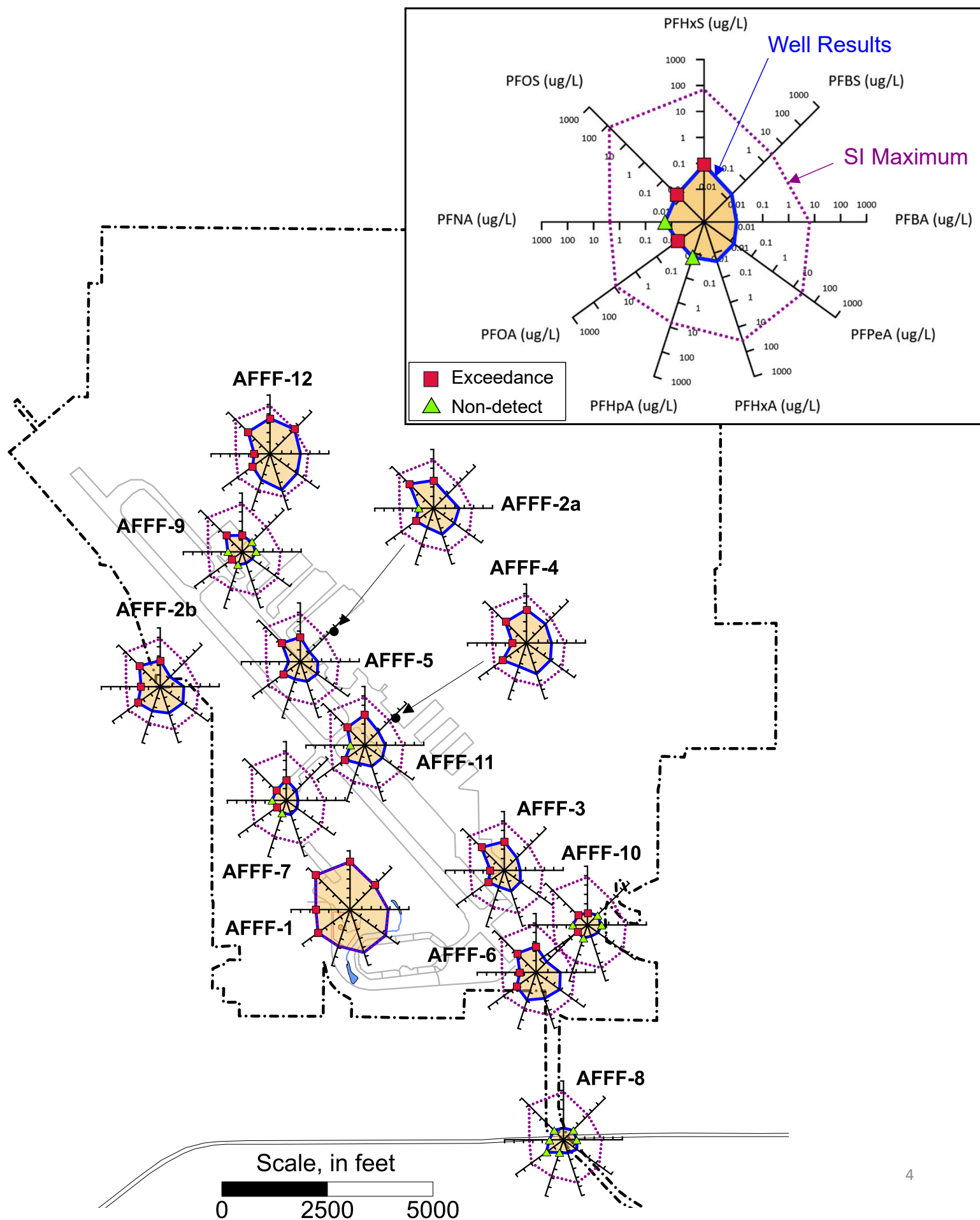


Table SI-2. Calculation of Proportion of Total PFCAs for AFFF Areas

Location	Proportion of Total PFCAs						Concentration (ug/L)						
	PFBA	PFPeA	PFHxA	PFHpA	PFOA	PFNA	PFBA	PFPeA	PFHxA	PFHpA	PFOA	PFNA	Total PFCAs
AFFF-01	7.4%	30.8%	41.0%	7.8%	10.3%	2.7%	6.5	27	36	6.8	9	2.4	87.7
AFFF-02a	23.0%	23.8%	37.2%	6.6%	9.5%	0.0%	0.29	0.3	0.47	0.083	0.12	<0.021	1.263
AFFF-02b	8.7%	26.1%	24.6%	14.5%	23.2%	3.0%	0.18	0.54	0.51	0.3	0.48	0.062	2.072
AFFF-03	8.0%	20.6%	34.3%	11.4%	20.9%	4.9%	0.028	0.072	0.12	0.04	0.073	0.017	0.35
AFFF-04	7.1%	21.1%	43.9%	6.6%	20.8%	0.5%	0.26	0.77	1.6	0.24	0.76	0.018	3.648
AFFF-05	10.8%	25.0%	23.6%	13.1%	25.0%	2.5%	0.041	0.095	0.09	0.05	0.095	0.0097	0.3807
AFFF-06	9.1%	30.9%	20.0%	30.4%	8.3%	1.3%	0.21	0.71	0.46	0.7	0.19	0.03	2.3
AFFF-07	13.4%	27.6%	40.5%	0.0%	18.4%	0.0%	0.0073	0.015	0.022	<0.015	0.01	<0.018	0.0543
AFFF-08	0.0%	64.6%	35.4%	0.0%	0.0%	0.0%	<0.015	0.031	0.017	<0.015	<0.1	<0.018	0.048
AFFF-09	0.0%	31.4%	31.4%	0.0%	37.1%	0.0%	<0.016	0.011	0.011	<0.016	0.013	<0.019	0.035
AFFF-10	0.0%	48.1%	29.6%	0.0%	22.3%	0.0%	<0.017	0.014	0.0086	<0.017	0.0065	<0.021	0.0291
AFFF-11	13.5%	17.3%	20.4%	9.6%	39.2%	0.0%	0.086	0.11	0.13	0.061	0.25	<0.018	0.637
AFFF-12	10.1%	20.6%	62.9%	5.0%	1.1%	0.3%	0.98	2	6.1	0.48	0.11	0.026	9.696

Note: PFCA concentration results are derived from the Aerostar (2019) report.

Table SI-3. Calculation of Total PFSA's for AFFF Areas

Location	Concentration (ug/L)			
	PFBS	PFHxS	PFOS	Total PFSA's
AFFF-01	2.6	71	82	155.6
AFFF-02a	0.055	0.51	2.5	3.065
AFFF-02b	0.017	0.34	0.74	1.097
AFFF-03	0.044	0.65	1.6	2.294
AFFF-04	0.4	2.1	0.79	3.29
AFFF-05	0.015	0.23	0.34	0.585
AFFF-06	0.022	0.33	0.4	0.752
AFFF-07	0.018	0.091	0.017	0.126
AFFF-08	<0.015	0.0089	<0.015	0.0089
AFFF-09	<0.016	0.032	0.16	0.192
AFFF-10	<0.017	0.012	0.014	0.026
AFFF-11	0.061	1	0.25	1.311
AFFF-12	2.8	3.4	1.1	7.3

Note: PFSA concentration results are derived from the Aerostar (2019) report.

Figure SI-3. Carboxylate pie charts for AFFF source areas with PFBA, PFPeA, PFHxA, PFHpA, PFOA, and PFNA.

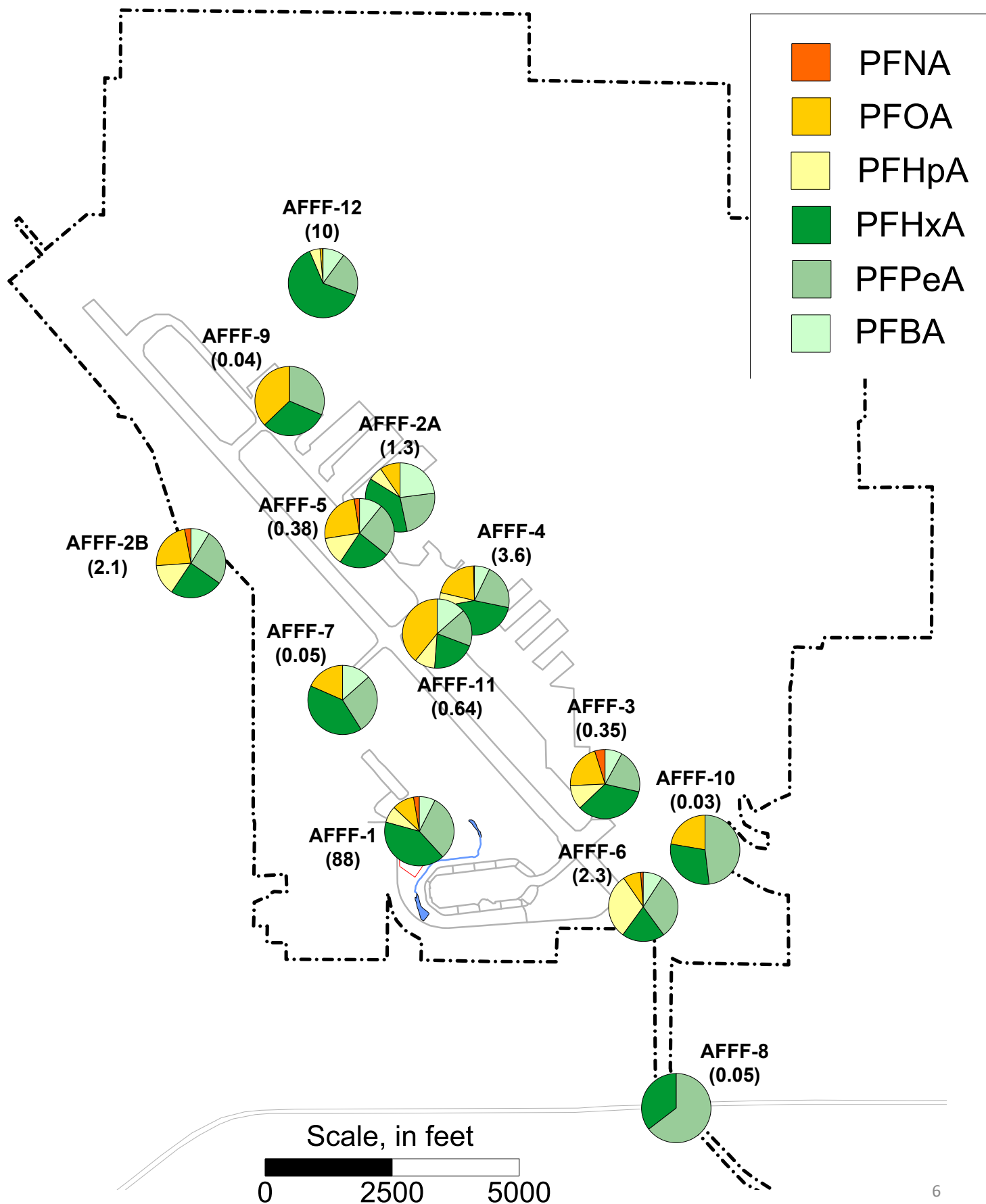


Figure SI-4a. Stacked bar map representing total sulfonates (bottom) and carboxylates (top) at AFFF source areas. Shaded bar intervals represent the proportion of these totals to the sum of total sulfonates and total carboxylates. Values in brackets below each source area label represent the sum of total sulfonates and total carboxylates in units of ug/L.

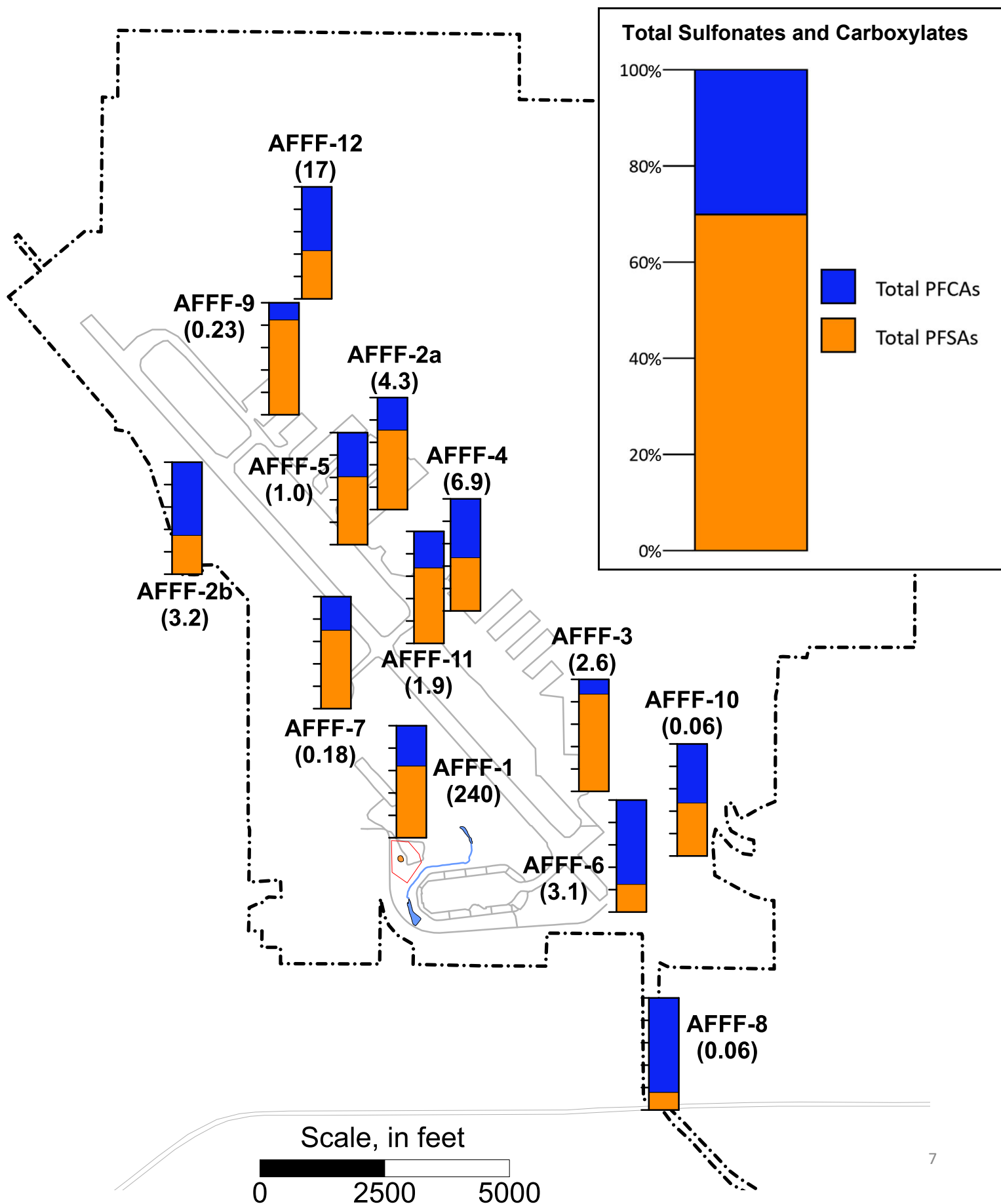


Figure SI-4b. Stacked bar map representing sulfonates at AFFF source areas. Shaded bar intervals represent the proportion of PFBS, PFHxS, and PFOS to the sum of these three sulfonates. Values in brackets below each source area label represent the sum of these sulfonates in units of ug/L.

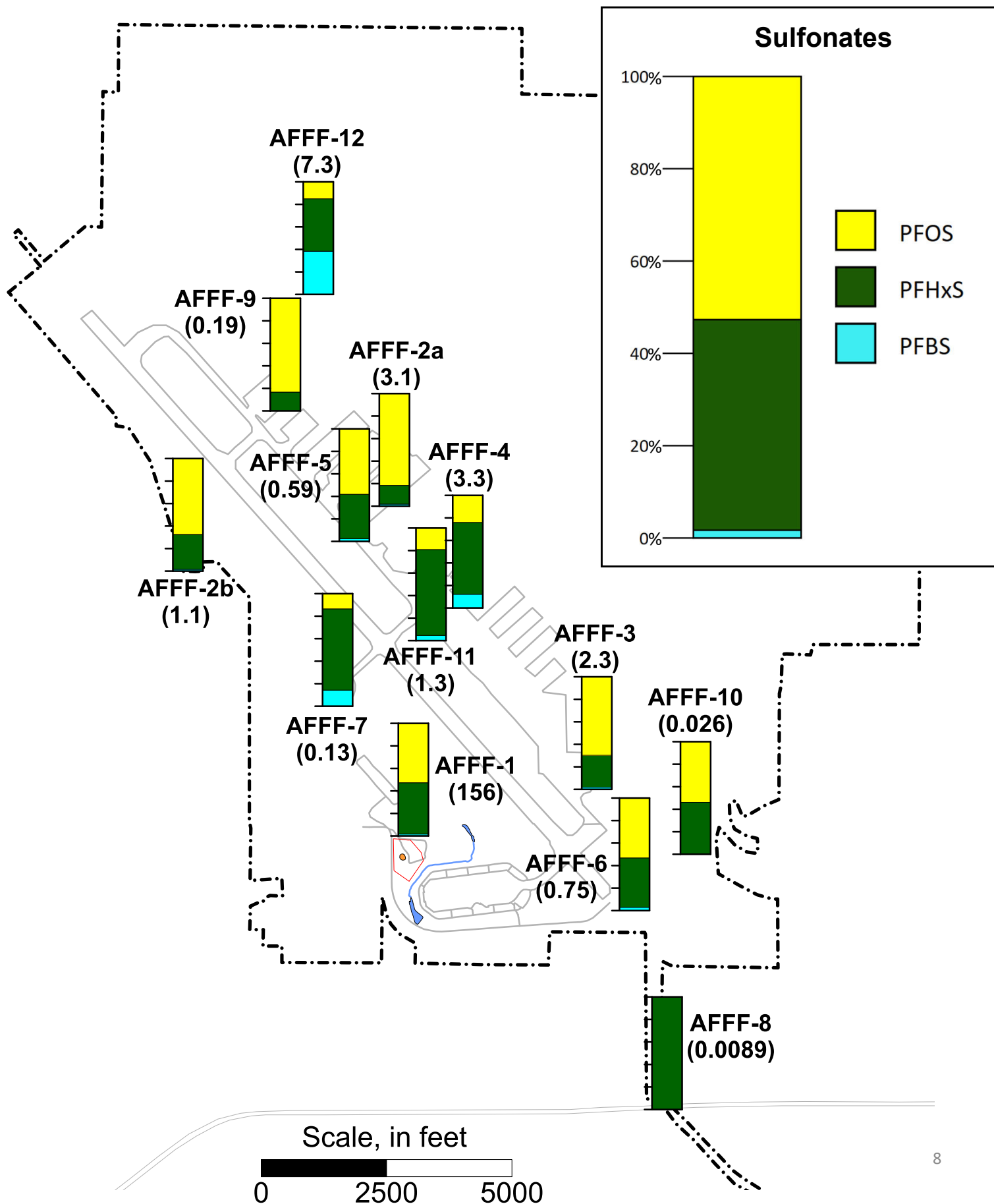


Figure SI-5. OU-1 radial diagrams with carboxylates (PFBA, PFPeA, PFHxA, PFHpA, PFOA, PFNA), and precursors 6:2 FtS and 8:2 FTS which may biodegrade to carboxylates in aerobic environments. Brown '+' symbols represent the former locations of dissolved oxygen infusion wells.

